Pan African University
Institute of Water and Energy Sciences

PAN-AFRICAN UNIVERSITY

INSTITUTE OF WATER AND ENERGY SCIENCES

(Including CLIMATE CHANGE)

Master Dissertation

Submitted in partial fulfillment of the requirements for the Master degree in

ENERGY ENGINEERING

Presented by

Constant KUNAMBU MBOLIKIDOLANI

"Design, simulation, prototyping and IoT-Based testing of an innovative tropical greenhouse with an energy efficient cooling system powered by a standalone Hybrid HAWT-Solar PV energy system: *Case study of DR Congo-Kinshasa /Plateau de Bateké weather conditions (savannah tropical climate).*"

Defended on 7th November 2020 Before the Following Committee:

Chair: ***Prof. Abdellatif ZERGA***	**(PAUWES, Tlemcen, Algeria)**
Supervisor: ***Prof. Venkata Ramayya***	**(Jimma Univ., Ethiopia)**
External Examiner: ***Prof. Kyandoghere Kyamakya***	**(AAU, Klangenfurt, Austria)**
Internal Examiner: ***Dr. Erick Tambo***	**(PAUWES, UNU)**

PAN AFRICAN UNIVERSITY
Institute of Water and Energy Sciences (including climate change)

Master Thesis title: "Design, simulation, prototyping and IoT-Based testing of an innovative tropical greenhouse with an energy efficient cooling system powered by a standalone Hybrid HAWT-Solar PV energy system: *Case study of DR Congo-Kinshasa /Plateau de Bateké weather conditions (savannah tropical climate).*"

Thesis submitted to Pan African University PAWES in partial fulfillment of the requirements for the degree of Master of Science in Energy Science, Energy engineering option

Full names**: Constant KUNAMBU MBOLIKIDOLANI**
Engineer in Oil, Gas and alternative energies

Supervisor: Professor Dr. **Venkatta Ramayya**

Submitted in 5th October 2020

Institute of Water and Energy Sciences (including climate change) in Algeria/ Tlemcen

THESIS APPROVAL

THESIS TOPIC: Design, simulation, prototyping and IoT-Based testing of an innovative tropical greenhouse with an energy efficient cooling system powered by a standalone Hybrid HAWT-Solar PV energy system: *Case study of DR Congo-Kinshasa /Plateau de Bateké weather conditions (savannah tropical climate).”*

Submitted by:

Constant KUNAMBU MBOLIKIDOLANI Signature Date

Approved by Examining Board

_____ _____ _____

Name of Examiner Signature Date

Thesis/ Dissertation Advisors

Dr.A.Venkata Ramayya_ 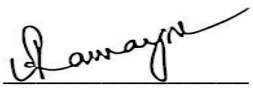 5th October

Name of Advisor Signature Date

Institute Dean

_____ _____ _____

Name of Dean Signature Date

Pan African University

_____ _____ _____

Name of Rector Signature Date

ACKNOWLEDMENTS

At the end of this research, we would like to warmly thank all those who have contributed from near or far to the completion of this Master thesis project.

I would like to express my gratitude to my supervisors, Professor Dr. Venkatta Ramayya, who has given me assistance to complete my Master thesis project and to whom, I have all esteem and scientific consideration.

I would like to thank the DAIPN center and TAMANO FOOD Company for providing me with internship despite the COVID 19 pandemic effect and providing me with helpful information on greenhouse related matters in Kinshasa and necessary testing environment for the developed prototype. I would like to thank particularly: Mr Ir Jean Jacques Mamba and Mr Jean Pierre MUKENDI KABONGO for their help and support in DAIPN center, and the occasional beverages which have made my field research enjoyable and memorable. I would not forget the helping hand of HALIME Abdoulaye Affadine in the equipment purchase in France and the one of Christian BAYI AYIKO during the testing phase, Thank you.

I would like also to thank the department of mechanical engineering of the University of Kinshasa, for giving me access to the laboratory where I have used Inventor and Ansys Fluent for the simulation of the proposed greenhouse. Particularly Mr. Derick Badibanga and Engineer Seba.

Last but not the least, my gratitude goes to my family for their love, support and encouragement during all my studies. Most of all I would like to thank my wife Therese KUNAMBU MASIKI for all the sacrifices that she has made to allow me to achieve my goal. I thank you from the bottom of my heart

Abbreviations and Acronyms

ANSYS: Analysis System

CDF: Congolese Franc

CFD: Computational Fluid Dynamics

COP: Coefficient of Performance

DAIPN : Domaine agro-industriel et présidentiel de la N'Sele

DHT: Digital Temperature and Humidity

DNA: Deoxyribonucleic Acid

DOD: Depth of Discharge

DRC: Democratic Republic of Congo

FRP: Fiber-Reinforced Plastic

GA: Genetic Algorithms

GPS: Global Positioning System

HAWT: Horizontal-Axis Wind turbine

HDPE: High-Density Polyethylene

HOMER: Hybrid Optimization of Multiple Electric Renewables

INERA : Institut National d'Etudes et de Recherches Agronomiques

IoT: Internet of Things

LED: Light Emitting Diode

MATLAB : Matrix Laboratory

METTELSAT : Agence Nationale de Météorologie et de Télédétection par Satellite

NTC: Negative Temperature Coefficient

NVAC: Naturally Ventilation augmented cooling

PE: Polyethylene

PET: Polyethylene Terephthalate

PNUD : Programme des Nations Unies pour le Développement

PV: Photovoltaic

SDG: Sustainable Development Goals

Contents

List of tables

List of figures

Abstract

Greenhouse is an agricultural structure that creates an optimal growth environment (microclimate) for the crops (especially vegetables and fruits). This work is geared towards identifying the current challenges that exist within the greenhouse sector in the savannah tropical climate and developing a new type of greenhouse more adequate, energetically efficient and affordable for small as well as large farmers thus, to boost their yield which remain low due to several reasons including the exclusive dependence on natural climatic factors such as rain and seasons. A meticulous design and simulations were carried out using Software, Ansys Fluent, helioscope and HOMER Pro respectively for an in-depth study of thermo-physical parameters distributed in the proposed greenhouse and for the design and sizing of the greenhouse energy supply system. The proposed greenhouse uses a new energy efficient cooling method designed and tested for savanna tropical climates in emphasizing more on the simplicity of technology, use of local materials, affordability and energy efficiency. It is mainly based on natural ventilation sustained by a misting system, a shading system and 6 exhaust fans. An effective and efficient coordination of the proposed cooling configuration was developed for an economical use of water and especially energy in the entire greenhouse. This configuration based on the designed energy usage planning saves significantly the entire greenhouse energy consumption; resulting in only 5.8382 KWh/day in summer months and 1.7KWh/day in winter months (for 24 hours). To optimize the energy consumption of the greenhouse, a specific timing was set for different cooling components (natural ventilation, misting system, shading system and exhaust fans). The first concept of the prototype was built in Kinshasa / Plateau de Bateké-Menkao in the Democratic Republic of Congo in the miniaturized design and provided 1°C to 7 ° C of cooling compared to the outside temperature. The cooling system proposed in this research has shown an increase in relative humidity of 1% to 24% during the testing phase. Design and sizing of a Hybrid Wind-Solar PV energy system with the storage system as a backup were meticulously carried out for the full-scale greenhouse. Finally, the cost of the proposed full-scale greenhouse was estimated to be 3.94 USA dollar per square meter, cost which made the proposed greenhouse affordable.

Keywords: **Energy efficiency, Hybrid energy system and Greenhouse cooling system**

Résumé

La serre est une structure agricole qui crée un environnement de croissance optimal (microclimat) pour les cultures (en particulier les légumes et les fruits). Ce travail vise à identifier les défis actuels qui existent dans le secteur des serres en climat tropical de savane et à développer un nouveau type de serre plus adéquat, énergétiquement efficace et abordable pour les petits comme les grands agriculteurs ainsi, pour booster leur rendement qui reste faible pour plusieurs raisons, dont la dépendance exclusive à des facteurs climatiques naturels tels que la pluie et les saisons. Une conception et des simulations minutieuses ont été réalisées à l'aide de Software, Ansys Fluent, hélioscope et HOMER Pro respectivement pour une étude approfondie des paramètres thermo physiques distribués dans la serre proposée et pour la conception et le dimensionnement du système d'alimentation en énergie de la serre. La serre proposée utilise une nouvelle méthode de refroidissement écoénergétique conçue et testée pour les climats tropicaux de savane en mettant davantage l'accent sur la simplicité de la technologie, l'utilisation de matériaux locaux, l'accessibilité et l'efficacité énergétique. Une configuration de refroidissement spécifique a été proposée en fonction de l'efficacité énergétique et du coût de fonctionnement. Le système de refroidissement de serre proposé est principalement basé sur une ventilation naturelle soutenue par un système de brumisation, un système d'ombrage et 6 ventilateurs d'extraction. Une coordination efficace et efficiente de la configuration de refroidissement proposée a été développée pour une utilisation économique de l'eau et surtout de l'énergie dans toute la serre. Cette configuration basée sur la planification de la consommation d'énergie conçue permet d'économiser de manière significative toute la consommation d'énergie de la serre ; seulement 5,8382 KWh / jour en été et 1,7 kWh / jour en hiver (pendant 24 heures). Pour optimiser la consommation d'énergie de la serre, un timing spécifique a été défini pour les différents composants de refroidissement (ventilation naturelle, système de brumisation, système d'ombrage et ventilateurs d'extraction). Le premier concept du prototype a été construit à Kinshasa / Plateau de Bateké-Menkao en République démocratique du Congo dans la conception miniaturisée et a fourni 1 ° C à 7 ° C de refroidissement par rapport à la température extérieure. Le système de refroidissement proposé dans cette recherche a montré une augmentation de l'humidité relative de 1% à 24% pendant la phase de test. La conception et le dimensionnement d'un système d'énergie hybride PV-Eolien avec le système de stockage en tant que sauvegarde ont été méticuleusement conçus pour la serre à grande échelle. Enfin, le coût de la serre à grande échelle proposée a été estimé à 3,94 dollars américains par mètre carré, coût qui a rendu la serre proposée économiquement abordable.

Mots clés : **Efficacité énergétique, System énergétique Hybride et système de refroidissement des serres**

INTRODUCTION

By 2050 the world population would be 9.8 billion (PNUD,2013), this put pressure on agricultural, water, as well as on energy sectors. Technological revolution is highly needed to sustain food production to meet the worldwide food demand.

In Africa, the food production faces numerous constraints, these have to be overcome so to feed the increasing population and to fight malnutrition. Those constraints include mainly technology limitation, poor energy access, dependence on rain-fed agriculture, low use of irrigation, poor water management, limited public investment and institutional support, climate change and gender gap in resources access.

In many countries of Africa notably the Democratic Republic of Congo farmers suffer from high yield losses, which mainly is as a result of unfavorable and/or unpredictable weather conditions (including climate change effect) for crops. Thus, in the quest to gain superiority over crop yield, there is the need to provide favorable micro climate conditions necessary for plants (vegetables and fruits) to produce maximum yield. The adoption of low-tech protected cultivation techniques affordable for farmers are believed to be able to meet these challenges.

It has become a necessity for researchers to come up with innovative solutions to curb on the one hand the issue of high yield losses and in another hand the energy access which is considered to be the plinth of modern agriculture. Among different innovative solutions adopted in the Democratic Republic of Congo especially in Kinshasa, the greenhouse technology is used to tackle the unfavorable and unpredictable weather conditions as well as climate change impact which cause the high yield losses impeding the development of sustainable agriculture able to sustain food security in the megacity of Kinshasa.

A greenhouse can be defined as an agriculture structure able to increase in extent the production season by offering a controlled indoor microclimate conditions adequate to the cultivation of diverse types of crops. Greenhouses increase crop yield and quality, and therefore have the potential to address the growing concerns of food security due to unfavorable, unpredictable weather conditions and climate change effects as well as urbanization spread. There is an emerging and expanding greenhouse industry in regions of the world relatively new to greenhouse technology. Due to food security concerns related to growing populations, rapidly declining soil quality, harsher climates (Lawrence et al., 2014; Stocking, 2003), and increasing awareness of declining freshwater availability (Al-Ismaili & Jayasuriya, 2016), greenhouses constitute a growing trend in regions of the Middle East, Africa, the Caribbean and Southeast Asia.

Various methods are used to control the microclimate found within a greenhouse notably, heating and cooling system. However, greenhouse cooling system can be more complex and far more difficult than heating. Unlike heating, for which the technology is well developed, greenhouse cooling frequently presents complex problems as it depends heavily on local environmental conditions, energy access, ease of operation and maintenance, and economic viability (Kumar et al., 2009; Sethi & Sharma, 2007).

Current cooling technologies demand large investments and involve high-energy consumption (Kittas et al., 2005). Natural ventilation is the preferred greenhouse microclimate control system as it is simple and cheap. Therefore, the study of the greenhouse microclimate under natural

ventilation has been the object of many studies. In most cases however, the outcome is informative but not generally applicable.

Although evaporative cooling solutions, such as pad-fan cooling systems, are successful in certain regions of the world, the optimization of greenhouse ventilation and cooling with respect to local climatic and economic conditions remains a challenge for many other regions (von Elsner, 2000, Sethi & Sharma, 2007). The lack of proper design, inaccessibility of suitable cooling technology, poor energy access and the unreliability of certain power grids renders greenhouse cooling systems that rely on forced ventilation and evaporative system unfeasible for many growers by constraining profits (Sachs, 2001). According to the World Bank, research in greenhouse technologies should concentrate on the design and engineering of lowest-cost controlled environment agriculture systems to be ventilated, cooled or heated as much as possible by natural phenomena and alternative energy sources.

In the Democratic Republic of Congo (DRC) there is a wide variety of climates and landscapes. Generally, the whole country moves under the average annual temperature, generally high. DRC has a hot and humid climate season on the greatest extent of its territory and an abundant rainfall, which is found in equatorial and tropical humid zone. DRC includes three main climates: the equatorial climate, the tropical climate (humid) and the mountain climate. The capital city, Kinshasa, is located in the west part of the country. It has a tropical savannah climate with dry winter. The annual average temperature is 25.3 ° C and the annual precipitation is 1,400 mm. It is the largest and megacity of the Democratic Republic of the Congo with an estimated population of more than 13 million. To feed this number of populations concentrated in Kinshasa requires mechanized modern agriculture. And one of the ways undertaken by the Government of Democratic Republic of Congo to promoted modern agriculture is the greenhouse technology used in DAIPN center (Domaine agro-industriel et présidentiel de la N'Sele) as well in many other farming compagnies dealing with greenhouses and aquaponic systems. Although greenhouse presents many benefits, local famers do not use this technology because of many challenges associated to its technical and economical aspect.

Global demand for food, especially vegetables and fruits keep soaring as populations explode. However, agriculture in DR Congo/ Kinshasa is still carried out in conventional way and lags behind in integrating modern technologies. Hence, there is the need to develop effectively the modern agriculture, which can increase the yield to meet the increasing demand for food.

These problems include; seasonal production of agriculture produce, post-harvest handling and resistant crop pests and diseases. Each of these problems has high negative impact on both the quality and quantity of food production. The seasonal farm production as a result of dependence on natural climatic condition, only allows a maximum of two seasons per year. The limit in season limits quantity of farm produce which is inversely proportional to the rate of consumption and population growth. It is reported that farmers loose up to two thirds (2/3) of the farm produce during the post handling period. This has not only caused financial losses but also discouraged a lot of farmers. The various pests and crops resistant to many of the pesticides is yet another challenge faced by the farmers practicing conventional open space farming. With modern technology in place such as greenhouse technology, all these farm challenges would be history and hence the Africa Agenda 2063 plus SDG 1, 2, 3, 7, 9, 12 will be well addressed. Recently, the evolution of Covid 19 pandemic and the associated international total / partial lockdown has been yet another wakeup calls for the Africa's agriculture sector and particularly

the one of Democratic Republic of Congo to embrace modern agriculture technologies which include greenhouse technology.

In addition, the impact of climate change is getting worse with high negative impact on the rain-fed agriculture. To sustainably feed Democratic Republic of Congo especially Kinshasa, modern and precision agriculture such as the use of greenhouse is highly needed to be introduced.

Based on the current market, a standard sized greenhouse which offers protection from aforesaid fluctuations can cost upwards of $5,000. This cost is far out of price range for most small-scale farmers. Nowadays, some large-scale commercial farmers in Democratic Republic of Congo try to use greenhouse system to increase their yield. Unfortunately, the greenhouse technology is facing many challenges in savannah tropical of Kinshasa. Some of the challenges this Master Thesis is geared towards realizing the solution to are mentioned below:

- **Local meteorological constraints for existed cooling technologies**: grasping the complexity of the savannah tropical weather condition of Kinshasa /Plateau de Bateke will help in designing the suitable efficient cooling technology to be used. The region has a heavy precipitation, high temperature and high relative humidity along the year with respectively annual average value of 1,400 mm, 25.3°C and 82.5%. For instance, as temperature and relative humidity are always strongly entangled in the greenhouse, decreasing temperature with one of the well-stablished borrowed cooling technologies, like Fan-Pad, will increase drastically the relative humidity and leading systematically to the failure of the entire greenhouse technology. Based on the local meteorological constraints, an efficient and affordable cooling technology in an innovative configuration will need to be designed, simulated and tested;

- **Lack of energy system and inaccessibility to electrical infrastructure issues**: Energy is the key factor for economic growth of any country to meet the basic human needs, in this case food production. Yet, in Democratic Republic of Congo (DRC) the national rate of electrification is currently 19% for all the country and 1% if we only take into consideration rural areas **(World Bank, 2016**). Our study zone is not covered by national grid, there is no electrical infrastructure. Thus, there is a need of identifying available energy resources, designing and sizing an affordable energy system to power the entire proposed greenhouse system;

- **High cost of greenhouse technology**: the greenhouse components and cooling technologies come with high cost of investments and involve high-energy consumption. Therefore, there is the need to come up with an adequate and energy efficient cooling techniques in accordance with the local weather conditions. An innovative well-designed greenhouse configuration and the experimentation of sustainable locally available material would have a significant impact on the cost of the greenhouse technology;

- **Proper greenhouse structure design issue**: a proper design based on local weather conditions plays a key role in the performance and the reduction of the cost of greenhouse technology as it contributes significantly in greenhouse energy and water efficiency. The conception of suitable greenhouse structure, the choice of optimal orientation and optimizing natural ventilation constitute the first step of an effective and

efficient greenhouse technology. It was hypothesized that different performances in terms of cooling system, indoor ventilation and food production yield will result from the greenhouse design in varying climates;

- **Optimization of Energy consumption:** high energy demand is generally required to power the entire greenhouse system especially for cooling system in tropical climate where the entanglement problem of high temperature and relative humidity putting a great stress on the energy system. A suitable optimization in terms of energy consumption is needed. Then, some alternative solutions such shading and lighting systems will be explored and experienced in a specific configuration;

Studies on greenhouse design, variations of microclimate in different shapes and understanding of the physical processes that drive natural ventilation have not reached the stage where the rates of air exchange can be predicted. Such information is required for the implementation of optimal environmental control strategies for regulation of summer or hot climate.

The Natural Ventilation augmented cooling (NVAC) greenhouse is an affordable design, using far less electricity than a fan-pad system in a comparably sized greenhouse. The test carried out in Trents, Barbados by McCartney and Lefsrud, in an empty NVAC greenhouse showed a cooling ranging from 1.3 to 3.6 °C relative to outside temperatures, while increasing relative humidity by 5.7-29.7%. This shows a deep ineffectiveness in regions like Kinshasa having high relative humidity and temperature along a year associated with a low average wind speed. In addition, the added inside roof proposed in the NVAC greenhouse design would have a potential impact on the penetration of solar radiation spectrum especially in regions with little solar radiation resource or poor sky clearness index. Less solar light penetration in a greenhouse structure can lead to a high energy consumption for powering the lighting system.

Although, the proven energy efficient cooling rate of the fan-pad system has shown its affordability in some specific regions, one of the limitations of this technology is the necessity for air tight greenhouse structure to guarantee that the airflow only passes through the cooling pads on one side and be extricated by the fans on the inverse side. This moreover implies that temperature conveyances will be uneven over the greenhouse, with greatest contrast of up to 11.4 C between the fans and the pads as it was observed by (Lopez et al., 2012) in their study. And fan-pad has been found to be ineffective in region with high and long relative humidity period over a year.

The significance of this study is unquestionable. The outcome of this research will help in boosting modern agriculture in Africa through a well-designed greenhouse technology using locally available material and powered by a low- priced clean energy system hence contributing to the Africa Agenda 2063 plus SDG 1, 2, 3, 7, 9 and 12.

Our proposed greenhouse is aimed at solving the pertinent aforesaid challenges faced by both large scale and small-scale farmers in Africa and particularly in Kinshasa/ Democratic Republic of Congo. The greenhouse proposed in this Master thesis offers an innovative cooling technology adequate to savannah tropical. The proposed cooling technology is an evaporative cooling system harnessing mainly natural ventilation associated to dehumidification equipment (exhaust fans), humidification equipment (misting system) and shading system used in intermittent way in a specific configuration. Our proposed cooling technology optimizes the natural ventilation. To implement all these, a specific structure design of greenhouse will be

carried out with a modified "shed roof opened" in the major direction of wind speed; the misting system will be strategically placed on the small roof longitudinal to the length of greenhouse structure using a well sized solar pump. Along the lateral sidewall 6 dehumidifiers (exhaust fans) will be placed. The entire proposed greenhouse system will be powered by a well sized standalone solar PV-Small Wind Turbine hybrid energy system.

A simple Arduino IoT based management system will be built for the testing phase. And a specific working configuration will be designed to smartly running the cooling system. This cooling system would be relatively very efficient than existing cooling technologies designed for savannah tropical climate, it will have the capacity of reducing temperature between 5°C to 10°C with no significant effect on relative humidity. The mounting system will be of wood (timber) with polyethylene plastic or PET covering system.

Our proposed greenhouse should be consuming very less energy than NVAC and fan-pad greenhouse. In addition, NVAC and Fan-Pad greenhouses have an important drawback of increasing relative humidity and uneven temperature within the greenhouse. Therefore, our proposed greenhouse would be designed and sized in the way of overcoming the challenge of increasing the relative humidity and should be far cheaper than others.

The objective of this research is of designing, sizing, simulating, prototyping and testing an innovative greenhouse with an energy efficient cooling system for the savannah tropical climate region of Kinshasa (Plateau de Bateke)/ DR Congo. In this research, we are emphasizing more on the energy efficiency, affordability and the use of locally available materials. The prototype includes:

- Design of greenhouse including the structure, cooling technology and energy system. The cooling system will be mainly based on natural ventilation with a misting system, exhausted fans backup and shading system. The cooling system will be based on evaporative cooling principle;
- The simulation of the geometrical structure adequacy, cooling components, air temperature, pressure distribution and air circulation within the greenhouse will be performed using Ansys-Fluent software before the construction of the prototype;
- Design and sizing of a solar PV-Small Wind Turbine energy system with battery storage system to power the greenhouse. The design will be based on the load demand, future scenarios and the available energy resources. The energy consumption will be estimated for the most common freestanding greenhouse size of 13.5 m wide and 32m long;
- Construction of the greenhouse prototype and installation of cooling system and covering system as well as solar irradiation shading system;
- The testing (IoT based and others) and demonstration of the greenhouse management system including cooling system.
- A cost estimation for the most common freestanding greenhouse size of 13.5 m wide and 32 m long.

CHAPTER 2. LITERATURE REVIEW

2.1. Greenhouse technology

A recent study suggests that greenhouse cultivation, of all crops combined, surpasses 5.4 million ha globally (Farrell et al., 2017). Most greenhouses are built in mild climate areas, and more than 90% of these are plastic film greenhouses (von Zabeltitz, 2011). Greenhouse plant production has become widespread because protected agriculture, in its various forms, has become important for local populations around the world as a source of reliable fresh food production and income. Greenhouses increase crop yield and quality, and therefore have the potential to address the growing concerns of food security due to climate change, population growth and urbanization (Lawrence et al., 2014).

Cultivation of plants in large scale greenhouses in temperate climates of Europe has been successfully carried out whereas in areas like Caribbean, Africa, and other warm climate regions especially those with tropics and subtropics climates face unique layout challenges due to the high temperatures and humidity that can occur in the hottest months (Cuce & Riffat, 2016) requiring a suitable air cooling system to overcome overheating (Sethi & Sharma, 2007). Air cooling in greenhouses is energy intensive especially with the use of mechanical cooling technologies. Suitable technological know-how is chosen relying on the desire of the crops, upkeep, operational ease, local environmental prerequisites and financial viability (Sanchez-Hermosilla, 2013).

2.2. Energy Balance in greenhouse

The transfer of energy inside and outside a greenhouse affects the indoor and outdoor environment, and determines what systems, such as cooling or heating systems, are needed for microclimate control. Energy balance models of varying complexity have been proposed to predict the performances of many greenhouse configuration operate under a variety of conditions and on a variety of crops (Nurarif & Kusuma 2013). A simplified equation can summarize the energy ratios of a greenhouse in warm climates, using greenhouse air as the control volume, greenhouse cladding, flooring, components inside the greenhouse and ventilation openings as control surfaces. Consequently, the energy transferred by these surfaces includes both sensible and latent heat exchanges. The energy balance equation is represented by the following equation:

$$\boldsymbol{Q_R + Q_G + Q_V + Q_S + Q_P + Q_L = 0}$$

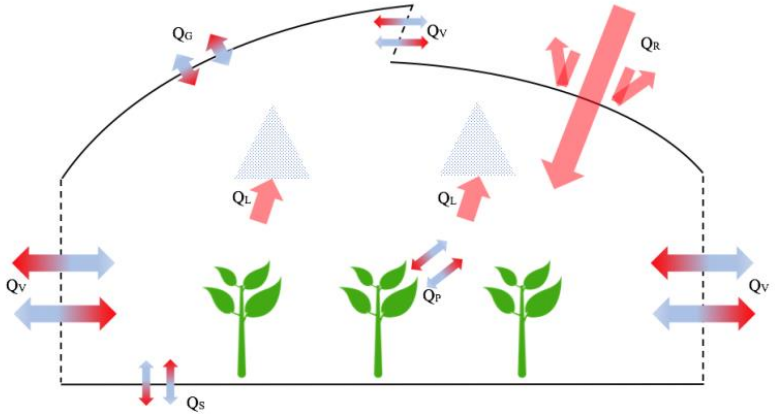

Figure 1. Heat transfer in a warm climate greenhouse. ((Nurarif & Kusuma 2013)

Q_R is the heat transfer by solar radiation. Q_G is the heat transfer across the cladding, Q_V is the heat transfer by ventilation, Q_S is the heat transfer between the ground and greenhouse air and depends on their temperature difference. Q_P is the heat transfer by the various greenhouse components and QL is the latent heat transfer of sensible energy in the air to water from evaporative cooling systems, if cooling is used.

2.3. Greenhouse Temperature and Relative Humidity

2.3.1. Temperature

Temperature is one of the most important key parameters to take into consideration in farming sector and particularly in greenhouse cultivations. Air temperature is an integral part of the greenhouse microclimate. Regardless of climate, air temperatures in the greenhouse are generally higher during the day and drops at night. Temperature fluctuations are the result of complex and interactive heat and mass exchanges between the indoor air and the different elements of the greenhouse. The yield potential of many common vegetable crops decreases at temperatures above 26°C, by which the fruit set is one of the first processes that is negatively influenced by the time of day Temperatures above 32 ° C and night temperatures above 26 % C, including specialized breeding varieties.((Nurarif & Kusuma 2013).

The ideal and approximate temperatures for best growth and quality of some vegetable crops are listed in Table 1 (Hochmuth 2007).

Mean Monthly Temperatures (°C)			**Vegetables**
Optimum	**Minimum**	**Maximum**	
Cool Season Crops			
12 - 24	7	29	Chive, Garlic, Leek, Onion, Shallot
15 - 18	5	24	Beetroot, Broad bean, Broccoli, Brussels sprouts, Cabbage, Horseradish, Kohlrabi, Parsnip, Radish, Spinach, Swiss chard, Turnip
15 - 18	7	24	Artichoke, Carrot, Cauliflower, Celeraic, Celery, Chinese cabbage, Lettuce, Mustard, Parsley, Pea, Potato

Warm Season Crops			
15 - 21	10	27	Lima bean, Green bean
15 - 24	10	35	Sweet corn, New Zealand spinach
18 - 24	10	32	Pumpkin, Squash, Vegetable marrow
18 - 24	15	32	Cucumber, Muskmelon, Sweet melon
21 - 24	18	27	Sweet pepper, Tomato
21 - 29	18	35	Chili, Eggplant, Okra, Sweet potato, Watermelon

Table 1. Approximate temperatures for best growth and quality of some vegetable crops

2.3.2. Relative Humidity

A recommended range of relative humidity in the greenhouse is between 40-70% (Wees, 2016), although this can vary considerably depending on air temperature, crop type and age of the crop. For example, a relative humidity level of 70 to 90% can be considered safe for most vegetable and flower crops in warm climates. The recommendations suggest that if the relative humidity out of daylight is less than 55-60% in warm climates, the relative humidity in the greenhouse should be increased by evaporative cooling((Nurarif & Kusuma 2013).

2.3.3. Solar radiation

Under normal conditions without greenhouse construction, a plant receives sunlight; the quantity, quality and duration of sunlight depends very much on the season, time of day, geographical location and weather conditions.

Plants use light as an energy source for photosynthesis. The term "photosynthesis" refers to the reaction between carbon dioxide and water in the presence of light to produce carbohydrates and oxygen. The rate of this process is highly dependent on the amount of light; the rate of photosynthesis is higher with increasing levels of Photosynthetic Active Radiation (PAR). Each plant species begins the process of photosynthesis at different levels of light energy; this is called the "light compensation point". This point is reached when there is enough light energy for the photosynthetic activity to produce more oxygen than the plant needs to consume for respiration (Lopez 2018).

Light quality refers to color or wavelength. The sun emits wavelengths between 10 and 2800 nm (97% of the total spectral distribution). They are divided into three areas: ultraviolet radiation (10-380 nm), visible radiation (380-780 nm) and infrared radiation (780-2800 nm). The highest energy corresponds to the shortest wavelengths; ultraviolet radiation has a higher energy than infrared radiation.

- ✓ Ultraviolet light: Ultraviolet light causes DNA damage, reduces the rate of photosynthesis, reduces flowering and pollination, and affects seed development. Ultraviolet light A (a sub-category) can cause plant elongation.
- ✓ Blue light: it is one of the absorption peaks, so the photosynthetic process is more efficient when blue light is present. Blue light is responsible for vegetative and leaf growth and it’s important for seedlings and young plants because it reduces stretch.

- ✓ Red light: This is the other peak of light absorption by the leaves. A phytochrome (a photoreceptor) in the leaves is more sensitive and responds to red light. This light is important in regulating flowering and fruit production. It also helps to increase stem diameter and promotes stem branching.
- ✓ Distant red-light: This light can cause plants to elongate and trigger flowering in plants with long days.
- ✓ Red light to distant red-light ratio: Plant elongation occurs when this ratio is low.

Different light sources distribute light differently : Incandescent lamp (blue spectrum and most of their light comes from the red spectrum); fluorescent lamp (most of their light in the blue, green and red spectra); high pressure sodium lamp (the highest peak is green, followed by red); halide lamp (the highest peak is in the green spectrum; the red spectrum accounts for about half of the energy peak coming from the green and lastly the blue) and light-emitting diodes (LEDs) (This type of light emits a specific wavelength. The manufacturer can produce these diodes in a specific color/wavelength according to customer requirements).

2.4. Greenhouse energy consumption

The energy transfer into and out of a greenhouse impacts the internal environment and determines what systems, such as cooling or heating systems, are needed for environmental control. Energy balance models of varying complexity have been proposed to predict the performances of many greenhouse designs under a variety of conditions and for a range of crops (Critten & Bailey, 2002; Singh et al., 2006).

In cold climate with a poor relative solar radiation, the energy (electricity) required for greenhouse lighting accounts for approximately 30% of operating costs. This leads often to the need of selection and use of low power consuming lighting system. As the light level of LED lighting can be easily controlled, it offers the potential to reduce energy costs by accurately matching the amount of additional light to the current climate conditions and lighting requirements of a crop (Watson, Boudreau, and van Iersel 2018)..

Greenhouse plant production is one of the most intensive parts of the agricultural production. It is intensive in terms of the yield of crop production, but also in terms of the energy consumption and investments. In order to reduce the costs and save the energy of greenhouse, many researches have to be conducted on greenhouse design and constructions based on specific local weather condition (solar radiation, wind data, temperature, rain and humidity...) and coverings including sensing and automated system for a suitable monitoring and controlling systems. (Djevic and Dimitrijevic 2009). Energy consumption varies for one greenhouse to another and regardless of the geographic climate condition the energy consumption rate of a greenhouse depends on its growth chamber, size, shape, monitoring and control system, lighting system and more. It also depends on how each facility is used: different crops and project goals naturally require different conditions (Ithaca 2020).

The most energy consuming part of a greenhouse is its cooling system. Current cooling technologies demand large investments and involve high-energy consumption (Kittas et al., 2005). This constitute the main challenge for greenhouse in tropical and hot regions.

2.5. Greenhouse cooling technologies

Mechanical systems are the foremost broadly utilized cooling systems for greenhouses. Mechanical cooling which uses fans, heat pumps and heat exchangers can keep up greenhouse temperature at low temperature, particularly in hot regions with high ambient temperatures and radiation levels (Kittas, Katsoulas, Bartzanas, & Bakker, 2013). Numerous studies explored and evaluated greenhouse mechanical cooling systems in hot regions.

Chou, Chua, Ho, and Ooi (2004) explored the effectiveness of a heat pump for heating, cooling and dehumidification of the greenhouse using simulation based on steady-state models. The results showed that the heat pump with a 3.7 kW compressor, 30.0 kW condenser capacity and 37.0 kW evaporator capacity was satisfactory to support a daytime temperature of 27 °C, night time temperature of 18 °C and relative humidity of 40% in a 270 m^2 floor area greenhouse. Based on the changes in climatic condition, the COP and heat pump's specific energy consumption varied between 1.2 and 4.0 and 1,000-16,000 kJ kg^{-1}.

Yang and Rhee (2013) studied the effectiveness of a greenhouse system that captures and use excess air thermal energy for heating and cooling. The system was made of a heat pump, fan coil units and heat storage tanks. The study highlighted that the amount of excess air thermal energy measured was between 258 and 6259 MJ per month for a 100 m^2 floor area greenhouse. And the maximum daily and monthly energy conservations were 76.3% and 25.7% respectively. However, the system was cumbersome and complex.

Katsoulas, Sapounas, De Zwart, Dieleman, and Stanghellini (2015) assessed the influence of the capacity of cooling system on the ventilation requirements of a semi closed greenhouses in different climatic conditions. The greenhouse climate and crop yields were simulated for several capacities of cooling system in the Mediterranean (Greece and Algeria) by applying a cooling module into an existing model of a greenhouse. The results showed that the increment in capacity of the cooling system results in the improvement of microclimate and decrease of water demand which improved the crop yield.

2.5.1. Natural ventilation cooling system

The natural ventilation is a well-known technique of providing cooling in greenhouses using wind and buoyancy driven flows (as shown on Figure 2) goes back to the start of controlled environments. This simple technique requires little or almost no external energy consumption to cool down a greenhouse. This technique can be under some specific conditions effective for greenhouse cooling applications in hot climates. It is driven by the difference in pressure between the greenhouse interior and outside environmental conditions. This is achieved by careful positioning of sidewall openings and roof openings. Researches have been carried out to investigate the influence of natural ventilation on the microclimate of greenhouse in hot climates. The most common approaches used for analysis that includes field experiments, laboratory scale testing and numerical modelling.

Figure 2. Natural ventilation cooling system ((Poly-Tex 2020)

Campen and Bot (2003) examined a naturally ventilated greenhouse utilizing three-dimensional modelling. Two roof opening arrangements were examined: rollup and fold window. The simulation results were validated with exploratory tracer gas measurements. The work revealed that the rollup window had higher ventilation rate due to the cover having larger openings.

Mashonjowa, Ronsse, Milford, and Pieters (2013) demonstrated the performance of a naturally ventilated greenhouse in Zimbabwe utilizing the Gembloux dynamic greenhouse climate model. The model comprises of a differential conditioning system based on the heat and mass balance of the greenhouse layers. The study showed that the wind impact and discharge coefficients were not only subordinate on the ventilation system but moreover on the climate conditions.

Baeza et al. (2009) examined the effect of side wall openings on the buoyancy driven flows in a multi span greenhouse employing an approved numerical model. The results appeared that the ventilation rate per unit ground area of a 20-span greenhouses with sidewall and roof openings was 2 times higher than that of a greenhouse with as it were roof openings. While in a 3-span greenhouse, the ventilation rate was 7 times higher for a combined roof-side wall opening configuration than a roof vent. In terms of temperature distribution, a large percentage of the area (48.3-79%) of the greenhouse had an indoor-outdoor temperature difference of 4 °C and higher for the roof only ventilation. With this combined ventilation configuration, those areas were 23.4-36.1%. The work concluded the importance of the optimum design of the side wall vents for buoyancy driven ventilation in particular for greenhouses with lower number of spans. Furthermore, addition of insect nets over the vents can reduce the ventilation rates by up to 87% when air exchange is buoyancy driven.

Teitel, Montero, and Baeza (2012) explored a new five span greenhouse design which had a 30° incline roof with side wall vents and roof vents for each span. Deflectors were included to the ridge of the windward and leeward ranges and on the sidewall vents to avoid hot and dry wind impinging specifically on the plants. The proposed plan was compared to atypical parral-type greenhouse with a shallow incline roof, little vertical and sidewall vents and no deflectors. The results showed that the proposed plan might give ventilation rates up to 4 times higher than the parral-type greenhouse. An enhancement within the air circulation and temperature distribution within the greenhouse was moreover observed. He, Chen, Sun, Liu, and Huang (2015) examined the impact of vent openings on a multi-span greenhouse microclimate amid the summer and winter.

Espinoza et al. (2017) assessed the influence of the configuration of ventilator on the flow distribution in a multi-span greenhouse in Spain, taking into account the impact of surrounding greenhouses. Two configurations were compared using experiments: a 2 and 3 half arch roof vents with side vents. Results showed that the 2 roof and side vents configuration had a lower overall ventilation flow rates but an improvement in the air movement was observed in the crop zone. Furthermore, the surrounding greenhouse on the leeward side decreased the ventilation capacity.

Li, Huang, and Zhang (2017) analyzed changes of temperature, humidity and sun-based radiation inside a naturally ventilated greenhouse during the sweltering seasons in Shouguang, China. Two single-slanted greenhouses were utilized for the test study. A thermal model was likewise evolved to build up the energy balance conditions and control the microclimate parameters of the greenhouses. The outcomes featured that air temperature changed between 21 ℃ and 26 ℃. while the relative humidity differed from 96% to 84%. It was additionally indicated that a shorter range and a more prominent rooftop tallness improved warmth conservation and energy saving in a single slanted greenhouse.

2.5.2. Evaporative greenhouse cooling system

The evaporative cooling is one of the foremost proficient technologies for giving appropriate greenhouse climatic conditions in hot and dry regions. It changes over sensible heat into latent heat through water evaporation provided straightforwardly into the greenhouse by means of fog or mist system, sprinklers or evaporative cooling pads (Kittas et al., 2013). This procedure can essentially decrease the air temperature below the surrounding temperature and increment the humidity to the essential levels. This cooling system can be separated into 3 distinctive technologies utilizing the same principle. We have:

Fan-pad system

This system frequently comprises of fans on one of the greenhouse sidewalls and pads on the converse sidewall. Evaporative cooling is fulfilled by sprinkling water over the pads and the active wind stream through the pads by the fans (Al-Helal, 2007) **Figure 3.**

Over a decade, a number of studies have experimented fan-pad frameworks for cooling greenhouses in hot and dry locales, and a number of arrangements have been proposed to move forward their execution. Ganguly and Ghosh (2007) worked on a floricultural greenhouse ventilated and cooled by a fan-pad system. Cooling was fulfilled by uniting a combination of fan-pad system and shading devices, while compelled ventilation was utilized to fulfilled dehumidification of the air. The research showed that the fan-pad ventilation framework was most successful amid the summer, while within the monsoon season it was less effective due to high humidity levels of outdoor air, which limits the viability of evaporative cooling.

Ahmed, Abaas, Ahmed, and Ismail (2011) moreover examined fan-pad framework but centered on assessing the thermal performance of diverse sorts of evaporative; pads celdek pads, straw pads and cut wood pads in Khartoum, Sudan. In addition, the highest cooling effectiveness was observed at the least air speed (0.25 m s^{-1}). However, a brief time cycle may cause fast ageing of the evaporative cooling pad. From the surveyed studies, it can be established that the fan-pad systems can be effective for greenhouse cooling and humidification in hot and arid regions. In order to realize ideal cooling, the water flow rate and dispersion system, capacity of pump, distribution and yield rate of the system must be carefully calculated and planned to supply

sufficient wetting of the pad and to avoid deposition of material. The normal thickness of the pad ought to be 100-200 mm. The pad surface depends on the airflow rate essential for the cooling system and the reasonable surface speed over the pad. Normal inlet speeds ought to be 0.75-1.5 m s^{-1}. Excessive speed may cause issues with water drops entering the greenhouse. The pad area ought to be almost 1 m^2 per 20-30 m^2 greenhouse area. The maximum fan-to-pad distance ought to be 30-40 m. The greatest distance of separation pad-pad ought to be 7.5-10 m, and fans ought to not discharge towards the pads of an adjoining greenhouse less than 15 m away (Kittas et al., 2013). In zones where water accessibility is a common concern such as dry and semi-arid regions, the water utilization of evaporative cooling technologies such as the fan pad systems must be taken into thought and minimized as possible. Pad water consumption calculation was addressed by the study of Sabeh, Giacomelli, and Kubota (2006) which explored the water utilization of an evaporative cooling pad system for greenhouses in semi-arid climate. Water utilization was primarily influenced by the air exchange rate. The pan fan system water utilization extended between 0.145 and 0.389 g m^{-2} s^{-1} when the air exchange rates were between 0.017 and 0.079 m^3 m^{-2} s^{-1}. The research highlighted that the fan-pad system consumed 14.8 l m^3 $.d^{-1}$ to preserve air temperature between 18 and 24°C.

Franco, Valera and Pena (2014) examined the water utilization of evaporative cooling cellulose pads for greenhouses. The study showed that the water utilization extended between 1.8 and 2.6 l h^{-1} m^{-2} $^oC^{-1}$ at incoming airflow speeds between 1 and 1.5 m s^{-1}. The system utilized a 2.2 kW centrifugal fan to supply the wind current. The research experiment demonstrated significance of controlling the air exchange rate within the greenhouse according to the necessities and energy consumption reduction.

Controlling the fans using solar PV is an alternative and has been also proposed. Although the capital might be high, this can be profitable in regions with irregular power supply. Davies, Hossain, Lychnos, and Paton (2008) proposed that the fan speed can be balanced based on the sunlight so as full speed is only required amid peak times. The research showed that the energy demand of the 5.5 kW/h in a day fans can be decreased by up to 40% when modulated as compared to constant speed operation. One of the disadvantages of the pan- fan system is the necessity for air tight greenhouse structure to guarantee that the airflow to only pass through the cooling pads on one side and be extricated by the fans on the inverse side. This moreover implies that temperature conveyances will be uneven over the greenhouse, with greatest contrast of up to 11.4 C between the fans and the pads as noted by (Lopez et al., 2012) in their study.

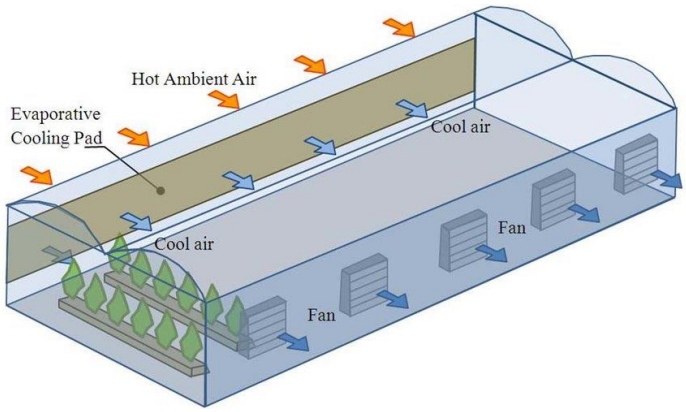

Figure 3. Pan-fan cooling technology (Franco, Valera, and Peña 2014)

Fog and mist system

This technology provides cooling by pressurizing and spraying water through minor nozzles to form micro-fine fog over the crops. The terminal velocity of the water droplets is low and the greenhouse air streams can easily transport water droplets. This will result in high evaporation rate of water whereas keeping the crops dry (Abdel-Ghany & Kozai, 2006). Several studies were carried out to explore mist and fog cooling systems for greenhouses.

Katsoulas, Baille, and Kittas (2001) considered the impact of misting on transpiration and conductance of greenhouse rose canopy. Tests were carried out amid summer with a mist system working when the relative humidity inside the greenhouse was below 75%. The results showed that the fog system contributed up to 20% to add up to evaporative cooling with only 40-50% of the mist water was being effectively utilized in cooling. On the other hand, calculated crop water stress index demonstrated that the crops were less pushed with misting conditions. In a further study, Katsoulas et al. (2006) explored the impact of fog cooling on microclimate and quality of soilless pepper crop in a greenhouse. The greenhouse had two compartments cooled by natural ventilation through roof openings that kept up air temperature below 26 °C and mist cooling with open roof vents to the greatest gap to keep relative humidity below 80%. The results showed that fog cooling can lower the insides air and leaf temperature by up to 3 °C as compared to natural ventilation. Moreover, the air vapor pressure deficit was lower than 2 kPa under fog conditions, indeed during the sultriest period of the day. It was also detailed that the fog system progressed the mean crop weight. However, it diminished impressively the total number of natural products per plant.

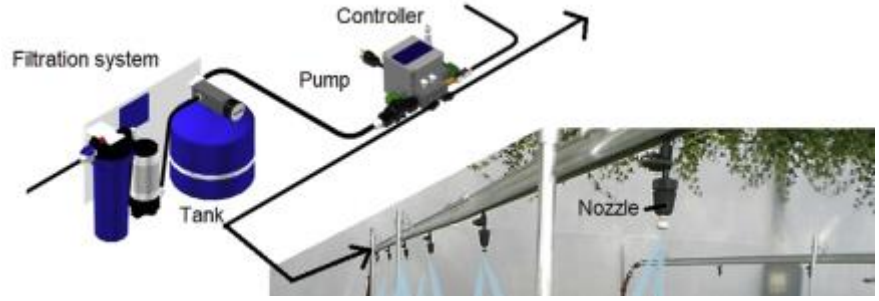

Figure 4. Fog/mist system (Yiming et al. 2007)

Natural Ventilation Augmented Cooling

General greenhouse designs rely on natural ventilation so as to reduce the cost due to the cooling system, unfortunately natural ventilation does not meet often the required microclimate for crops under greenhouse. The Natural Ventilation Augmented Cooling (NVAC) greenhouse is naturally **ventilated** and improved by augmenting the thermal buoyancy with a strategically placed misting system as shown in Figure 5. The greenhouse structure is made of tall sidewalls, oversized side vents, a roof vent, and an additional inside roof (McCartney and Lefsrud 2018). The misting system plays key role in the cooling process and it is placed above the gutter level of the greenhouse and sprays a mist of water between the top roof and the added inside roof. The added roof guides the cooled air towards the main space of the greenhouse and prevents water droplets from reaching the crop. Testing was carried out in Trents, Barbados, where an empty NVAC greenhouse showed a cooling ranging from 1.3 to 3.6 °C relative to outside temperatures, while increasing relative humidity by 5.7-17.7%. This is in contrast to inside temperatures being warmer than outside temperatures in most natural ventilation greenhouses.

The NVAC greenhouse is an affordable design, using far less electricity than a pad and fan system in a comparably sized greenhouse. The NVAC misting system can be used intermittently or continuously to reduce greenhouse temperatures year-round or to extend growing seasons. Site-specific conditions such as natural variations in weather must be considered as they play a role in the performance of the NVAC greenhouse. Accordingly, an automation system can help improve usage.

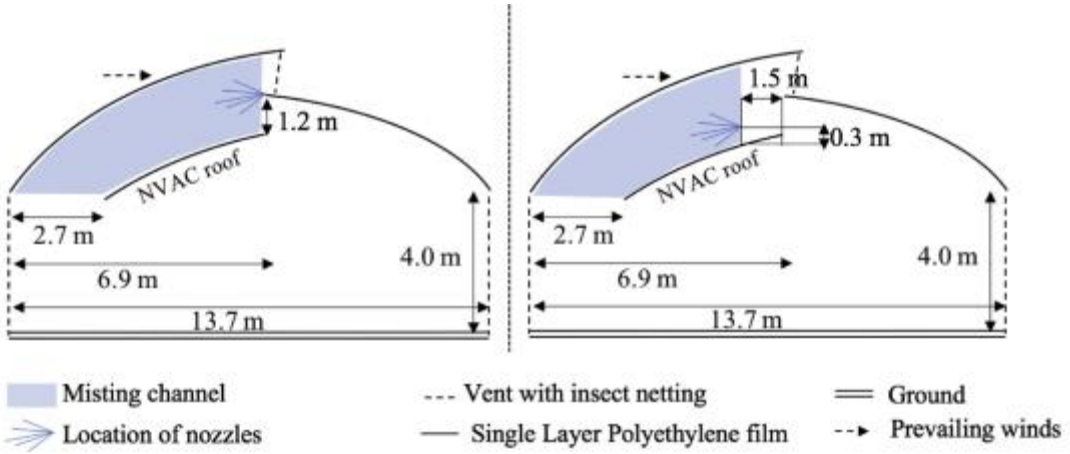

Figure 5. Configurations tested for NVAC (McCartney and Lefsrud 2018)

External surface/roof evaporative cooling

As the greenhouse has its largest roof area exposed to solar radiation, they are also responsible for most of the cooling requirements. Therefore, allowing water to evaporate on the surface can reduce heat flux through the roof. This can be achieved through thin film of water on exterior surfaces, since the surface is heat sensitive to the latent heat of vaporization for water evaporation. Part of the sun's rays falling on the moisture and the surface is reflected and the rest is absorbed for water evaporation. A mathematical model of a greenhouse, with evaporation and cooled by a film of water that moved across the outer shade cloth was developed by Ghosal, Tiwari and Srivastava (2003).

2.6. Hybrid greenhouse cooling systems

One cooling procedure may not be satisfactory to supply the desired crop climate under hot and dry conditions. In order to attain ideal greenhouse cooling in hot climates, cooling methods can be combined. Hybrid systems can decrease energy utilization whereas improving greenhouse cooling performance. Over the recent years, numerous analysts have presented combinations of diverse cooling methods. Ganguly, Misra, and Ghosh (2010) demonstrated an integrated system for greenhouses, comprising of solar PV, polymer electrolyte layer fuel cell stacks and electrolyzer bank. The study revealed that 51 solar photovoltaic modules each of 75 Wp, 3.3 kW electrolyzer and two 480 W fuel cell stacks were able to supply the energy necessity of a floriculture greenhouse with 90 m^2 floor area prepared with fan-pad ventilation system.

Guan, Bennett, and Chime (2015) explored a hybrid air conditioning system to set up the benefits of multi-operating modes of a low-energy coordinate evaporative cooler in different hot climate districts in Australia. The system was an adjusted direct evaporating cooler,

comprising of an open cycle-closed cycle cascade system, counting different modes of operation like natural ventilation cooling, constrained mechanical ventilation cooling, evaporative cooling and mixed heating. A new climate evaluation instrument was set up to evaluate the crossover system's performance. The device can measure and assess the working hours for each working mode under several climate conditions and necessities. The results demonstrated that the potential for coordinate evaporative cooling is critical in Australian climates. The system was installed in a 2304 m^2 glass multi-span greenhouse. The study revealed that the fan-pad system can be an effective option for cooling greenhouses in humid climates under some specific conditions. It was also observed that by combining evaporative cooling pad with shading, the greenhouse can be kept 2-3 ℃ lower than the ambient temperature at 80% relative humidity. The internal thermal screens prevented solar radiation from entering the lower part of the greenhouse during the summer.

Banik and Ganguly (2017) developed a thermal model of a conveyed fan-pad evaporative cooler coupled with sun-based desiccation utilized in a floricultural greenhouse in Indian sub-continent. The study considered the impact of crop transpiration and other parameters such as zone index and characteristic length of crop leaf. The study concluded that coupling desiccants with evaporative cooling provides improved cooling impact. The greatest temperature within the greenhouse was anticipated as 26.6 °C in June, whereas the temperature of the ordinary fan-pad system reached up to 28 °C. The predicted payback period for the system was generally brief (6 years). However, the system was less compelling when the surrounding relative humidity increases. From the surveyed studies, it is highlighted that the combination and concurrent utilization of natural ventilation, evaporative cooling and shading has the potential to diminish greenhouse energy requirement and give ideal indoor conditions for year-round cultivation. A hybrid cooling system must be helped by a compelling control procedure to guarantee that the specified temperature and humidity levels and distributions are kept up within the greenhouse.

2.1.1. Solar powered cooling

Over the past years, various analysts have proposed sun based fueled systems for greenhouse cooling in hot regions in order to diminish energy costs.

Lychnos and Davies (2012) built and tried models of a solar-powered liquid desiccant cooling system for greenhouses in hot climates (Figure 6). The open-air at first flows through the desiccator which is made of permeable fabric and is dehumidified before being cooled by the evaporative cooling pad. The system uses a sun-based regenerator to supply the specified latent heat to evacuate the water from the liquid desiccant and reestablish the dehumidifying capacity. The desiccator moreover incorporates cooling tubes to evacuate the latent heat of condensation of the desiccant. Air is driven through the greenhouse utilizing an exhaust fan. The results were compared with past studies that utilized other liquid desiccants. The execution of the cooled greenhouse was predicted for hot regions including Chittagong, Bangladesh; Messina, Italy; Mumbai, India; Muscat, Oman; Havana, Cuba and Sfax, Tunisia employing a computational model. The results showed that magnesium chloride fluid desiccant system decreased the greenhouse temperature by 5.5 -7.5 °C within the chosen areas, as compared to standard evaporative cooling. Moreover, at periods of year when the fluid desiccant system gives lower temperatures than wanted, it could run in evaporative cooling mode only. The work recommended that further testing ought to be carried out by means of pilot scale trials.

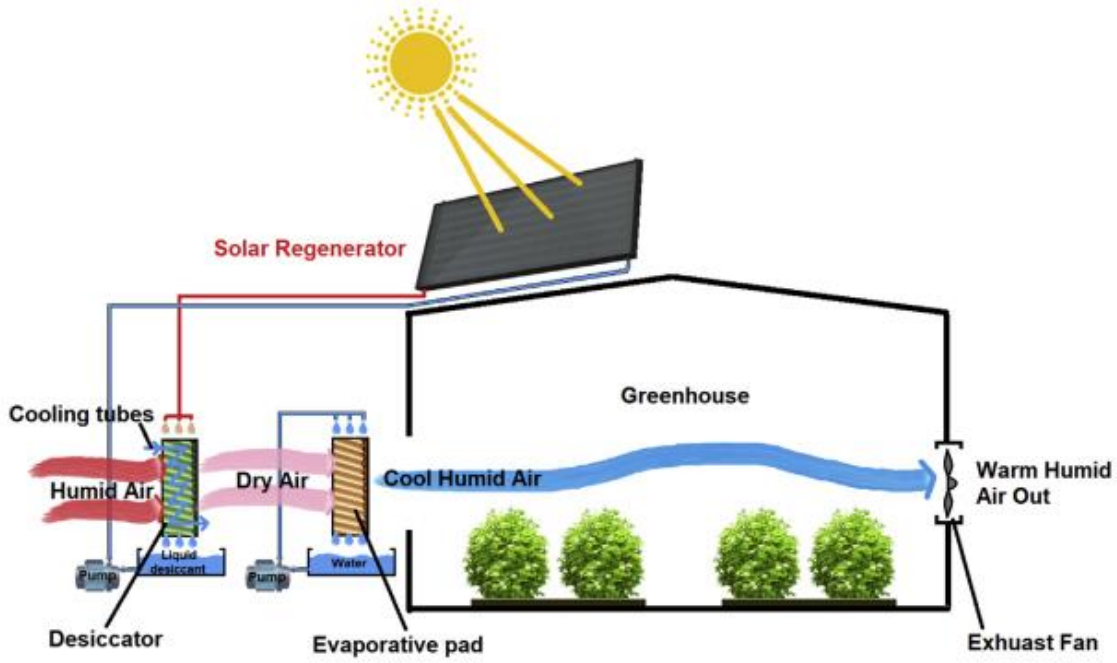

Figure 6. the solar powered liquid desiccant cooling system for greenhouses (Ghoulem, 2019).

Likewise, Ghosh and Ganguly (2017) studied a solar powered evaporative desiccant cooling system for a greenhouse in hot and humid climates, but focusing on a partially closed configuration. The study developed a thermal model which was validated with data from the literature. Work has shown that the cooling system's COP varied between 0.64 and 0.74 during the wettest months of the year while maintaining the indoor temperature conditions required for the target crop (lettuce). Campiotti, Morosinotto, Puglisi, Schettini and Vox (2016) also proposed a solar system for cooling greenhouses but designed a plant with absorption cooling for thermal control. The facility consisted of a Libr-H2O single-acting absorption chiller powered by vacuum tube solar collectors. A simulation model was developed at MATLAB-Simulink to study plant configurations and controls and perform a dynamic simulation of cooling demand and solar field production. The study showed that the proposed system could achieve significant energy savings for greenhouse cooling. However, solar collectors have a low thermal COP (0.70).

2.6.1. Solar technology economic analysis

Hassanien, Li and Lin (2016) reviewed the solar technology used in agricultural greenhouses. Economic research shows that in mild European climates the benefit of solar thermal cooling is lower than in warm climates. Photovoltaic and solar thermal systems are reported to be practical options for greenhouse cooling, especially in desert areas. Lower prices for photovoltaic modules will make photovoltaic greenhouses and solar pumping systems more feasible in the near future, and reduce the payback period.

Yildirim and Bilir (2017) studied a mixed greenhouse cooling system consisting of a geothermal heat pump, which is operated by a grid integrated solar system. In order to obtain even solar radiation in the greenhouse, the photovoltaic panels or 77.8 square meters of solar collector areas were covered only 50 percent on the south side of the roof. Design Builder and Energy Plus software are used to predict heating, cooling and lighting loads that take into account the ideal growing temperature of the plants. Results show that photovoltaic electricity can meet 33 to 67 per cent of greenhouse fuel gas demand in summer, depending on the type of crop with different internal temperatures: tomato (20°C), cucumber (26°C) and lettuce (14°C). The literature on solar cooling in greenhouses shows that the use of solar energy improves overall energy efficiency and reduces energy costs. This technology can be combined with ground-source heat pump systems to optimize greenhouse cooling in warm climates. In wet weather, it can be combined with a desiccant-based cooling system to provide the heat required for desiccant regeneration.

2.6.2. Ground cooling systems/geothermal heat pump

Attar et. al., (2014) used experiments to evaluate the effectiveness of soil thermal energy to cool a chapel greenhouse. Capillary polypropylene heat exchangers suspended in the air and buried in the soil have been used to store or use excess solar energy. A theoretical study was carried out to find the optimal distance between buried heat exchangers. The results showed that the use of heat exchangers with cold water flowing through them reduced the temperature of the air in the greenhouse by 12 °C and made it suitable for the cultivation of pepper. However, the configuration used in this study may cause air stratification.

Ceylan, Ergun, Acar and Aydin (2016) performed a thermodynamic and psychrometric analysis of a soil source evaporation cooling system that is suitable for greenhouses in warm areas. The system includes cooling water circulation, a cooling pad and a soil source cooling pipe. The system was examined by modifying the amount of air blown and absorbed by the site and the amount of water mist. The results showed that the relative humidity of the environment is between 50.2% and 59.3% behind. The efficiency of the system was low compared to mechanical systems and a significant amount of water was required for cooling.

2.7. Optimization and simulation of climatic condition of a greenhouse

Several studies have focused on the use of different methods to analyze and optimize the climatic conditions of greenhouses in high temperature climates. A comparison of various evolutionary algorithms, including evolutionary planning, evolutionary strategies and genetic algorithms, was made to calibrate the parameters of the climate model, which simulates the distribution of air temperature and relative humidity in greenhouses where tomatoes are grown. The results show that evolutionary planning is more efficient and provides precise estimates of

temperature and relative humidity values. Accurate forecasting and assessment of climatic conditions in greenhouses helps farmers control agricultural production and helps designers to optimize climate control systems. Hasni, Taibi, Droui and Boulard (2011) studied the use of simulation-based genetic algorithms (GA) and particle population optimization algorithms to determine the optimal size of greenhouse in Mediterranean climates at controlled temperatures and pressures. The proposed algorithm significantly improved the computation time and accuracy in identifying physical parameters of a horticultural greenhouse model.

2.8. Greenhouse shapes

The alignment of the greenhouse and the shape of the roof play a key role in optimizing solar radiation exposure to maximize heat gain or reduce cooling loads. Gupta and Chandra (2002) examined the effects of different forms, orientations and energy saving strategies such as glazing, fabric insulation and curtains on greenhouse energy consumption. To study a greenhouse in Delhi (India) during the summer, he developed a mathematical model based on heat and moisture balance. The additional insulation of the north wall of an east-west oriented gothic greenhouse can save up to 30% energy.

Mobtaker, Ajabshirchi, Ranjbar and Matloobi (2019) studied the effects of six types of greenhouse ceiling shapes, including uneven, uniform and wide greenhouse shapes, arch types, vineyards and Quonset shapes, on the availability of solar radiation. The results showed that the east-west oriented greenhouse received 8% more sunlight than the other ceiling shapes throughout the year.

Soriano, Hernández, Morales, Escobar and Castilla (2004) pointed out that the results of radiation studies in single-field greenhouses are not suitable for multi-field greenhouses. The results of their study showed that for a multi span greenhouse, relevant differences in radiation transmission was observed in different locations for example higher transmission was observed in the southern located span of the roof. In another study, Soriano et al. (2004) investigated the effect of the roof slope and shape on the transmission of solar radiation in multi-span greenhouses using scaled experiments. The study showed that the increase in roof slope resulted in the significant increase in the transmission of direct solar radiation.

Gupta, Tiwari, Kumar and Gupta (2012) also estimated the total amount of sunlight for different orientations by examining the distribution of solar radiation transmitted by the incident sunlight on the floor and internal walls of a greenhouse in New Delhi, India.

Another study was conducted by El-Maghlany, Teamah and Tanaka (2015), focusing on the shape of the greenhouses, to optimize the transmission of solar energy. they proposed an analytical model that examines the influence of the aspect ratio of the curved surface of the ellipse on the captured solar energy.

Stanciu, Stanciu and Dobrovicescu (2016) estimated the received solar radiation using a clear-sky isotropic analysis model, which was applied to a simplified thermal greenhouse model to simulate diurnal temperature. It was reported that the E-W oriented greenhouse had lower indoor air temperatures and solar heat gains relative to the N-S orientation, resulting in an energy saving of 125 kWh d^{-1}. The optimal choice of orientation and shape of a greenhouse depends on the geographic location, the amount of solar radiation, the number of sections, the size of the plot, the type and quantity of plants and the technology used.

2.9. Greenhouse covering system

The covering material and its properties play a crucial role in optimizing energy consumption, performance and greenhouse economy. The covering material plays a bi-functional role, as it blocks far infrared radiation and allows the solar radiation necessary for plant growth. Many studies have been conducted on covering materials incorporating radiation-preventing techniques used to meet greenhouse cooling challenges in cold and arid regions.

Xiao-wei, Jin-yao, and Xiao-ping (2013) established a model to study microclimate variables in a typical plastic greenhouse in China. A common radiation model was adopted and the effect of shape, configuration of openings and cover material on airflow patterns inside and outside the greenhouse were established. Validation of the model was carried out using experiments and the difference between the temperature values ranged between 0.8 and 1.7 °C.

Feuilloley and Issanchou (1996) studied the thermal properties of cover materials for plastic films and glass greenhouses. Experimental tests showed that condensation caused a temperature increase of 0.2°C - 2.2°C or 0.4% C for plastic film and glass covers. The total heat transfer coefficient was expressed as a linear function of the temperature of the outer surface, the sky and the wind speed. Shen and Yu (2002) suggested that under hot and humid conditions, a combination of fans with near infrared reflector cover materials can effectively reduce heat loads and avoid very humid conditions in greenhouses.

Abdel-Ghani et al. (2012) studied a greenhouse covering system containing a near infrared reflector. The author has demonstrated the feasibility of near infrared reflective plastics as economical and simple coatings in greenhouse environments in dry climates at high temperatures, which can reduce internal temperatures by up to 5 ° C. However, this is not enough in regions where ambient temperatures can exceed 45 ° C in summer, and more work is needed to improve the NIR reflective plastic cover.

Although plastic sheeting can effectively reduce the temperature of greenhouses, they can also be destroyed by sunlight and chemicals used in agriculture. Therefore, it has been proposed to use fluoropolymers in greenhouse plastic membranes to reduce waste and environmental pollution. To obtain the desired growth environment, it is important to choose the appropriate covering material. To do this, the thermal performance of the material must be measured with precision and under conditions similar to those of a greenhouse.

The covering material has been shown to improve the cooling of the greenhouse by reducing the amount of solar radiation allowed to pass through and simultaneously controlling the amount of radiation needed to enter the greenhouse by controlling the growth of the plant. When choosing the appropriate roofing material for a greenhouse, several factors must be taken into account, such as location, temperature and humidity curves required in the greenhouse, as well as plant requirements, durability of the material and the cost. Abdel-Ghany (2016) studied the most common umbrella techniques in summer greenhouses. The cooling effect of the sun on the microclimate of the greenhouse has been studied to determine the best method for masking the sun in dry and hot areas. These studies show that the combination of sun protection methods such as painting or sunscreens with evaporative cooling and / or natural ventilation can reduce the temperature of indoor air by up to 10 ° C increase the relative air humidity by 20% and reduce direct sunlight by 50%. This will reduce water and energy consumption and improve the productivity and quality of plants. Marucci and Cappuccini (2016) proposed a system of

rotating photovoltaic (PV) panels and a high reflector for use in the shade of the greenhouse to combine plant production and electrical energy. In the warm weather of Lazio, Italy, the energy balance in the completely clear sky was checked to determine the energy flow from the factory. The extent of the shadow is determined based on the relationship between the projection length of the photovoltaic panel and the distance from the point of rotation. The results show a 15% reduction in relative humidity in the greenhouse, a change in solar radiation measured in the greenhouse from 100 to 950 W m^{-2} and ambient solar radiation from 700 to 950 W m^{-2}. However, the system uses mechanically actuated panels, which means higher maintenance costs and lower reliability.

Murakami, Fukuoka and Noto (2017) introduced another technology that provides two new NIR cutting nets with high transparency for visible light and is in the NIR range (700-2500) Nm) to improve the sweetness of melon fruits in summer. The net was attached to the tube chamber on the polyolefin membrane. For natural ventilation, the film was rolled up to 1.5 m on the north and south sides of the greenhouse. The near infrared cutting network reduced the greenhouse temperature by 5 ° C on a sunny summer day and increased the sugar concentration of ripe fruit. Santolini et al. (2018) using computational fluid dynamics (CFD), studied the effects of the black net on the distribution of air flow in the Bologna greenhouse in Italy. The two interior walls were parallel to the exterior wall, while the third interior is mounted horizontally between the roof. In addition, black shutters were installed on the roof. Studies have shown that the use of umbrellas can distribute air more evenly in greenhouses than in the absence of umbrellas, especially near growing areas

2.10. Numerical modelling for greenhouse ventilation and cooling technologies

Computational modeling of fluid dynamics (CFD) has been used to improve the design of greenhouses, optimize cropping systems, control the climate and design technologies for cooling and heating greenhouses (Boulard, 2011). CFD is useful for studying complex fluid flows. For example, it is useful for simulating complex multiphase flows in evaporative spray systems in greenhouses (Chen, Cai, Xu, Hu and Ai, 2014). The CFD provides a detailed analysis of the data on the relevant parameters, for instance speed, temperature, humidity, CO2, etc. This is important for analyzing the distribution of indoor climatic parameters and should be optimized for crop production. On the other hand, CFD modeling makes it easy to assess different greenhouse design configurations (Santolini et al., 2018). The CFD model has been actively used in practice to predict air flow and thermal models in natural and mechanical ventilation greenhouses (Flores-Velazquez, Montero, Baeza & Lopez, 2014); Piscia, Munoz, Panad and Montero, 2015).

Tamimi and Kacira (2013) also focus on increasing the uniformity of humidity in the greenhouse using a high-pressure mist cooling system. Likewise, discrete species and phase models are used to simulate the evaporation of droplets and the vapor of evaporation. Validation shows that the expected temperature value is between 6 and 16% of the experimental data, while the relative humidity value is between 14 and 27%. The study highlights the possibility for the model to optimize the internal conditions by modifying the position and the angle of the nozzle.

Key findings	Research gap identification	Justifications
In the literature review part of this research, it has been shown that the major greenhouse energy consumption inducing high cost of the entire greenhouse installation in hot and arid climate regions is mainly due to the indispensable greenhouse indoor air temperature reduction and cooling need so as to maintain and control the greenhouse microclimate in the range of the crop requirements. It has been demonstrated through previous researches and studies reviewed that for designing and constructing an affordable energy efficient greenhouse, different parameters have to be taken carefully into consideration notably, the geographic location with the local weather conditions like solar irradiation energy, wind speed, temperature, relative humidity, rainfall, seasonality and climate change effect. The greenhouse intrinsic parameters such as cooling technology, greenhouse structure including roof shape and covering system have to be carefully taken into consideration. Researches have highlighted different greenhouse cooling technologies with their effectiveness as well as their cost in terms of energy consumption. Natural ventilation, evaporative cooling technologies, ground cooling systems/geothermal heat pump and solar powered cooling system have been reviewed in this chapter. In terms of affordability and energy consumption, evaporative cooling such Fan-Pad cooling technology and Natural Ventilation augmented cooling (NVAC) have been showed to be widely used and affordable. In some specific area and weather conditions, the NVAC technology has been demonstrated to have an affordable design, using far less electricity than a Fan-Pad system in a comparably sized greenhouse.	• Studies on greenhouse design, variations of microclimate in different shapes and understanding of the physical processes that drive natural ventilation have not reached the stage where the rates of air exchange can be predicted. Such information is required for the implementation of optimal environmental control strategies for regulation of summer or hot climate. • The NVAC greenhouse is an affordable design, using far less electricity than a fan-pad system in a comparably sized greenhouse. The test carried out in Trents, Barbados by McCartney and Lefsrud, in an empty NVAC greenhouse showed a cooling ranging from 1.3 to 3.6 °C relative to outside temperatures, while increasing relative humidity by 5.7-29%. This shows a deep ineffectiveness in regions having high relative humidity and/or with low wind speed. In addition, research should be conducted to highlight or to overcome the prospective impact of the added inside roof specific design structure of NVAC on light transmittance inside the greenhouse especially in regions with average or little solar irradiation resource. Less penetration can lead to high energy consumption for powering lighting system. • Research is required to establish how buoyancy and wind driven ventilation is influenced by ventilator configuration, greenhouse size and geometry. While there is considerable progress in the evaluation of new cladding materials to reduce the heat load, but understanding and predicting the light distribution pattern in the greenhouse have not moved far. Moreover, the information applicable to tropical and subtropical climate is scarce. • Although, the proven energy efficient cooling rate of the fan-pad system has shown its affordability, one of the limitations of this technology is the necessity for air tight greenhouse structure to guarantee that the airflow only passes through the cooling pads on one side and be extricated by the fans on the inverse side. This moreover implies that temperature	Kinshasa (case study) has a specific and complex climate. According to the Köppen-Geiger climate classification, Kinshasa has a tropical savanna climate (tropical wet and dry climate) with a dry winter -Aw. The temperature variation within a year ranges between 20-31°C. Kinshasa has a very high average relative humidity 82.5%, expanded in 11 months of a year. The rainfall is abundant in 10 months of a year with an average wind speed 3 m/s influenced by its topography with a high wind direction variation within a year. The average solar radiation is of 4.62 $KWh.m^{-2}d^{-1}$. The Objective pursued in this Master thesis research is of designing and building an innovative and sustainable greenhouse with an energy efficient cooling system suitable to the tropical savanna climate region of Kinshasa (Plateau de Bateke)/ DR Congo. We will emphasize more on the energy efficiency, affordability and the use of locally available materials. The entire greenhouse system will be powered by a hybrid HAWT- solar photovoltaic energy system. To overcome the limitations showed by Fan-Pad and NVAC, a hybrid energy efficient cooling system will be studied for local weather conditions of Kinshasa/Plateau de Bateke. That hybrid cooling system will be made of natural ventilation, exhausted fans, misting system and shading system. The misting system will be intermittently intervened when it is needed.

Theorical and experimental studies have been conducted on different covering materials to test their effectiveness in terms of energy saving and greenhouse protection under specific solar radiation conditions. Many covering materials have proved their effectiveness in cold as well as in arid areas notably PE covering material and some others were proposed to be studied. Photovoltaic and solar thermal systems were reported to be practical options for greenhouse cooling powering system, especially in desert areas. Lower prices for photovoltaic modules are making photovoltaic greenhouses more feasible nowadays and in the near future, and reduce significantly the payback period.	conveyances will be uneven over the greenhouse, with greatest contrast of up to 11.4 C between the fans and the pads as it was observed by (Lopez et al., 2012) in their study. And fan-pad has been found to be ineffective in regions with high relative humidity for a long period over a year. • The greenhouse covering materials play a bi-functional role by blocking far infrared radiation, allowing solar radiation and at the same time contributing in energy saving required for cooling system. Research should be conducted on covering materials to be used in tropical climate conditions as the thermo physical requirement is different than in cold and hot regions.	The new proposed greenhouse structure with its hybrid cooling system will be properly designed and simulated with different software notably Ansys-fluent, so to analyze the greenhouse indoor air circulation, wind speed, the indoor air temperature and relative humidity distribution. And a good design will help to overcome the high temperature and relative humidity of Kinshasa weather condition. Always concerned with promoting the energy efficiency, affordability and the use of locally available materials in a smart greenhouse, a new plastic covering system will be tested. That covering plastic will be made of simple Polyethylene or the polyethylene terephthalate $(C_{10}H_8O_4)_n$. The valorization of this plastic might present many prospective benefits such as its availability as well as its affordability in Kinshasa.

Table 2. Key findings, research gap identification and justifications

CHAPTER 3. METHODS

This research is aimed at devising an affordable and energy efficient greenhouse for savannah tropical climate region of Kinshasa /Plateau de Bateke. To achieve the goal of this research, a design was made and prototype built for performance analysis in field environment. In general, the method of conducting this research and building the prototype were based on methodology detailed below.

3.1. DESCRIPTION OF CASE STUDY AREA

The Democratic Republic of Congo (DRC) was the case study area for this research, country in which the prototype has been built and tested. In DRC, the research was conducted in and DAIPN/Kinshasa (technical research center of greenhouse farming and modern agriculture) and Tamano food centers. In DRC there is a wide variety of climates and landscapes. Generally, the whole country moves under the average annual temperature, generally high. DRC has a hot and humid climate season on the greatest extent of its territory and an abundant rainfall, which is found in equatorial and tropical humid zones. DRC includes three main climates: the equatorial climate, the savannah tropical climate and the mountain climate.

The capital city, Kinshasa, is located in the western part of the country. The city of Kinshasa covers an area of 9,965 Km^2 with an average altitude of about 300 meters. Located between latitudes 4° and 5° and between longitudes 15° and 16°32, the city of Kinshasa is limited:

- In the East, by the provinces of Mai-Ndombe, Kwilu and Kwango;
- In the West and North, by the Congo river thus forming the natural border with the Republic of Congo Brazzaville;
- In the South, by the province of Central Kongo.

Figure 7. Location of Kinshasa in DRC map, (source Ministère de plan)

It is the largest and megacity of the Democratic Republic of the Congo with an estimated population of more than 13 million. Kinshasa has a tropical savannah climate with dry winter.

The annual average temperature is 25.3 ° C and the annual precipitation is 1,400 mm. The driest months are July and August with only 3 mm of precipitation and, March and April the wettest with 196 mm of precipitation.

To feed this number of populations concentrated in Kinshasa requires a modern agriculture. One of the ways promoted by the Government of Democratic Republic of Congo is the greenhouse (for vegetables and fruits) used in DAIPN center as well as in many other organizations dealing with greenhouse and aquaponic systems. Still, the use of greenhouse technology faces a lot of challenges including technical and economic challenges. Although greenhouse presents many benefits, local famers do not use this technology because of many challenges associated to its technical and economical aspect.

3.2. DATA COLLECTION AND DATA ANALYSIS

3.2.1. Data collection

The data collection was conducted in **INERA**/Kisangani center (**I**nstitut **N**ational d'**E**tudes et de **R**echerches **A**gronomiques) and some of data were collected in Kinshasa, DAIPN center, TAMANO and on the research site based in Menkao (79 Km from the Kinshasa town).

The National Institute of Agronomic Studies and Research (INERA) is the main agricultural research agency in DR Congo; it works under the Ministry of Higher Education and Scientific Research and it is responsible for research on agricultural crops, livestock, forestry and fisheries.

Data collected from INERA originated from **METTELSAT** (**A**gence **N**ationale de **M**étéorologie et de **T**élédétection par **S**atellite). The National Agency for Meteorology and Remote Sensing by Satellite (**METTELSAT**) was created by Decree No. 12/040 of October 2, 2012 with the missions of observation, meteorological and climatological monitoring as well as the study and evaluation of natural resources so to empower the effective planning and management of natural resources for a sustainable development of the country.

The headquarters of METTELSAT is in Kinshasa, Chaussé Mzée L.D Kabila, Binza-Météo/Kinshasa-Ngaliema, B.P4715 Kinshasa II N° Impot A/1007464A, website www.meteordc.org/. The data acquisition was conducted from 1975 to 2005. The data package was provided in excel format. For a deep analysis and understanding, we have processed them and expressed the results in different tables and graphics (see Data analysis).

The data collection mainly included:

- ✓ The effect of climate change (season unpredictability) on food production in DR Congo/ Kinshasa Plateau de Bateke;
- ✓ Relative humidity data of Kinshasa;
- ✓ The rainfall data of Kinshasa;
- ✓ Temperature data of Kinshasa;
- ✓ Solar irradiation resources in Kinshasa;
- ✓ Wind speed in Kinshasa and particularly in Plateau de Bateke -Menkao;
- ✓ The evaluation of the level of greenhouse management in DAIPN center and TAMANO firm in Kinshasa/Plateau de Bateke and to evaluate the technics and

cost of energy consumption of the greenhouse system in tropical climate of Kinshasa/Plateau de Bateke;

3.2.2. Data analysis and interpretations

a. Effect of climate change on food production in DRC

The DRC has more of 80 million hectares of arable land and 4 million hectares of irrigable land. Its well-diversified climate, materialized by the existence of several agro-ecological zones and its important hydrographic network allow a varied range of agricultural speculations, spread out throughout the year.

The Congolese agricultural sector employs more than 60% of its working population. It is therefore the only sector that offers real and sustained economic growth possibilities, capable of providing real added value and real wealth, especially since relatively few resources are needed to restart the agricultural sector and make it contribute significantly to real national economic growth

Despite these advantages, it should be noted that only 10% of arable land and 3% of irrigable land are currently exploited (INERA and PNUD, 2012). This means the bulk of Congolese agriculture is provided by small farmers, occupants of small areas, practicing traditional agriculture essentially dependent on the climate (the rhythm of the rains) and therefore quite vulnerable to climate changes. Climate is the key factor to agricultural production. Below is the illustration of most common climate risks in DRC:

RISK	IMPACT	LOSS OF HUMAN LIFE	DURATION (DAYS)	EXTENDED (Km^2)	FREQUENCY (%)	TREND
RAIN INTENSE	5	2	3	4	3	↑
SEASONAL DROUGHT	2	1	2	4	3	↑
FLOODS WATERFRONT	3	2	2	2	2	↑
CANICULAR CRISIS	3	2	2	4	3	↑
COASTAL EROSION	5	1	2	2	2	↑

Table 3. Most common climate risks in the DRC (PNUD)

Impacts: 1 = $1 per capita, 2 = S 10, 3 = S 100, 4 = $ 1000, 5 = $ 10.000
Loss of human life: 1 = 1 person per event, 2 = 10 persons,
3 = 100 persons, 4 = 4.000 persons.
Duration: 1 = 1 day, 2 = 2 days, 3 = 100 days (a season), 4 = 1.000 days (over one year)
Spatial extended: 2 = 10Km^2, 3 = 100 Km^2, 4 = 1.000 Km^2
Frequency: 1 = 1% probability (some years), 2 = 10 % probability,
3 = 100 % probability (annual)

Trend indicators :

- average increase: ↑
- significant increase: ↑

According to INERA and PNUD (Programme des Nations Unies pour le Développement) reports (2012), the evidence of climate change is materialized by increasingly persistent hot weather, increasingly torrential rains and limited in terms of number of days, and other effects are visible across the country.

On the socio-economic side, despite the diverse potential in natural and other resources, the GDP per capita remains slightly below US $ 1 per day.

The informal and rural-agricultural sector (dominated by small farmers 60% of active population) are constantly weakened by the country's current slow progress (access to education, health care, energy access, costs of means of transport and accessibility to shopping centers, etc.), to which are added the effects of climate change.

The insufficiency of reliable statistical data and the difficult accessibility to existing ones, make the design and application of adaptation policies and / or strategies rather difficult, or at least hazardous.

Therefore, it is established that the level of vulnerability to climate change is fundamentally proportional to the level of poverty of a given population, the integration and promotion of activities aimed first at achieving food security and then integrated human development, are prerequisites for real adaptation measures to climate change. And, agriculture (more than other sectors of the national economy) has a very high potential to serve as a safe adaptive intervention against the known and predicted harmful effects of climate change.

b. Solar irradiation in Kinshasa

The length of the day in Kinshasa does not vary substantially along the year. In almost each year, the shortest day is around June 20, with 11 hours, 52 minutes of daylight; the longest day is around December 21, with 12 hours, 23 minutes of daylight. The average solar irradiation is 4.62 $KWh/m^2/day$.

Average daylight / Average sunshine Kinshasa, Democratic Republic of Congo

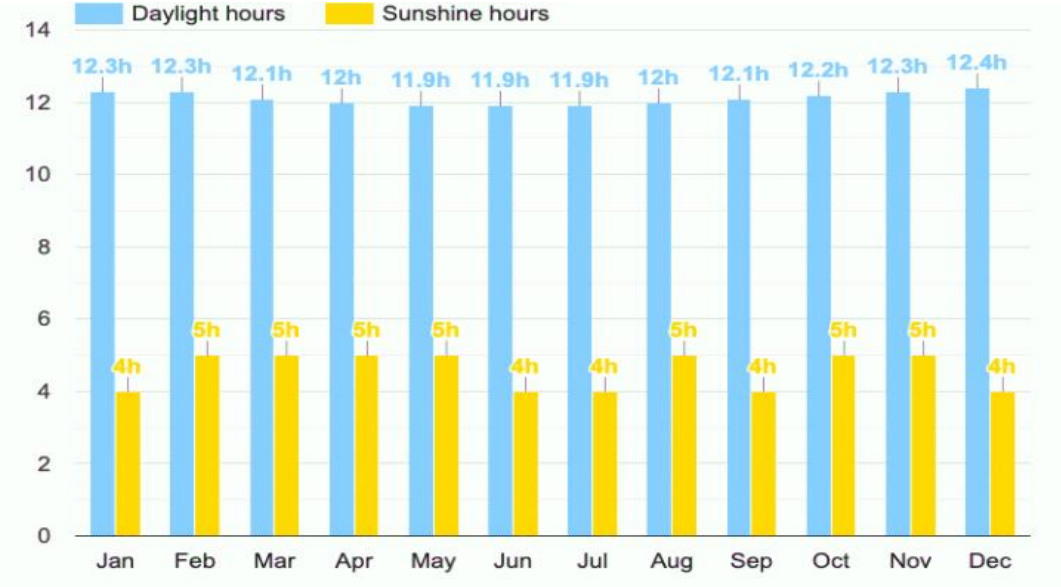

Figure 8. Average Daylight hours /Sunshine hours -Kinshasa /Democratic Republic of Congo

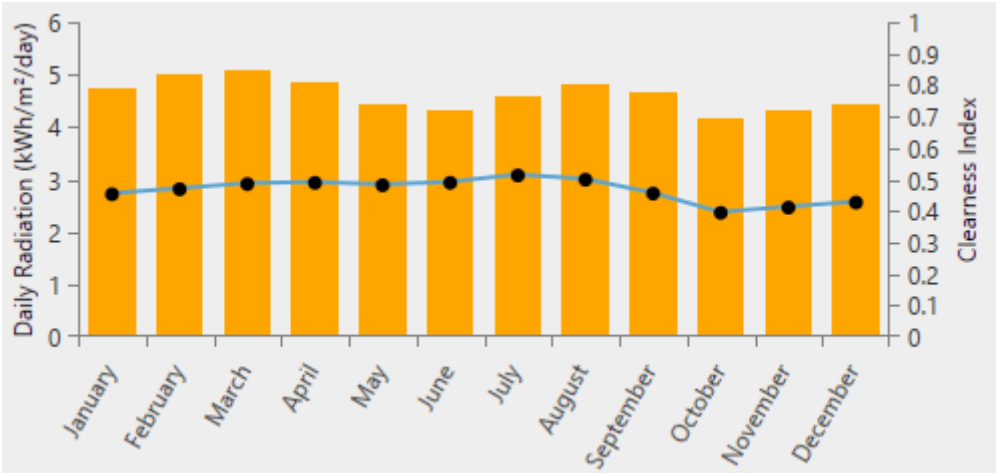

Figure 9. Monthly average solar global horizontal irradiation

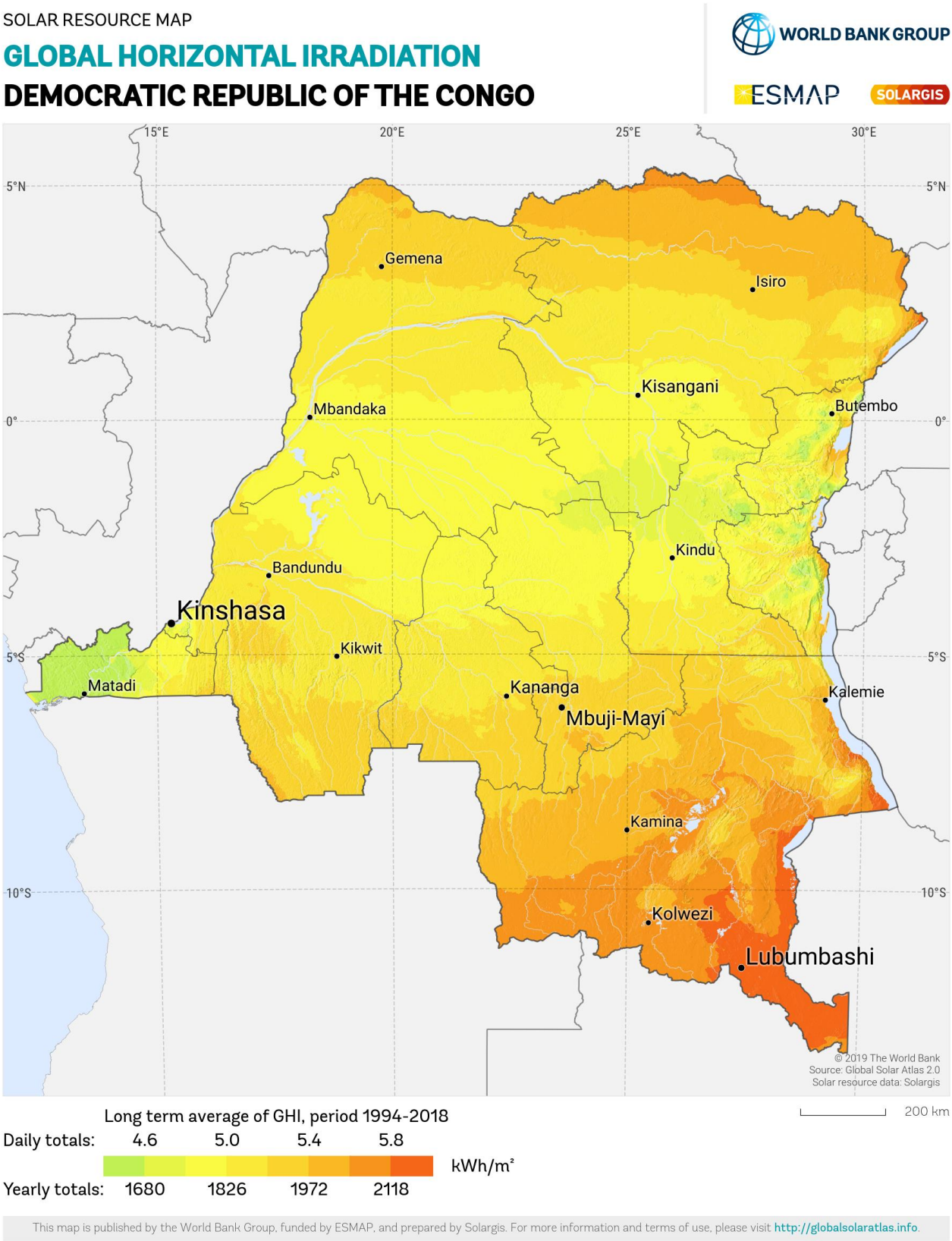

Figure 10. Global Horizontal Irradiation (World Bank)

The average solar irradiation received in a day (for five hours) is 4.62 KWh/m^2/day. The average solar radiation clearly indicates that the solar energy resource in Kinshasa is exploitable.

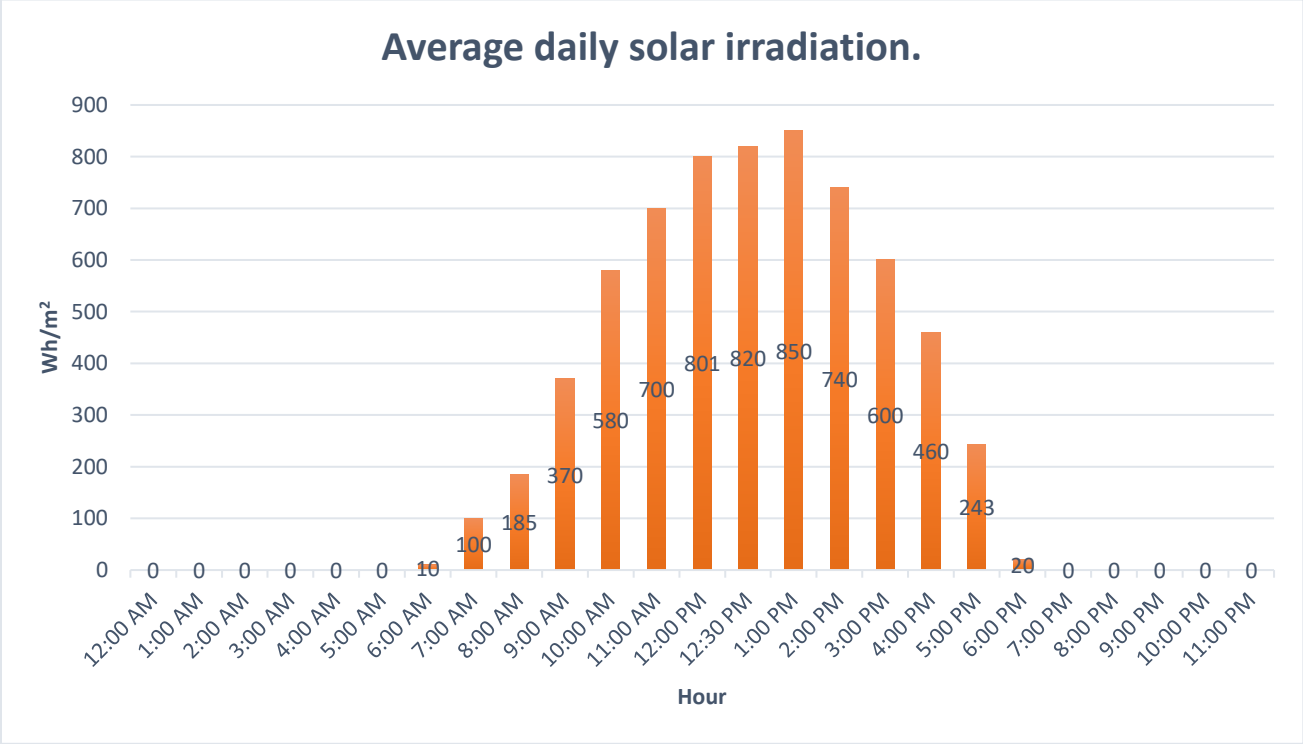

Figure 11. Daily distribution of solar irradiation in Kinshasa

c. Temperature in Kinshasa

The hot season lasts for 3.3 months, from February 3 to May 12, with an average daily high temperature above 30°C. The hottest day has an average high temperature of 32°C and the lowest day has an average low temperature of 22°C.

The cool season lasts for 1.8 months, from June 16 to August 8, with an average daily high temperature below 28°C. The coldest day of the year is around July 17, with an average low of 18°C and high of 27°C.

Max and min temperature in Kinshasa, Democratic Republic of Congo

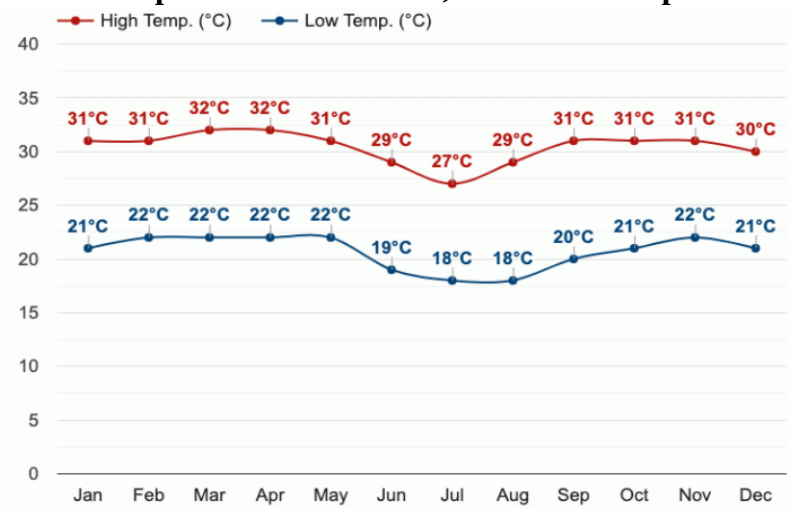

Figure 12. Max and min temperature in Kinshasa, Democratic Republic of Congo

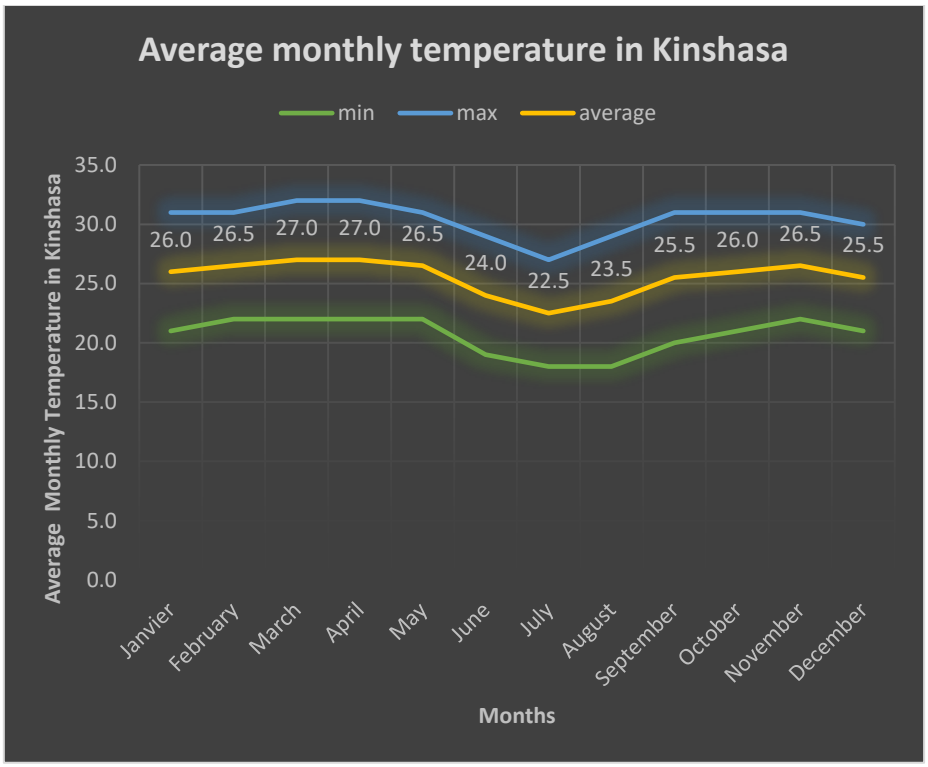

Figure 13. Average monthly temperature in Kinshasa (in orange color)

d. Precipitation

In Kinshasa, during the entire year, the wetter season lasts 7.9 months, from September 25 to May 22, with a greater than 44% chance of a given day being a wet day. And the chance of a wet day peaks at 87% around November 11. The drier season lasts 4.1 months, from May 22 to September 25.

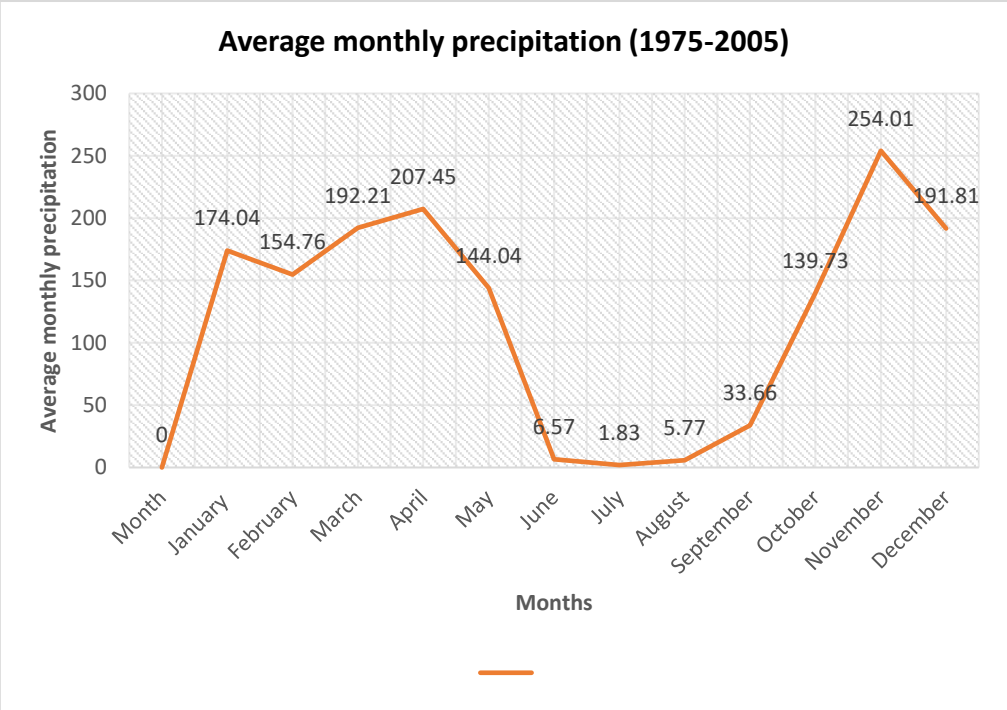

Figure 14. Average monthly precipitation (1975-2005)

e. The Relative Humidity in Kinshasa

Kinshasa experiences an extreme seasonal variation in terms of humidity. The muggier period of the year lasts for 10.6 months, from early September to the end of July. The muggiest months of the year are early May, the end of December and early January, with muggy conditions which can reach 98%.

The least muggy months of the year are, August and early September with muggy conditions 76% of the time.

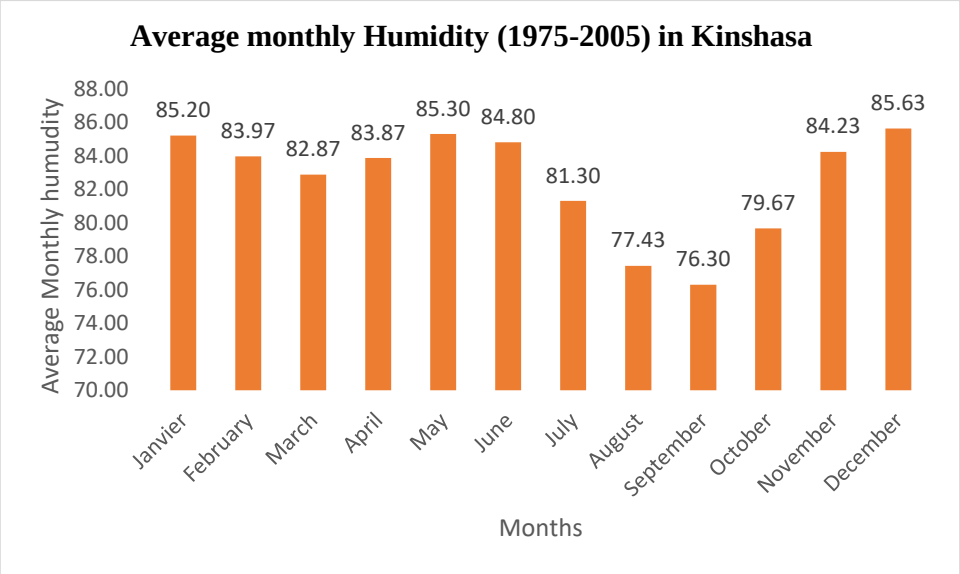

Figure 15. Average Monthly humidity 1975-2005

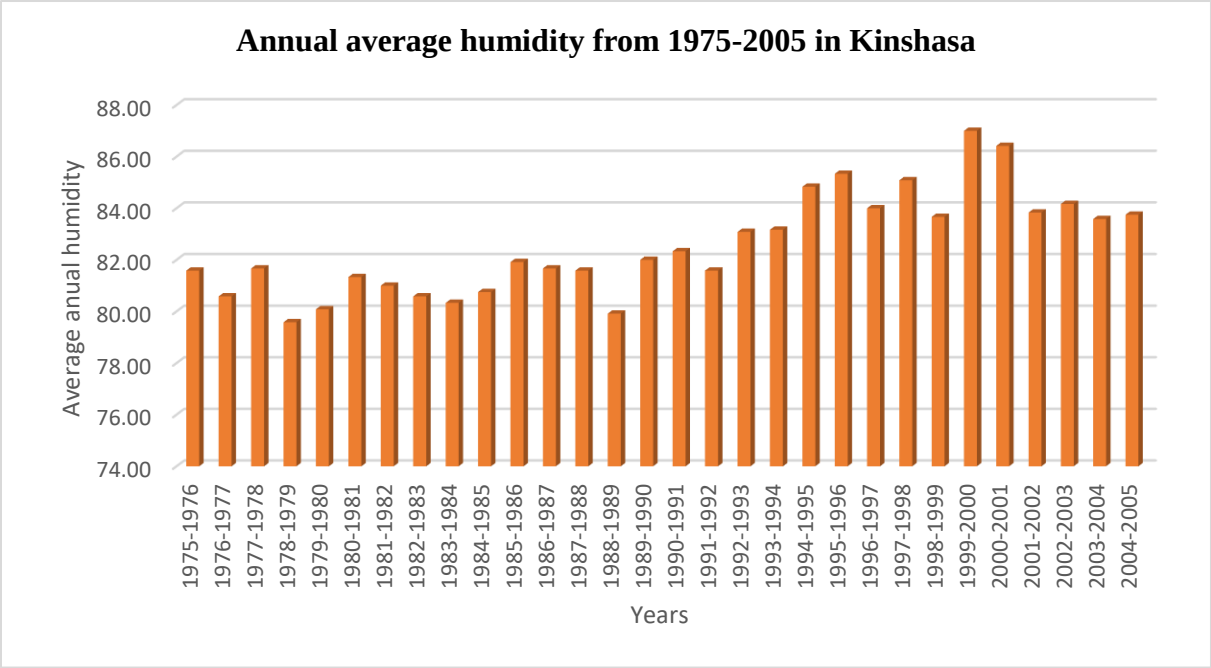

Figure 16. Annual average humidity in Kinshasa.

f. Wind speed and direction in Kinshasa weather conditions

The wind experienced at any given location is highly dependent on local topography and other factors, and instantaneous wind speed and direction vary more widely than hourly averages.

The average hourly wind speed in Kinshasa experiences mild seasonal variation over the year.

The windier part of the year lasts for 3.1 months, from June 22 to September 26, with average wind speeds of more than 4.8 miles per hour. The windiest day of the year is August 12, with an average hourly wind speed of 6.1 miles per hour.

The calmer time of year lasts for 8.9 months, from October to June. The calmest months of the year are the end of November, December and January.

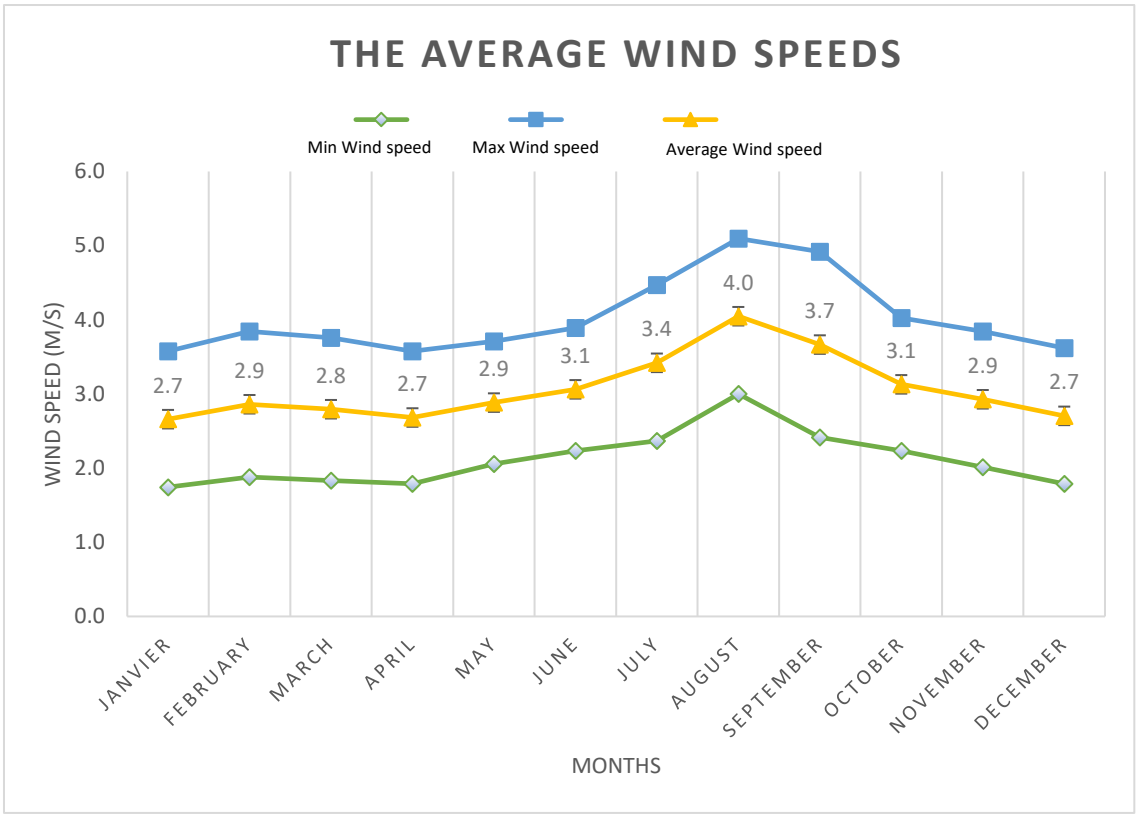

Figure 17.The average of mean hourly wind speeds (orange line)

Our site in Kinshasa/Plateau de Bateké has a particular topography, favorable to harness wind resources. The topography by large plateau (a largely level expanse of land at a high elevation) with a significant altitude compared to the rest part of Kinshasa province. The average wind speed is 3.0 m/s.

At the end of our internship in DAIPN center (located in Kinshasa/Plateau de Bateké), we conducted a brief acquisition campaign for three days from August 07, 2020 to August 13, 2020. Wind speed data were measured using an anemometer (type Neoteck Anemometer, version NTK060-EN P1-3) coupled to a NTC thermometer.

The NTK060-EN P1-3 instrument specification:

Air velocity measurement specification				
Unit	**Range**	**Resolution**	**Threshold**	**Accuracy**
m/s	0-30	0.1	0.1	±5%
Ft/min	0-5860	19	39	
Knots	0-55	0.2	0.1	
Km/h	0-90	0.3	0.3	
Mph	0-65	0.2	0.2	

Table 4. Air velocity measurement specification

Temperature measurement specifications			
Unit	**Range**	**Resolution**	**Accuracy**
°C	-10 to 45	0.2	±2%
°F	14 to 113	0.36	±3.6%

Table 5. Temperature measurement specifications

Data collected with Neoteck Anemometer **NTK060-EN P1-3** (wind speed and temperature)

Date	Time	Wind speed (m/s)	Temperature (°C)
August 7, 2020	9. 31 am	4.1	22.3
	10.47 am	5.1	22.9
	12.03 pm	5.3	24
	2 pm	4.6	23
August 10, 2020	8. 51 am	3.8	21
	11 am	6.1	22.3
	1.22 pm	5.4	24
	2.46 pm	5.8	26
August 13, 2020	9.04 am	3	24
	10.05 am	3.5	25.4
	2.26 pm	4.1	23.6

Table 6. Data collected with Neoteck Anemometer NTK060-EN P1-3

Wind direction

The predominant average hourly wind direction in Kinshasa varies throughout the year.

The wind is most often from the east for 1.0 months, from April to May, with a peak percentage of 36%. The wind is most often from May to June, with a peak percentage of 41% on June. The wind is most often from the west for 10 months, from June to April, with a peak percentage of 84% on August.

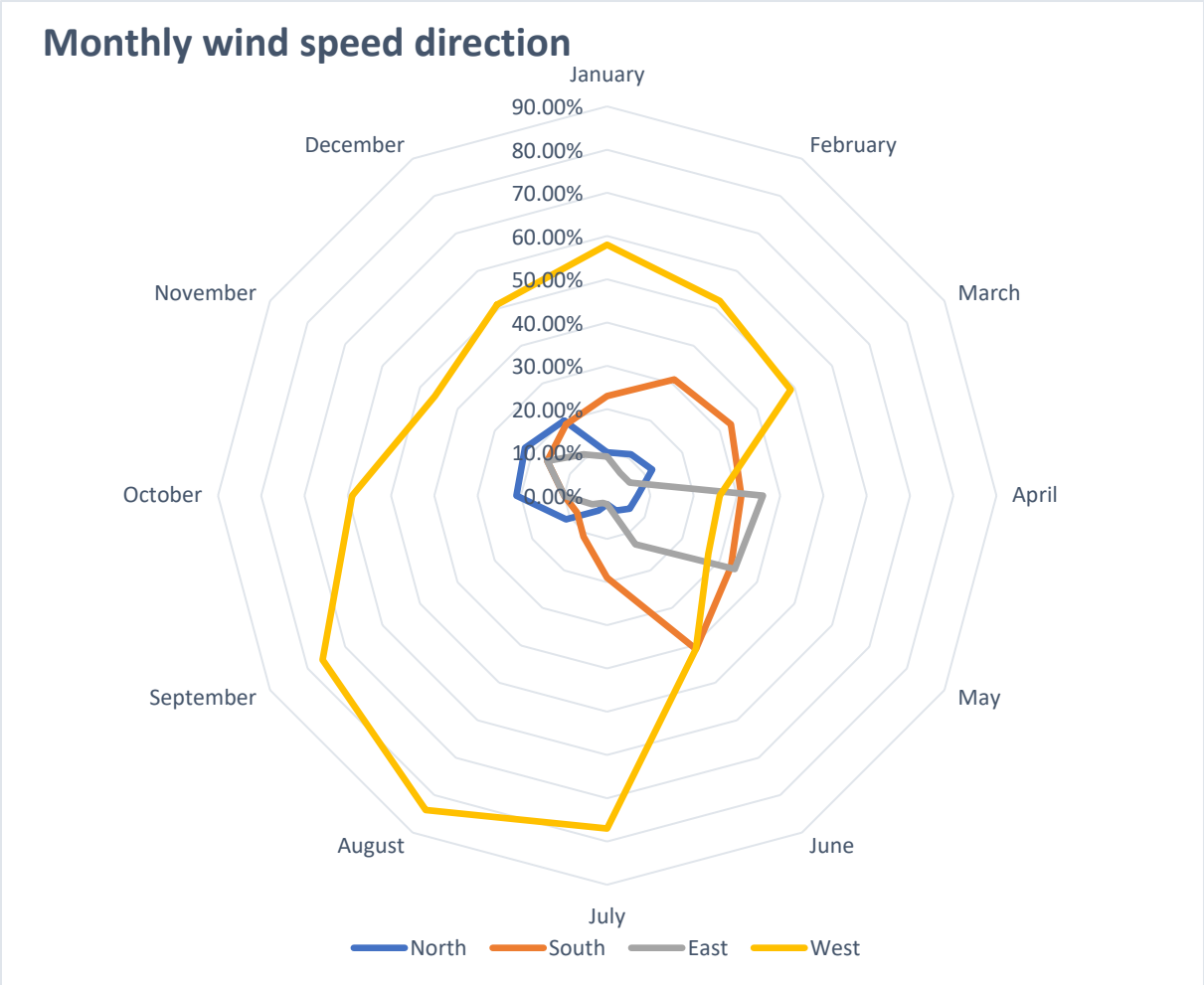

Figure 18. Wind direction in Kinshasa

The percentage of hours in which the mean wind direction is from each of the four cardinal wind directions per month, excluding hours in which the mean wind speed is less than 0.447m/s.

3.2.3. Summary of data analysis

The summary of data analysis is presented in the below table for further understanding of local weather conditions in Kinshasa.

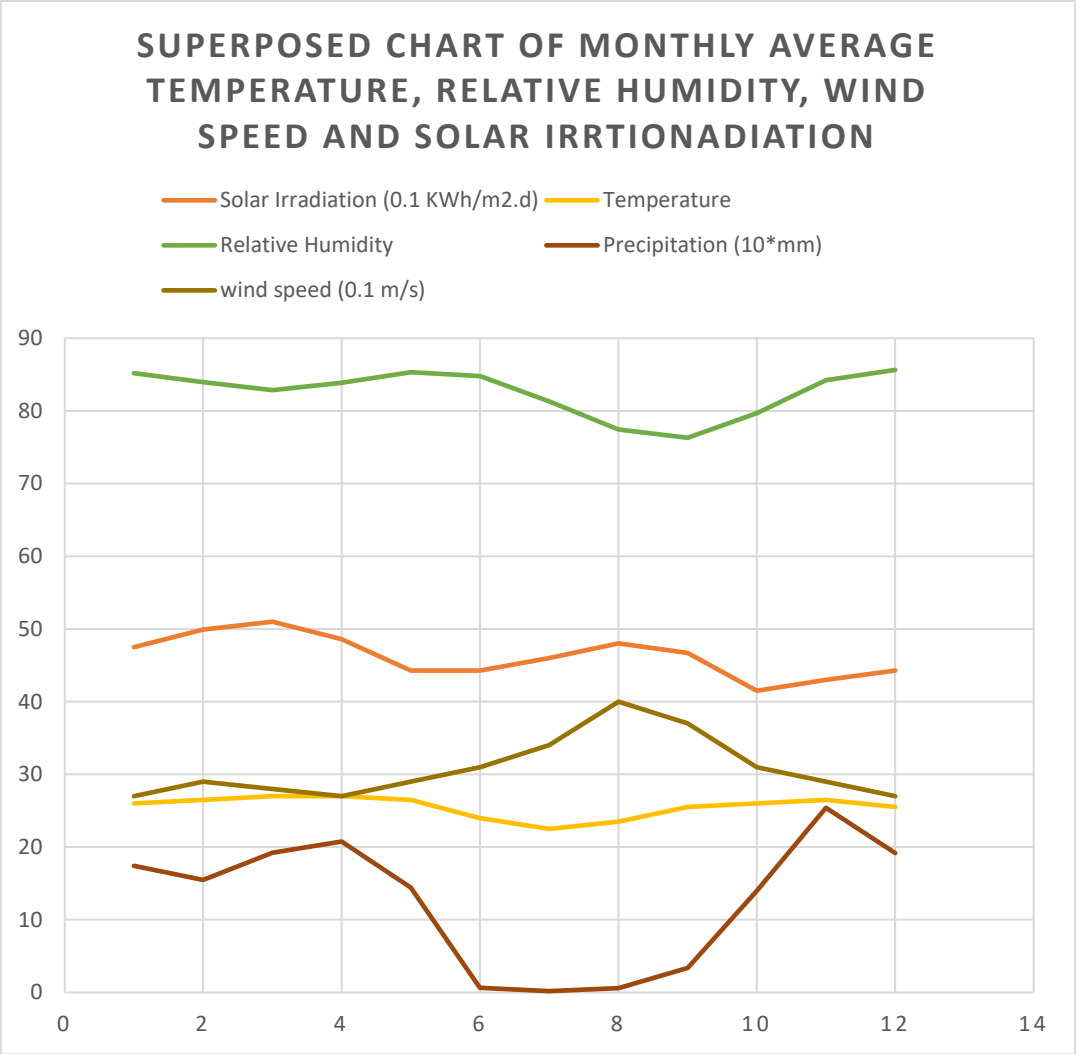

Figure 19. Superposed chart of Temperature, Relative Humidity, Wind speed and irradiation

3.2.4. The level of greenhouse management in Kinshasa

Greenhouse technology is not widespread in Kinshasa, because of the economic aspect behind and lack of electrical grid in agronomical zones of Kinshasa as well as the unawareness. Among vegetable and fruit farming companies found in DR Congo and particularly in Kinshasa, only few of them use greenhouse, notably DAIPN and TAMANO

3.3. GREENHOUSE ENVIRONMENTAL DESCRIPTION

The greenhouse is generally represented as a one-dimensional system made up of four distinct environments: the wall separating the inside from the outside, the indoor air, the plants and the soil. It is considered that each of them is homogeneous, with the exception of the soil, because of the heterogeneity of its composition and its humidity. These environments are the seat of thermal and evapocondensative exchanges. A distinction is made between short wavelength radiative exchanges, both direct and diffuse, which are transmitted, reflected or absorbed by the considered area. We can also distinguish the long wavelength radiative exchanges between these areas, the sky and the outside; the conductive and convective exchanges and finally the mass and evapocondensative exchanges which are strongly linked to plant transpiration. However, these different modes of exchange do not have the same importance depending on the degree of precision required and the objective of the simulation implemented.

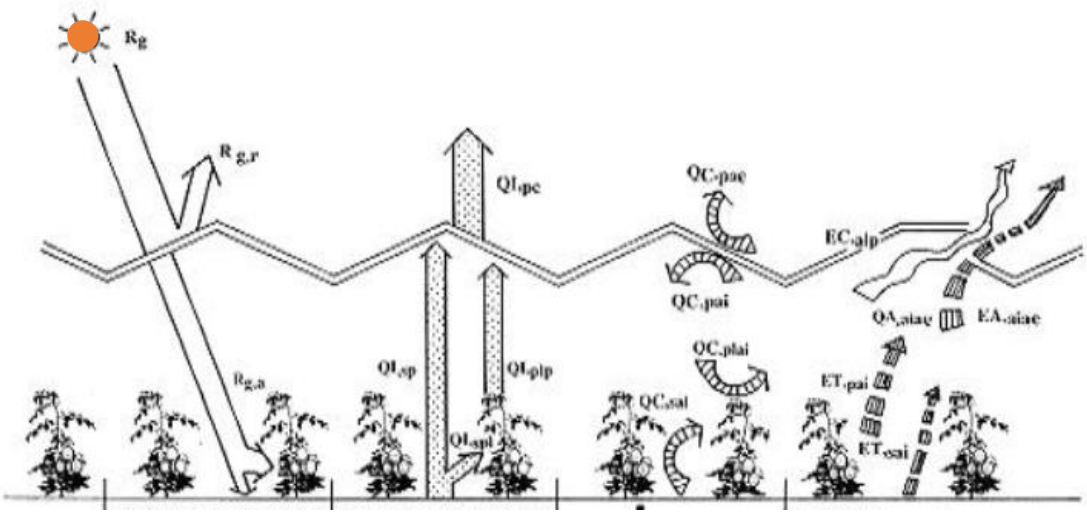

Figure 20. Thermal interactions

3.3.1. Greenhouse design

The proposed greenhouse is aimed at solving challenges faced by both large scale and small-scale farmers in Africa and particularly in Kinshasa/ Democratic Republic of Congo. The greenhouse proposed in this Master thesis offers an innovative cooling technology adequate to savannah tropical climate. The proposed cooling technology is an evaporative cooling system harnessing mainly natural ventilation associated to dehumidification equipment (6 exhaust fans), humidification equipment (misting system with 16 nozzles along 32m) and shading system used in intermittent way.

This proposed cooling technology optimizes the natural ventilation. For implementing all these, a specific structure design of greenhouse is done with a "modified shed roof" opened in the major direction of wind; the misting system is strategically placed on the top of the small roof longitudinal to the length of greenhouse structure using a well sized solar pump. Along the lateral sidewall 6 exhaust fans are placed. The entire greenhouse is powered by a standalone solar PV-Small Wind Turbine hybrid energy system.

An IoT based testing was used to test the cooling system performance including, exhaust fans, misting system and shading system. In this proposed greenhouse, a strong emphasis has been put on affordability, availability of material (equipment) in DR Congo, ease of access to technology, and energy efficiency.

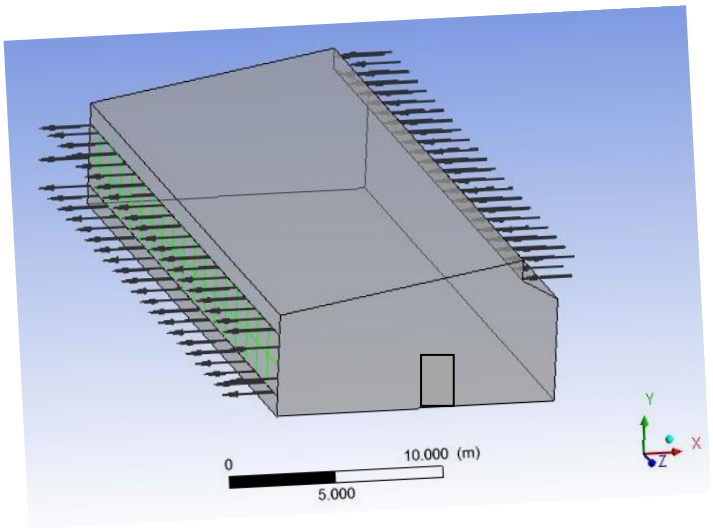

Figure 21. The geometrical structure of the proposed greenhouse

3.3.2. Physical Model of the proposed system

To study the phenomena seen in a greenhouse under different conditions, physical models are often used which consist of the numerical solution of transport equations (fluid mechanics equations).

These models allow us to characterize the greenhouse indoor climate with a fine field knowledge of these parameters, such as: temperature, humidity, pressure and air speed etc.

The numerical modeling of fluid flows, which is in fact a mathematical representation of the studied phenomenon, consists in determining at any point and at any time the state variables representative of the flow (velocity, pressure, temperature), by solving a system of partial differential equations, with a set of boundary and initial conditions drawn from the problem. This system of equations governing the phenomenon is deduced in general, from the application of the principles of conservation of mechanics, thermodynamics and the introduction of a number of simplifying assumptions to the system of basic equations of:

- Mass conservation equation;
- Momentum equation;
- Energy equation.

This general system is valid for all flow regimes.

In this part of our work, we have exposed the complete physical model which simulates the movements of air in our greenhouse and which is based on the basic equations called the Navier-Stokes equations;

In order to characterize the turbulent transfers in the greenhouse, we presented the different turbulence models, in particular the standard k-ε model used during this study.

Solving a convection problem means determining at any point in the field of study and at any time the characteristic quantities of the fluid studied (air for our study), namely:

- The pressure;
- The temperature;
- The wind speed field.

In this part, we present the equations that govern the phenomenon of natural convection in a turbulent regime inside a greenhouse, we are interested in the balance equations governing the average motion of the fluid and the consequences of turbulence on the resolution of these equations. So, we will end up with a system of equations. To solve all the equations considered in this study, it is necessary to specify the initial conditions and the boundary conditions of the entire boundary of the flow domain. The equations expressing the flow phenomena are mainly those derived from the physical laws of conservation of mass, conservation of momentum and energy conservation.

a. Mass conservation equation (continuity)

This is the equation that expresses the law of conservation of mass for a material control volume. In the case of a medium without a source or sink of matter, the equation of continuity is expressed mathematically in the following form:

$$\frac{\partial \rho}{\partial t} + div\,(\rho.V) = 0$$

Where ρ is the density, and V is the velocity vector.

b. Momentum equation

The principle of conservation of momentum enables the establishment of the relationships between the characteristics of the fluid and its movement and the causes that produce it. Where we can state that the rate of change of momentum contained in the control volume is equal to the sum of all external forces applied to it. It is written in the following form:

$$\rho \frac{d\vec{V}}{dt} = \rho.\vec{f} - \vec{\nabla} p + \vec{\nabla} \tau$$

This equation expresses the balance between the rate of change of momentum per unit volume and the external forces applied to the unit of volume: the volume forces $\rho\vec{V}$, the pressure force $\vec{\nabla}P$, and the force of viscosity $\vec{\nabla}\tau$.In the case of Newtonian fluids, the equation takes the simplified form of the Navier-Stokes equations:

$$\rho \frac{d\vec{V}}{dt} = \rho.F - grad(p) + \mu \Delta V + \frac{\mu}{3} grad(div(V))$$

Where μ: is the dynamic viscosity of air. F: force per unit of volume.

c. Energy equation:

The energy conservation equation is obtained from the first principle of thermodynamics. This principle connects the different forms of energy, namely:

$$\frac{d}{dt}(\rho c_p T) = \Delta(\lambda T) + q + \beta T \frac{dp}{dt} + \mu \phi$$

- $\frac{d}{dt}(\rho C_p T)$ **:** the total energy change;
- $\Delta(\lambda T)$: the energy variation by conduction;
  q : the dissipated power density;
- $\beta T \frac{dp}{dt}$: the energy variation due to compressibility
- $\mu\rho$ **:** irreversible dissipation due to viscous friction.

The coefficients Cp, λ, and β are respectively the heat capacity, the thermal conductivity and the isobaric coefficient of expansion of the fluid.

Simplifying assumptions

To build sufficiently detailed and precise models, in order to reduce this system and facilitate its resolution, we make certain approximations and simplifying assumptions:

- The fluid (air) is viscous and Newtonian.
- The fluid is assumed to be incompressible.
- The thermophysical properties of the fluid are assumed to be constant.
- The viscous dissipation is negligible due to the low speeds involved (ϕ = 0)
- The heating power by compression is negligible compared to other energy terms. **βT dp / dt =0**
- The volume forces are limited to the gravitational forces.
- The dissipated density power is negligible (**q = 0).**

In a certain number of situations, the hypothesis of an incompressible fluid is not justified and it is necessary to take into account the very small variations in density produced by a temperature or pressure gradient. In the case of natural convection, the flows in the greenhouses are the result of variations in density due to temperature gradients within the fluid itself. It is assumed that the airflow speeds are low enough that the density variations produced by the pressure variations are negligible.

d. Boussinesq approximation:

For flow patterns in a greenhouse, the resultant of external forces is limited to gravitational forces so that the influence of natural convection caused by temperature gradients is evident. When buoyancy forces occur in the flow, the design of fixed physical properties no longer matches the behavior of the fluid flow. The effect of natural convection is taken into account in the momentum equation by the change in density. If by taking a reference thermodynamic state (density $\boldsymbol{\rho_0}$ and a temperature $\mathbf{T_0}$), the state equation for density ρ becomes using the Taylor expansion:

$$\rho = \rho_0(1 - \frac{T-T_0}{T_0} + \cdots)$$

By limiting this equation to the first-order development:

$$\rho = \rho_0(1 - \beta(T - T_0))$$

β: is the isobaric coefficient of expansion of the fluid, namely:

$$\beta = -\frac{1}{\rho}(\frac{\partial \rho}{\partial T})$$

In fact, it is the variation in the density of the fluid which is the origin of the phenomenon of natural convection, creating a driving force volume (Archimedes) which is opposed in particular by a friction force viscous.

Boussinesq's approximation consists in neglecting the variations in mass volume in conservation equations, except its implication as driving force in the F term of the conservation equation for the amount of movement.

We can express the volumetric force F, the motor of natural convection by:

$$\boldsymbol{F = g\beta(T - T_0)}$$

We admit that in the other terms of the conservation equations, the density ρ can be considered as constant (Boussinesq approximation).

System of equations used:

After introducing the hypotheses given above, we can consider that the following equations describe the phenomenon of natural convection inside the greenhouse.

$div(\rho.V) = 0$;

$$\frac{DV}{Dt} = \frac{\partial V}{\partial t} + (V.\nabla)V = -\frac{1}{\rho}\nabla p + v\Delta V + g\beta(T - T_0)$$;

$$\frac{DT}{Dt} = \frac{\partial T}{\partial t} + (V.\nabla)T = a\Delta T$$

Where: $v = \frac{\mu}{\rho}$ is the kinematic viscosity,

$a = \frac{\lambda}{\rho C_p}$ is the thermal diffusivity of the fluid.

In the case of a stationary **(∂ / ∂t** = 0) and two-dimensional flow, the system of equations relative to a cartesian coordinate system is expressed:

e. Continuity equation:

$$\frac{\partial u}{\partial x} + \frac{\partial v}{\partial y} = 0$$

f. Equation of momentum following x:

$$u\frac{\partial u}{\partial x} + v\frac{\partial u}{\partial y} = -\frac{1}{\rho}\frac{\partial p}{\partial x} + v\left(\frac{\partial^2 u}{\partial x^2} + \frac{\partial^2 u}{\partial y^2}\right)$$

g. Equation of momentum following y:

$$u\frac{\partial v}{\partial x} + v\frac{\partial v}{\partial y} = -\frac{1}{\rho}\frac{\partial p}{\partial y} + v\left(\frac{\partial^2 v}{\partial x^2} + \frac{\partial^2 v}{\partial y^2}\right) - g\beta(T - T_0)$$

h. Energy equation:

$$u\frac{\partial T}{\partial x} + v\frac{\partial T}{\partial y} = a\left(\frac{\partial^2 T}{\partial x^2} + \frac{\partial^2 T}{\partial y^2}\right)$$

The differential equations of continuity, momentum, and energy form the mathematical model of laminar flow.

3.4. DIGITAL MODEL AND ANSYS FLUENT SIMULATION

The current development of numerical methods and simulation software helped us to obtain the approximate solutions for the aforementioned system of equations. The CFD (Computational Fluid Dynamic) uses powerful numerical methods such as, finite volumes and finite elements for fine discretization of the study area. They are very efficient for the numerical resolution of Navier-Stokes equations.

Their advantages over experimental trials lie in the substantial reductions in time, computational cost and their ability to study complex systems where experimental study is impossible.

The ANSYS FLUENT software (the one we used) uses the finite volume method to model varied flows in more or less complex configurations. It is able to solve any number of transport equations.

The finite volume method was developed by Patankar in the early 1970s. It was first used in the simulation of viscous and two-dimensional flows.

The computational domain is divided into a finite number of elementary subdomains, called control volumes. The finite volume method consists of integrating the partial differential equations on each control volume.

3.4.1. Ansys Fluent overview

Fluent is a CFD (Computational Fluid Dynamics) software for performing numerical simulations of fluid flow problems. The Ansys Fluent package relies on the finite-volume method to solve the equations governing the motion of a flowing fluid and includes different physical models such as:

- Flow in 2D and 3D geometries using unstructured adaptive meshes.

- Incompressible and compressible flow.
- Stationary or unsteady analysis.
- Non-viscous, laminar or turbulent flow.
- Newtonian or non-Newtonian flow.
- Heat transfer by convection, natural or forced.
- Heat transfer by radiation.
- Inertial (stationary) or non-inertial (rotating) reference marks
- Multiple moving reference frame, including sliding interfaces and mix planes.

3.4.2. Choice of mesh type

The location of the variables of the problem which must be calculated is defined by the mesh which corresponds to a discrete representation of the physical domain.

The simulation domain is then divided into a finite number of control volumes. In the different codes of calculation using the finite volume method, there are mainly two types of mesh:

1. Structured mesh

It is much easier to generate it using multi block geometry.

Its advantages:

- ✓ Economical in number of elements, has a lower number of mesh compared to an equivalent unstructured mesh;
- ✓ Reduces the risk of numerical errors because the flow is aligned with the mesh.

Its disadvantages:

- ✓ Difficult to generate in the case of a complex geometry;
- ✓ Difficult to obtain a good mesh quality for certain complex geometries.

2. Unstructured mesh

The elements of this type of mesh are generated arbitrarily without any constraint as to their arrangement.

Its advantages:

- ✓ Can be generated on a complex geometry while keeping a good quality of the elements;
- ✓ The algorithms for generating this type of mesh (tri / tetra) are very automated.

Its disadvantages:

- ✓ Very greedy in number of meshes compared to the structured mesh;
- ✓ Generates numerical errors (false diffusion) which can be more important if we compare with the structured mesh.

In this master thesis, the simulations use the structured mesh.

3.5. BOUNDARY CONDITIONS

Ansys Fluent gives the choice between a certain number of types of boundary conditions, very different.

Most of the physical problems described mathematically by a partial differential equation (or system of equations) are defined in an unbounded domain.

If one wishes to solve problems of evolution numerically in all the space, one is thus brought to confine the field of computation.

Several methods can be considered, such as the use of integral equations for acoustics or electromagnetism, or even infinite element methods.

The method undoubtedly the most used consists in defining an artificial domain of computation and thus to bring back the total problem on a truncated domain. This truncation necessarily induces the search for boundary conditions adapted on the fictitious border of the domain of computation. This general approach therefore leads to the determination of artificial boundary conditions. These boundary conditions are not contained in the formulation of the original problem: they must be obtained by a transformation. This transformation must provide an approximation of the solution on the unbounded domain by the solution calculated in the finite domain with the artificial frontier. This methodology has already been successfully applied in several fields of applied mathematics such as for example electromagnetism, fluid mechanics, etc. .... Clearly, these artificial conditions must make it possible to consider computation domains of minimal size, and thus to potentially build fast algorithms for computing solutions. However, this goal cannot be achieved without some difficulty. First: it is necessary to know how to define these boundary conditions, which are most often non-local in space and time.

Second, the numerical processing (approximation, stability, efficiency) of analytical conditions is a delicate question.

The specification of boundary conditions consists of knowing the type of the boundary condition, the placement where it applies and the value of the variables that must be defined on this condition.

CFD software gives the choice between a number of very different boundary conditions that can describe the boundaries of a large number of flow domains.

3.6. GREENHOUSE SIMULATION PROCESS

For the climatic conditions considered:

3.6.1. Definition of the geometry:

Our geometry was built on "Inventor Autodesk",

- ✓ The geometry is of plastic greenhouse of the "modified shed roof" type and classic shape, its geometric characteristics are: 13.5 m wide, 32 m long and an upper roof height of 8 m. The air ventilation in the proposed type of greenhouse is obtained through opening window installed on the top of the secondary roof of the greenhouse;

- ✓ To cover this type of greenhouse, polyethylene is chosen. This material is transparent in the visible light range.

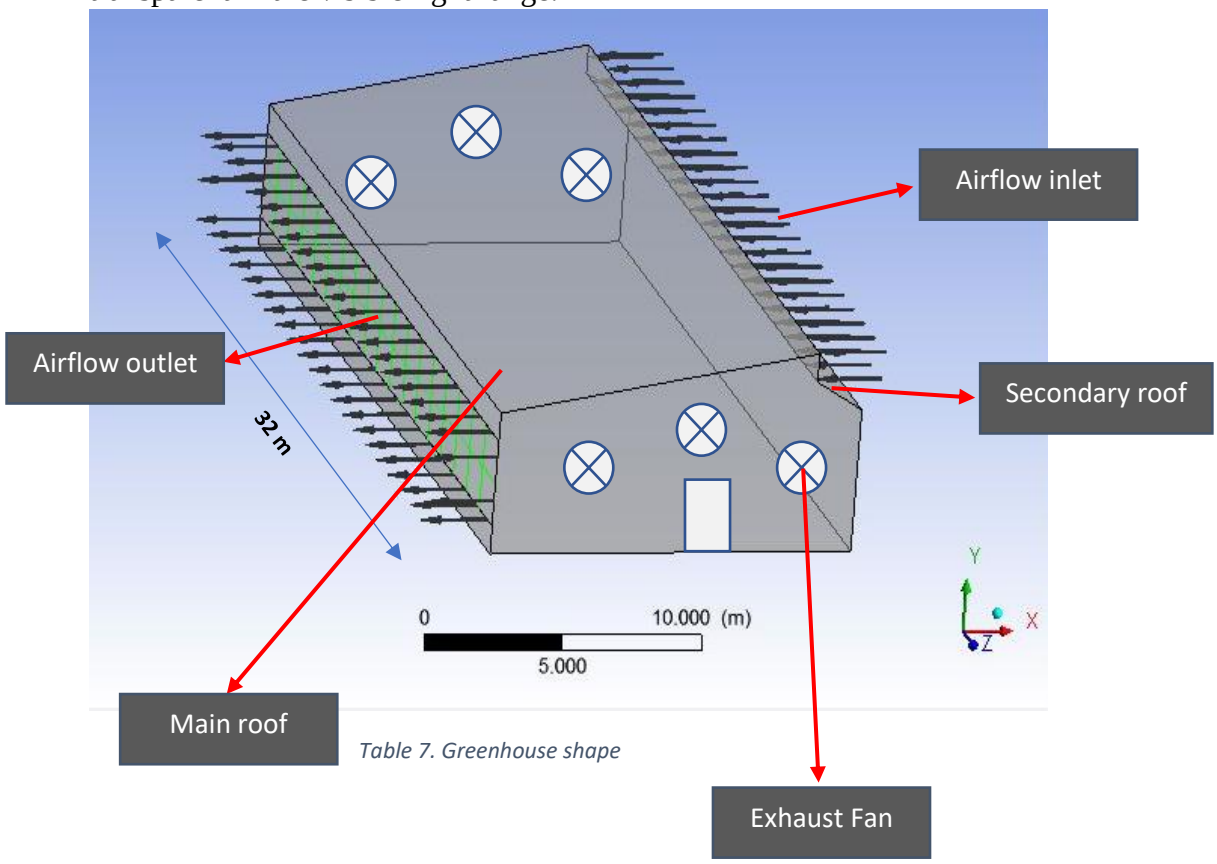

Table 7. Greenhouse shape

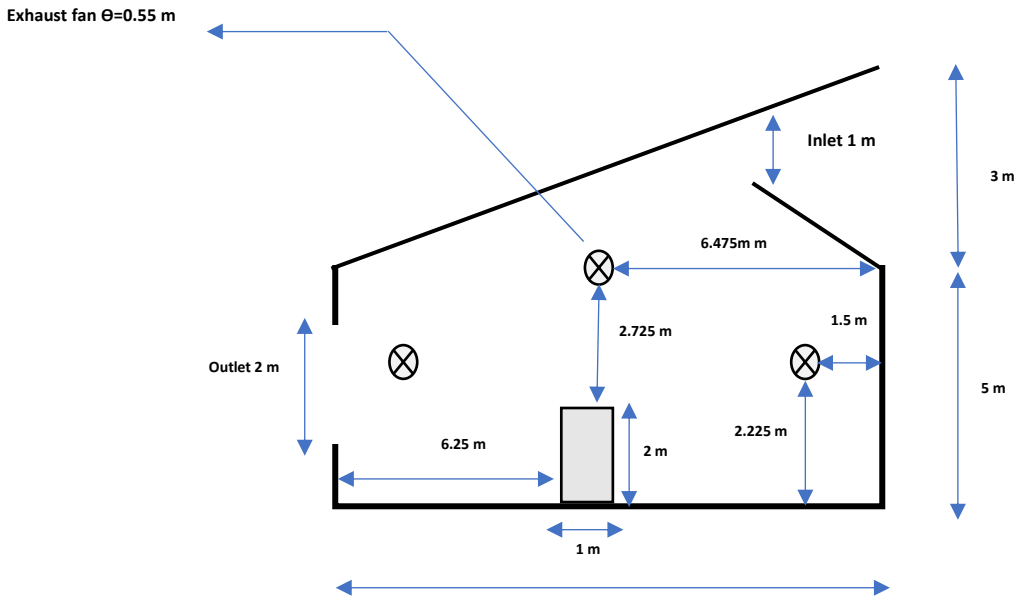

Figure 22. Proposed shape geometry and Sizing

3.6.2. Condition at the inlet (humidifiers):

Knowing the geometry of inlet (1*32m) and the weather conditions (average temperature, relative humidity and wind speed) in the Kinshasa. The conditions at the inlet used in the simulations were the following: the air temperature T = 25 ° C (air density ρ_{25} =1.184Kg/m^3 at Kinshasa altitude level, 290m average) and the absolute humidity ω = 0.016 Kg wet / Kg dry air (RH = 80%). The mass flow rate is calculated by the following formula $Q = \rho_{air\ at\ 25°C} \times A \times V$ where the A is the surface area of inlet and V the air wind speed entering the inlet. In this research, A=1m× $32m$ and V_1=1.5m/s and V_2=3m/s

mass flow rates of Q1 =56.832 Kg/s; and Q3=113.664 kg /s (for velocity V_1 and V_2).

Q1 = 204585.2 Kg/h mass of air entering in hour = 204585.2 Kg n_1=79.74511 h^{-1}
Q2 = 409190.4 Kg/h mass of air entering in hour = 409190.4 Kg n_2=159.498 h^{-1}
Volume $_{greenhouse}$ = 2166.798 m^3 **q = n*V** **n**: air change rate (h^{-1})
Time =1h **q**: fresh air supply
air density (T=25°C) =1.184 Kg/m^3 **V:** volume of structure

The conditions are summarized in the below table:

Condition in the entrance		
Relative humidity	80%	
Temperature (°C)	25	
Air velocity (m/s)	1.5	3
Mass flow rate (Kg / s)	56.832	113.664
Air change rate (h^{-1})	79.74511	159.498

Table 8. Conditions at the inlet

3.6.3. Outdoor conditions (thermal and dynamic)

The ANSYS FLUENT software gives choice of boundary conditions in number. These boundary conditions are very different from one to another and can describe the boundaries of a large number of flow domains.

In our simulations, we apply "WALL" type boundary conditions to the sidewalls and roof. For the thermal condition, we choose to impose heat flows on these walls and roof.

We can summarize the boundary conditions for the case of our greenhouse in the following diagram:

+

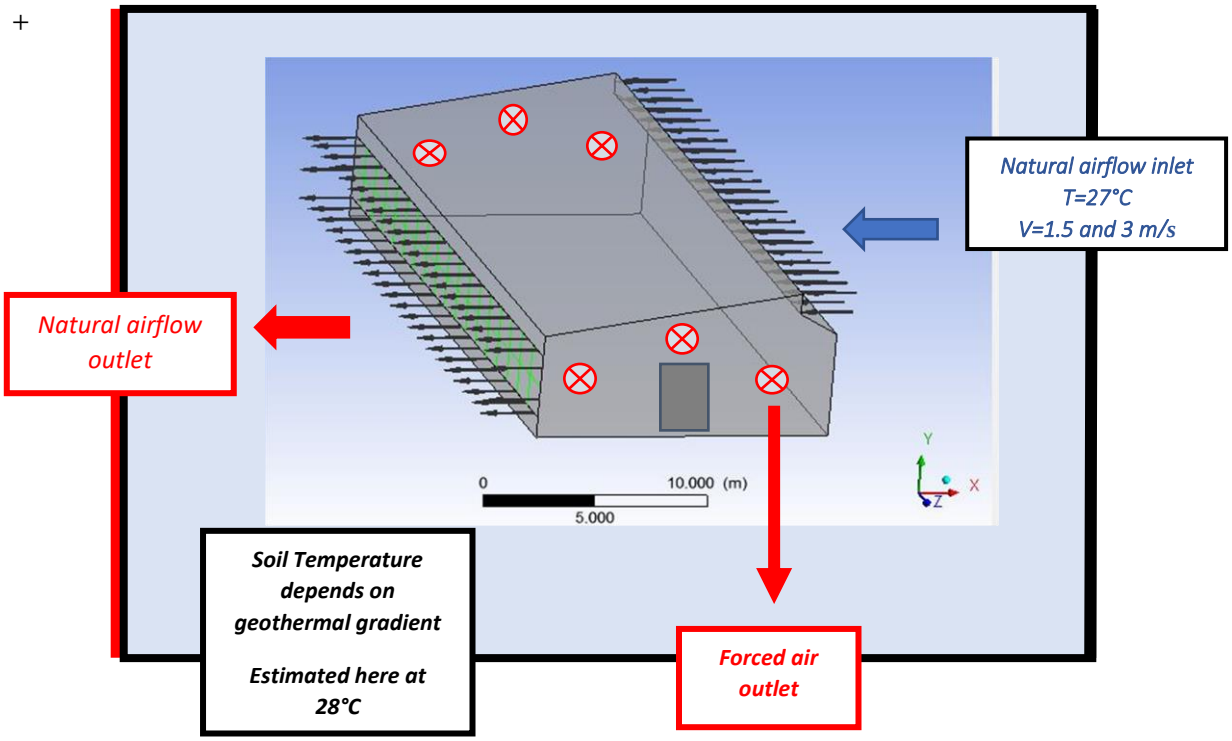

Figure 23. Limits conditions in the case of our greenhouse

3.6.4. Greenhouse wall:

They are considered semi-transparent, exposed to incident solar radiation (heat flux) of 1000 W/m^2, of which 200 W/m^2 are diffuse.

- ✓ Natural convection on all surfaces of the greenhouse;
- ✓ The ground surface is adiabatic.

3.6.5. The covering system:

Plastic polyethylene is used in this experiment for covering all wall and the roof with **Transparent FRP roof fiber glass**. The heat flux is 1000 W/m^2. This material is transparent in the visible domain, its properties are represented in the board:

Properties - sidewall	
Materials	Plastic polyethylene
Density (kg/m^3) Specific heat (J/kg.K) Thermal conductivity (W/m.K) Thickness (in micron meter) Heat transfer coefficient W/m^2.K	1400 1046 0.17 200 0.33
Properties- roof	
Materials	Transparent FRP roof fiberglass
Light transmittance	55%
UV protection	UV protection
Heat transfer coefficient W/m^2.K	0.55
Density (kg/m^3)	1550
Thermal conductivity (W/m.°C)	0.57
Thermal expansion (10^{-6} m/m. °C)	20
Thickness	1mm
FRP: Fiber-reinforced plastic is a composite material made of a polymer matrix reinforced with fibers.	
Netting system	
Material	100% HDPE+UV
Mesh hole size	2x2 mm
Type of mesh	10 Mesh
Open area	60.8%
Ventilation reduction	25.088m^2

Table 9. Physical Properties of covering and netting system.

3.6.6. Flow state

In this study, we have chosen to consider flow with heat transfer.

3.6.7. Fluid properties

We have chosen air as fluid; its properties are represented in the table below.

Proprieties	Numerical values
Dynamic viscosity Specific heat Thermal conductivity Density	1.7894. 10^{-5} kg/m.s 1006.43 J/Kg.K 0.0242 W/m.K Incompressible-ideal-gas

Table 10. Fluid properties (air)

3.6.8. The characteristics of fans (exhaust fans)

For the model of our greenhouse we will need a total of 6 exhaust fans, the characteristics of which are shown in the table below:

Blades Diameter(mm)	Blades Rotational Speed(rpm)	Motor Rotational Speed (rpm)	Air flow $m^3/hr.$	Input power (W)
200	**1400**	**1400**	**2000**	**120**

Table 11. Exhaust fan characteristics

3.6.9. Cooling technology objectives

The pursued target of our cooling system is that the temperature and relative humidity inside our greenhouse may be kept between T = 23-27 ° C and the relative humidity between H = 70-85%. For this, the shading system, misting system and exhaust fans will be installed and use in a specific ways described in . However, it should be noted that the goal in this work is to optimize the use of natural ventilation.

3.6.10. Simulations parameters

In the work, we needed to identify and determine the following physical and thermodynamic parameters: Velocity field, indoor air circulation, temperature field, the distribution of relative humidity and pressure inside our greenhouse:

- ✓ For velocity field: we use the wind speed (in inlet) of 1.5m /s and 3m / s, (profile and magnitude of velocities);
- ✓ Temperature and pressure profile will be presented both in YZ and XZ planes.

3.6. 11. Meshing

The mesh information for CFX1 (V_1=1.5 m/s) was the same as for CFX2(V_2=3 m/s). Nodes=18659 and Elements=83997 (boundary conditions employed with details are shown in Appendix)

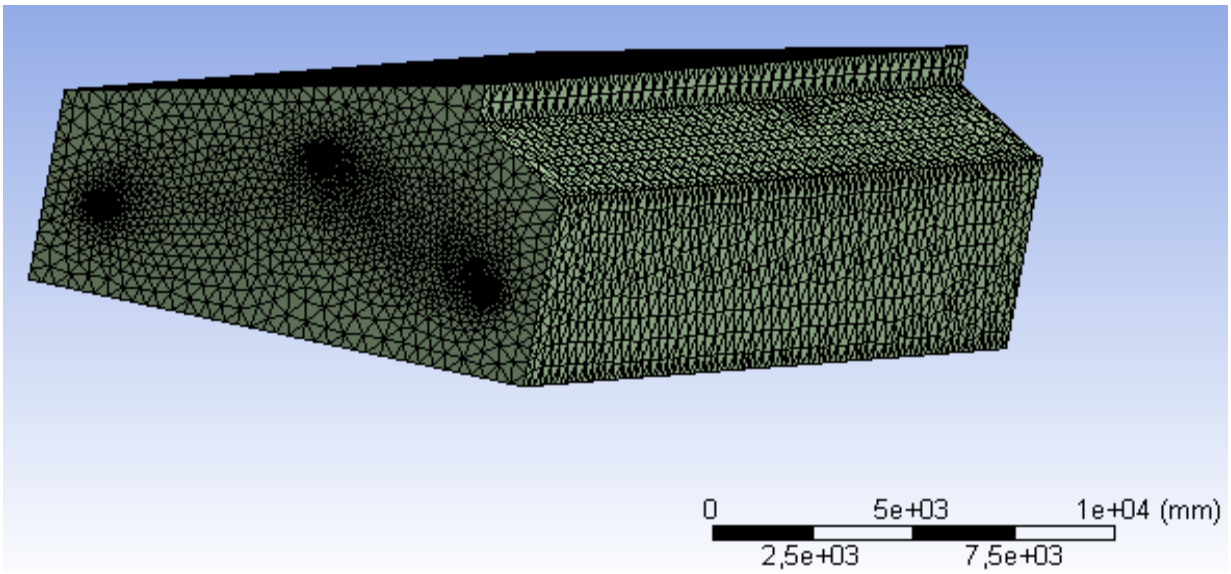

Figure 24. Meshing geometry

3.6.12. Interpretation of simulation results

For flow without energy addition in between inlet and outlet, velocity and pressure are inversely proportional to each other. However, in case of flow with energy addition in between inlet and outlet, (including the case with fans working) velocity and pressure are directly proportional to each other. For the results presented here are those with fans working and that without working. In any case energy addition from the roof through solar irradiance is present which contributes to energy addition between inlet and outlet.

For the flow of a gaseous fluid such as air. Pressure and temperature are directly proportional to each other.

Wind speed field

The circulation of air inside our greenhouse is shown on the Figure 25 and Figure 27. On the Figure 25 the proposed greenhouse uses only natural ventilation and the wind speed in the entrance is 3m/s. While on the Figure 27 the proposed greenhouse uses natural ventilation and exhaust fans (6 fans) with the wind speed of 1.5m/s.

Predominant airflow bypass in the upper corridor tend to produce a shielding effect of most part of the domain of the Greenhouse where plants are located.

We can also see that the increase in wind speed with Fans generates an increase in air circulation in the proposed greenhouse, homogeneity of flow over the entire right part of the greenhouse is mainly due to the shape of the greenhouse. Recirculation regions can also be seen in the middle part of the greenhouse.

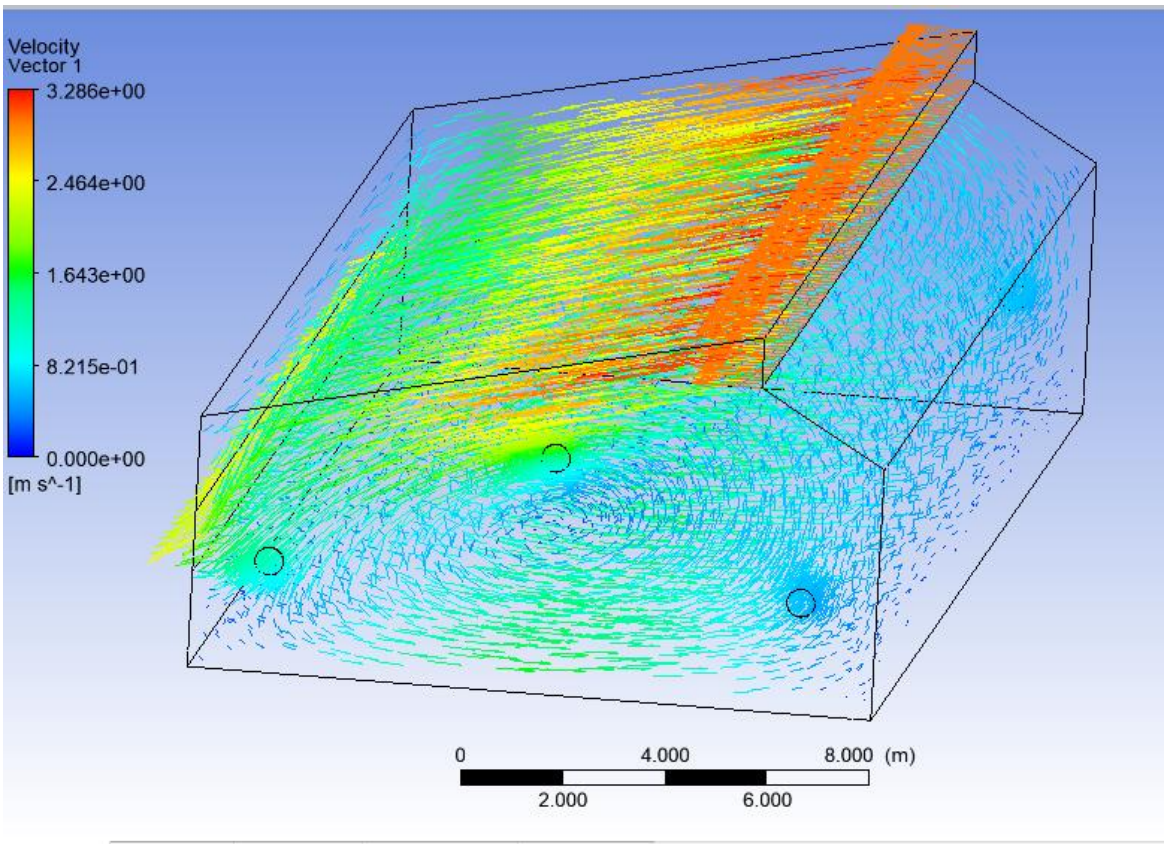

Figure 25. Airflow profile with v=3m/s (no exhaust fan)

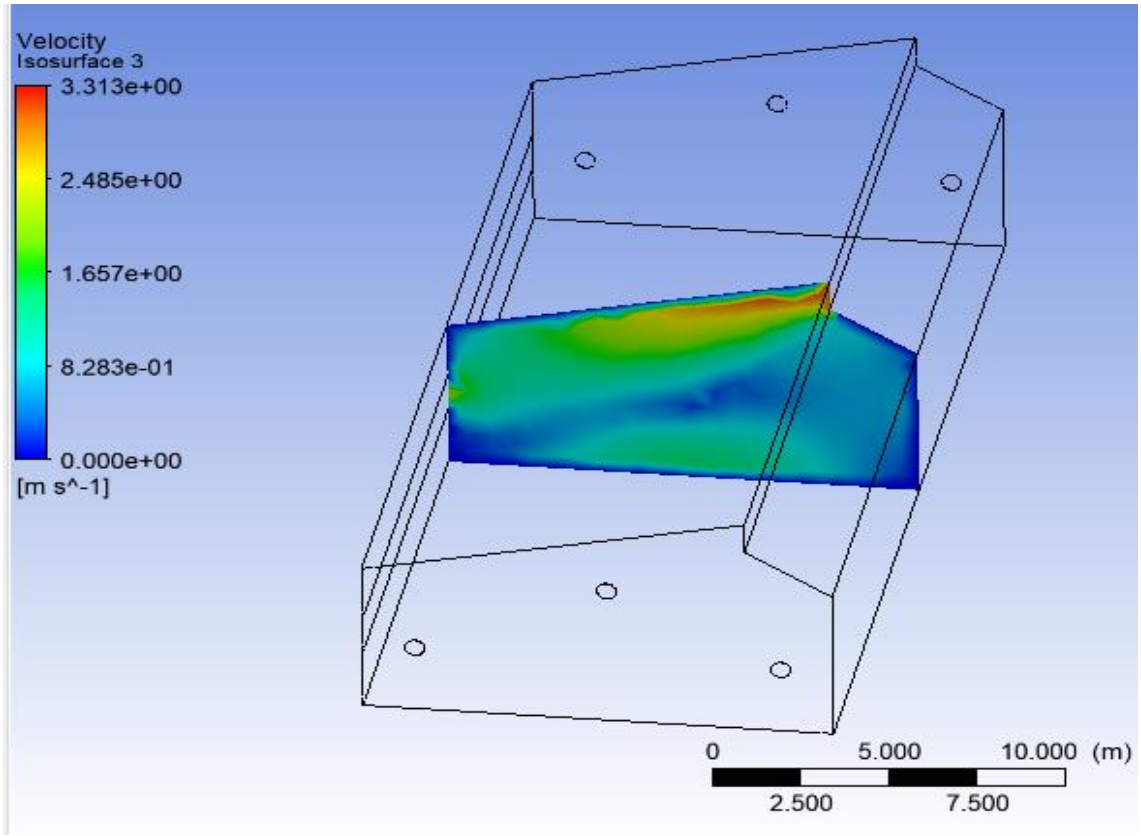

Figure 26. Figure 14. Airflow profile in the XZ plane with Y = 16 m with v=3m/s (no exhaust fan)

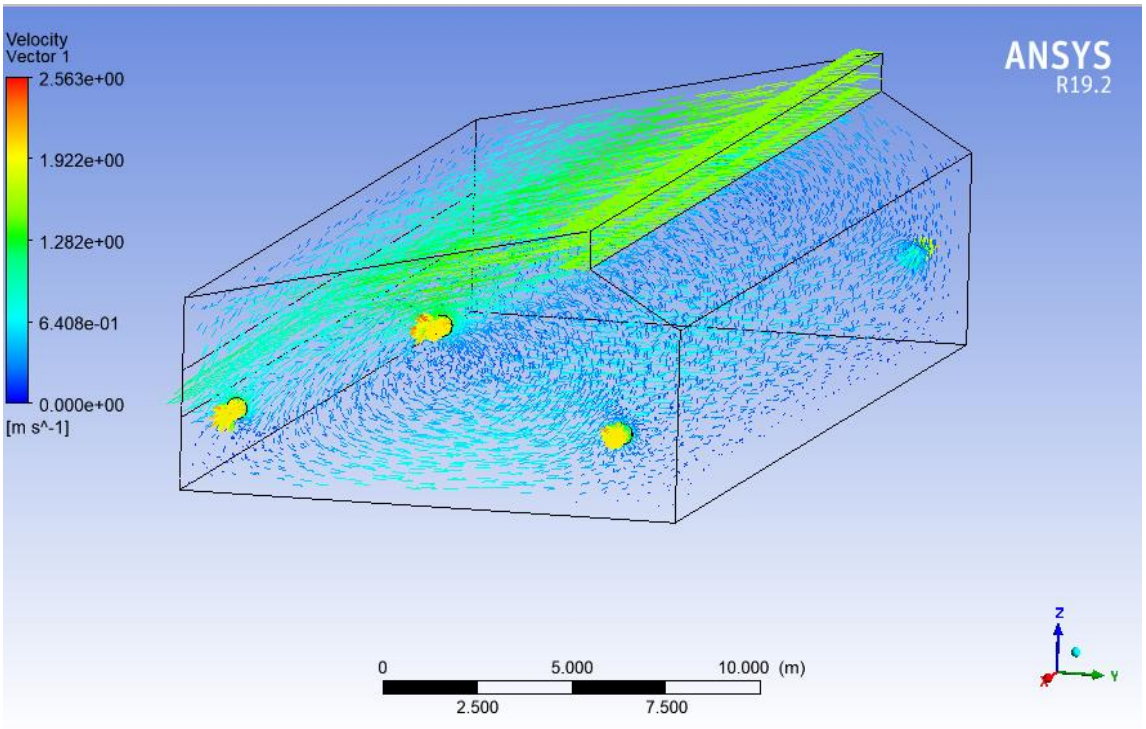

Figure 27. Airflow profile with v=1.5m/s (with six exhaust fans working)

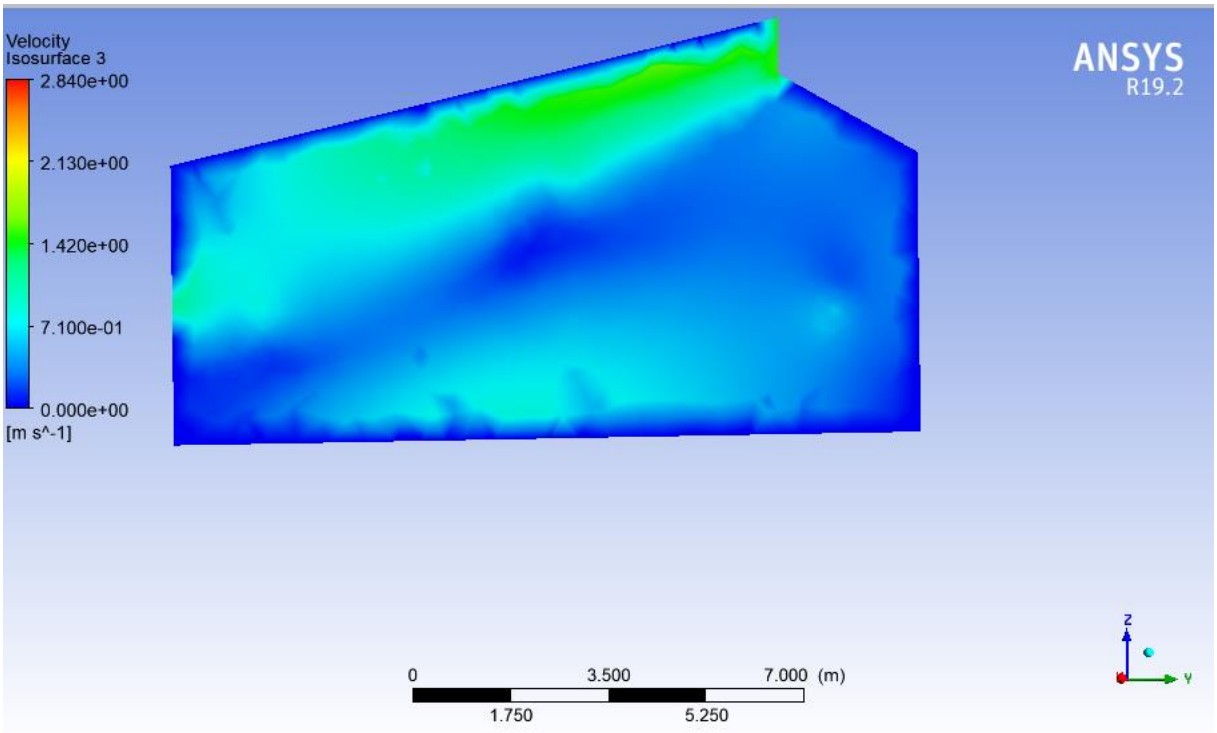

Figure 28. Airflow profile with v=1.5m/s (with exhaust fan)

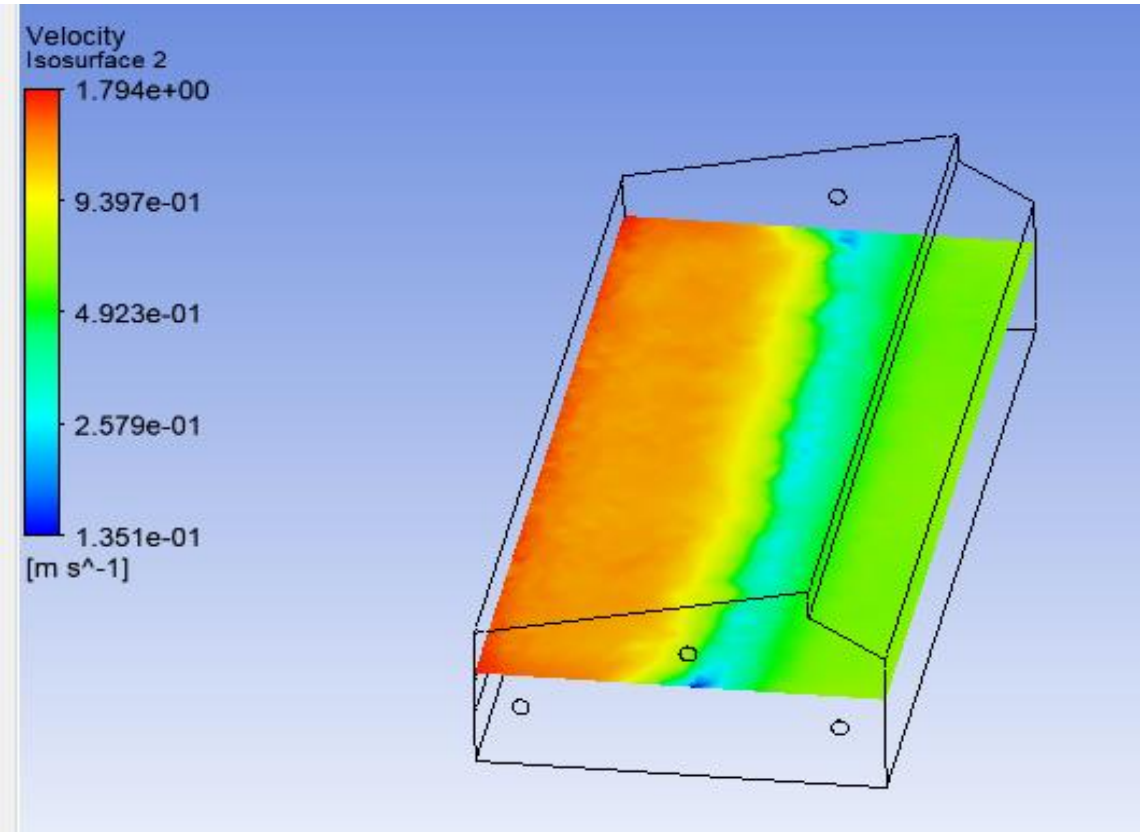

Figure 29. Airflow profile in the XY plane with Z = 4.5 m for v=1.5m/s

In those figures, we see that the air speed is maximum near of the air entry because of the slope of the main roof, also for the exit opening the wind speed is high, and decreases slightly in the middle of our proposed greenhouse structure. On the other hand, it is much weaker in the inlet downstream side. We can easily see the air recirculation phenomenon from those profiles. The airflow pattern as such will influence the temperature field in the entire domain.

Temperature field

Figure 30 and Figure 31 show the temperature field, a first note of observation is: increasing wind speed implies increasing temperature inside the greenhouse around the outlet, this increase would be mainly due to the stagnation of the flow in that part of the greenhouse, since the figures Figure 26 and Figure 29 clearly show that the increase in wind speed results in an increase in the air inside the greenhouse.. Figure 31 shows how the temperature is constant and well distributed when v=1.5 m/s. The temperature distribution acroos the cross section is shown in Figure 30.

In addition, in Figure 34 we can see how the pressure in outlet increases when the wind speed increases

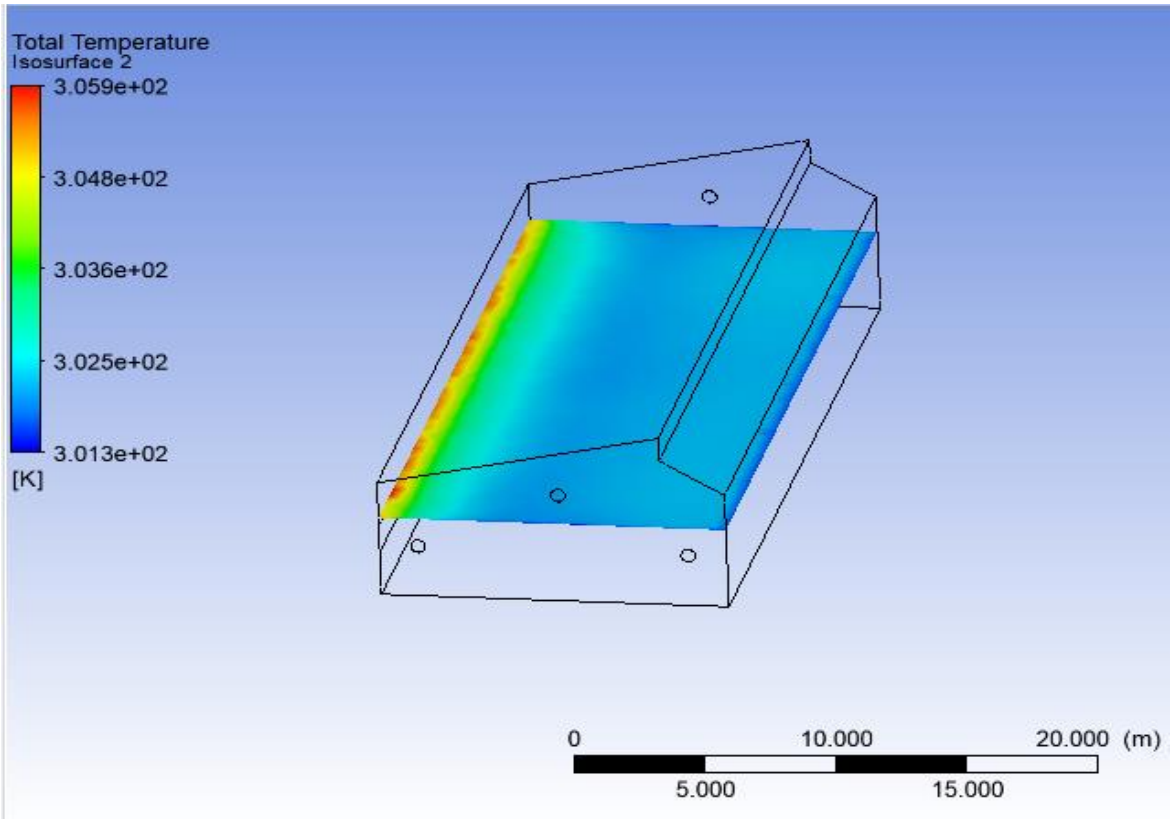

Figure 30. Temperature profile in the XY plane with Z = 4.5 m for v=3m/s

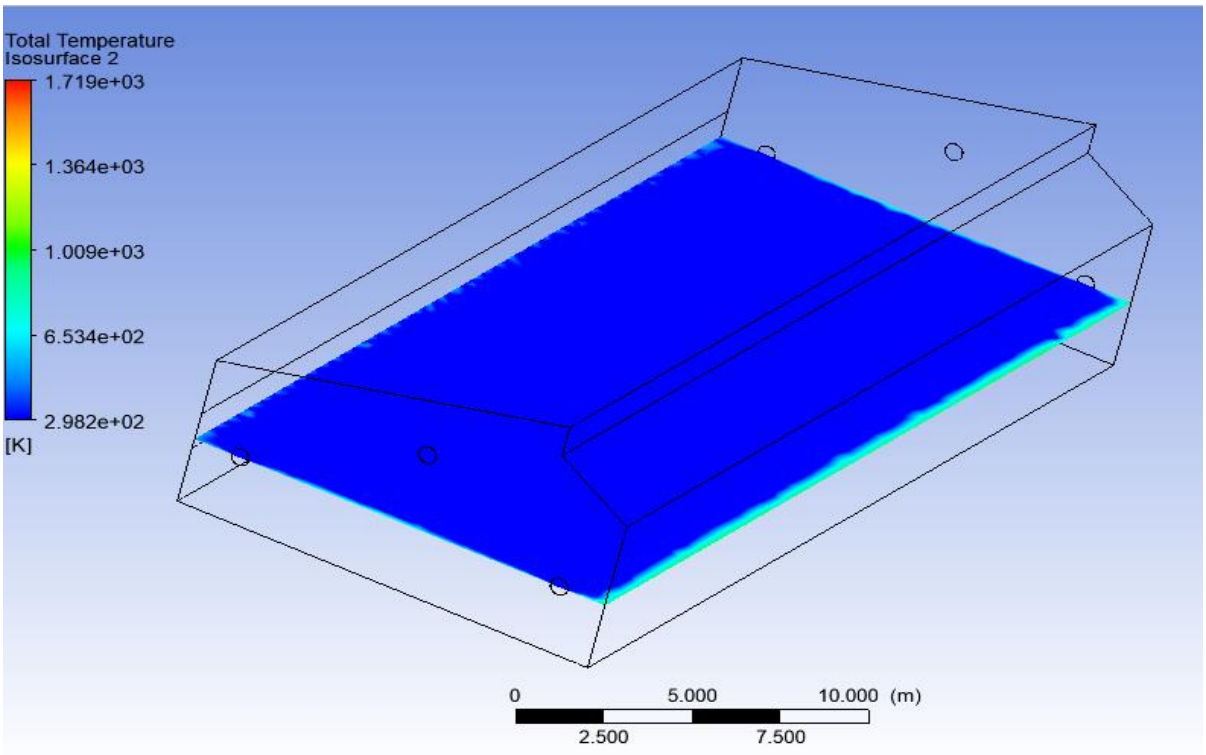

Figure 31. Temperature profile in the XY plane with Z = 2.5 m for v=1.5m/s

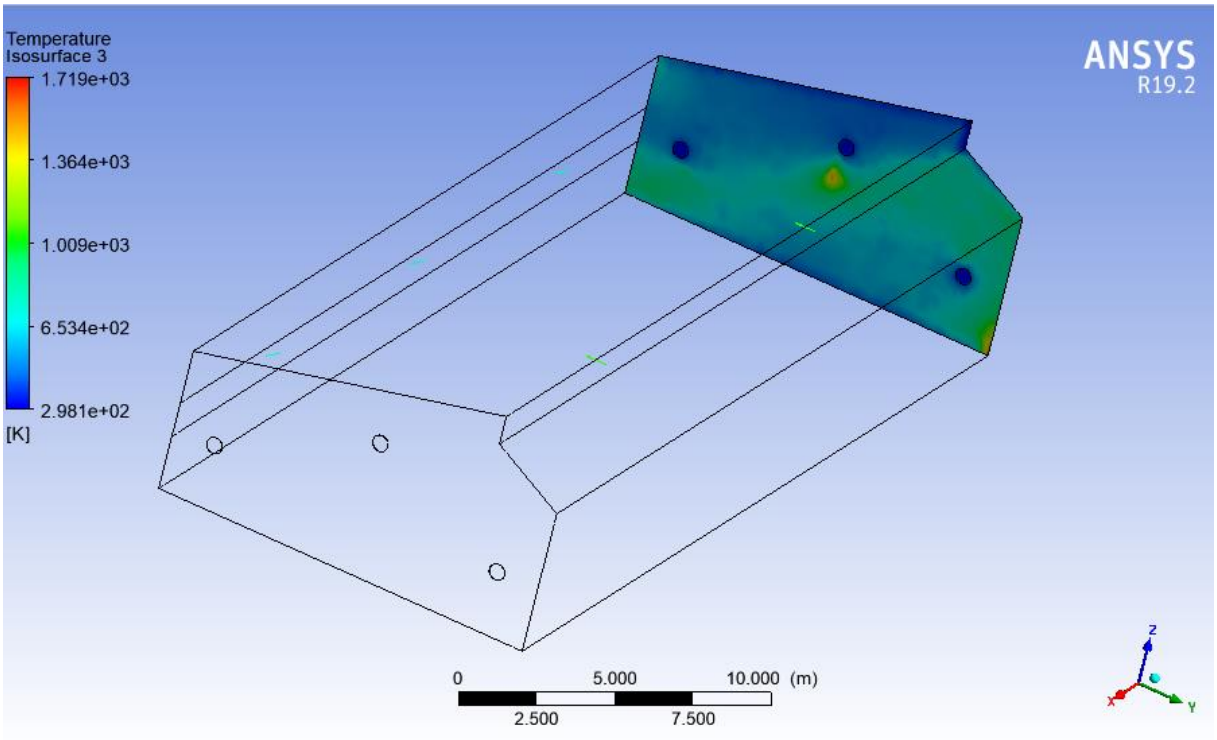

Figure 32. Temperature profile in the XY plane with X = 0 m with v=1.5m/s (with exhaust fan)

The Figure 32, represents the profile of the air temperature across the cross section of the greenhouse. This figure indicates the development of a thermal gradient important near the secondary roof, near the outlet and near the openings.

Pressure field

Figure 33- 33 show the increase of pressure with the increase of velocity, even though the comparison is at two different elevations resulting in the same pattern. The increase in pressure in the inlet and outlet regions of our greenhouse is mainly due to the shape of our greenhouse. The development of recirculation shown in earlier would result in a pressure drop due to internal dissipation.

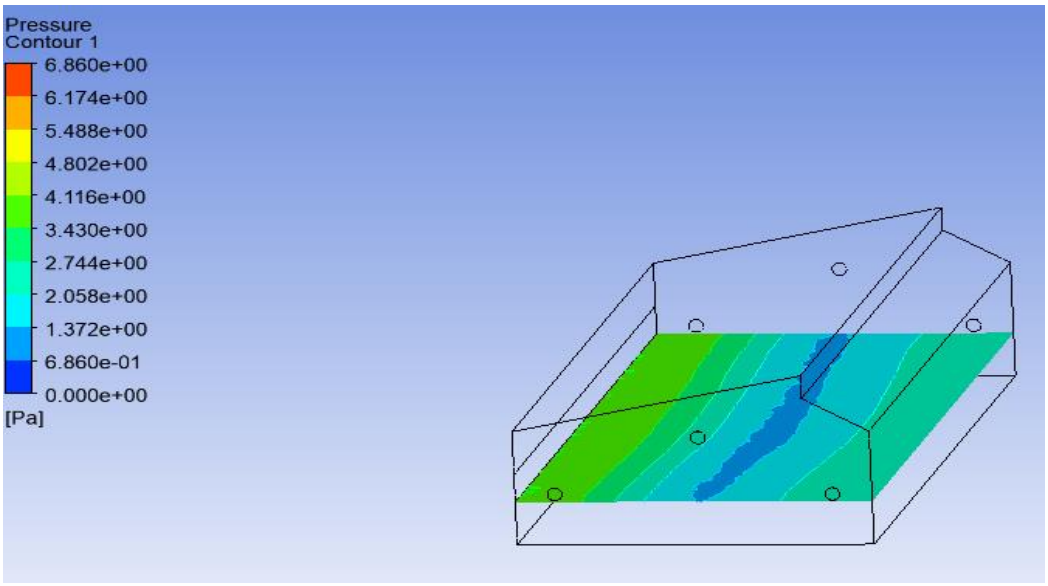

Figure 33. Pressure in the XY plane with Z = 2.5 m for v=1.5m/s

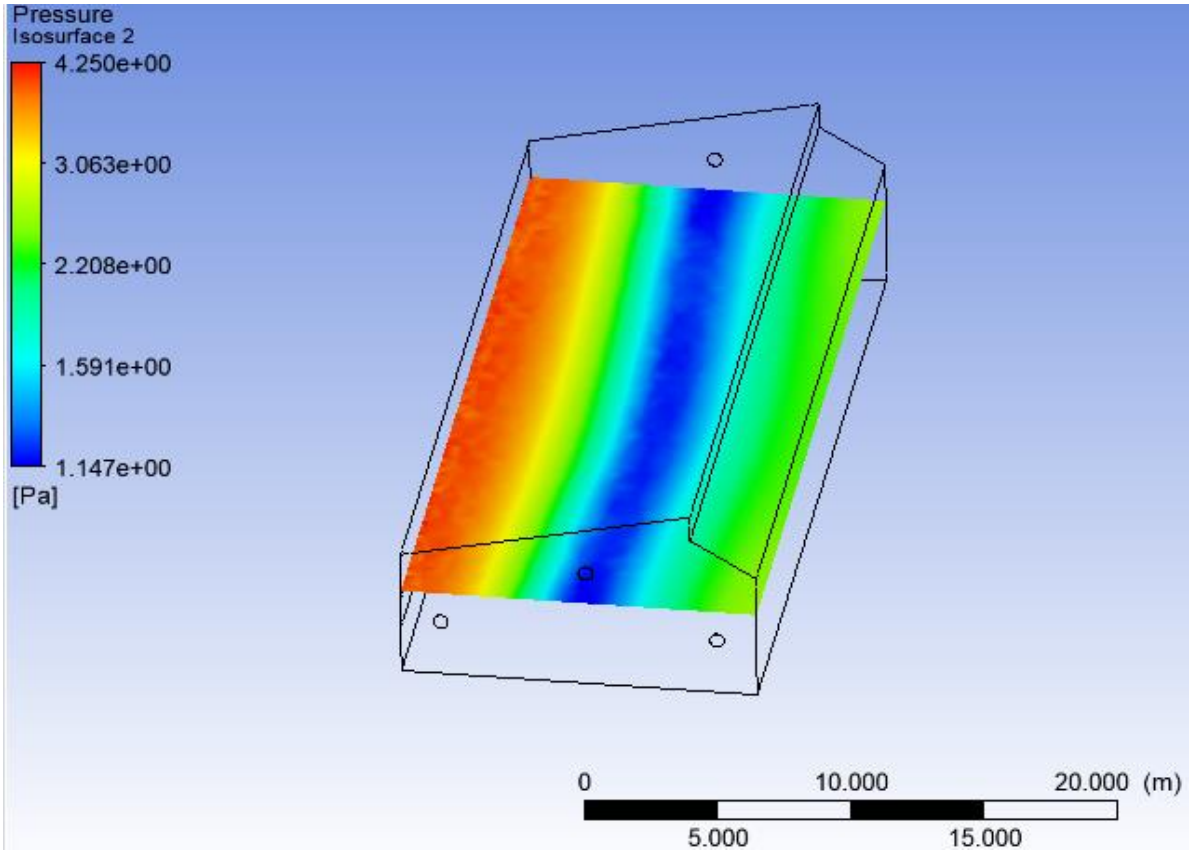

Figure 34. Pressure profile in the XY plane with Z = 4.5 m for v=3m/s

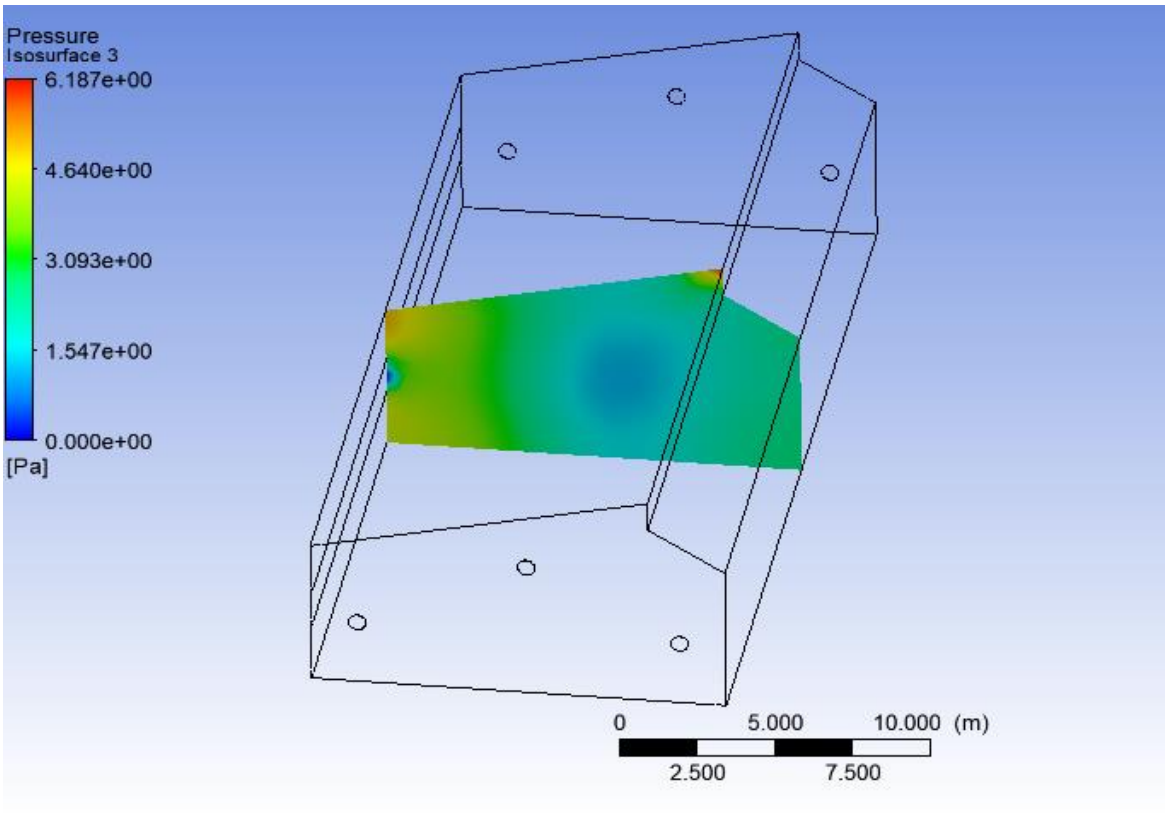

Figure 35. Pressure profile in the XZ plane with Y = 16 m for v=3m/s

The simulation of our greenhouse has given clues to the velocity, temperature and pressure field inside enabling an understanding of the microclimate inside the domain of the Greenhouse. Then the design of Greenhouse energy system and construction of the prototype are the next phase of our research.

3.7. DESIGN AND SIZING OF THE POWER ENERGY SYSTEM

To power our greenhouse, a small hybrid energy system of Solar PV-HAWT (Horizontal Axis Wind Turbine) has been designed and sized to meet greenhouse energy demand. Hybrid energy systems represent a very promising sustainable solution for power generation in stand-alone applications, especially in remote regions far from the grid.

Hybrid energy system is often defined as the integration of several types of energy generation equipment such as electrical energy generators, electrical energy storage systems, and renewable energy sources. Hybrid energy systems may be utilized in grid-connected mode, isolated from grid, and special aims. In this research an isolated mode has been used.

The hybrid energy design and sizing are convolution processes, there is no unique list of steps to follow. However, in this research we have followed the below steps the design and sizing of our greenhouse:

- Definition of the available energy resources: we have chosen solar PV and Wind energy;
- Load determination: we have determined the magnitude and duration of the electrical load on average daily and seasonal bases
- The selection of the battery capacity: based on the desired period, maximum and average daily depth of discharge, application requirements;

- Optimizing PV array tilt angle: based on site geographical information;
- Insolation: from available site insolation data, calculate insolation falling on the array at the calculated tilt angle
- Determination of PV array size and wind turbine capacity in hybrid configuration;
- Estimation of the cost of the system;
- Determine the control strategy to be used for battery protection

3.7.1. Planification of the greenhouse energy usage and load demand per day

The planification is mainly based on the daily solar energy distribution presented in Figure 8, Figure 11Figure 10 and Figure 11. The proposed greenhouse cooling system combines a misting system, a shading system and exhausted fans, used intermittently. For optimizing the greenhouse energy consumption, the proposed cooling system will be used from 11:00 AM to 3:00 PM in each summer. From 11:00 AM to 1 PM, the shading system will be used to regulate the temperature and relative humidity inside the greenhouse. From 1 PM to 3 PM the misting system will be used with exhaust fans to cool down the air temperature and balance the inside relative humidity.

N°	Greenhouse Electric Load /day	Power (W)	Quantity	Power load (KW)	Working time in a day (hour)	Usage time of a day	Energy consumption (KWh/day)
1.	Lighting (to fill the light transmittance deficit due to the use of the shading system from 11:00 AM to 1 PM and providing light in the greenhouse from 6:00PM to 4:00 AM)	40	2	0.08	12	11:00 am-1:00 pm; 6:00 pm-4:00am	0.96
2.	Solar submersible Water Pump for misting system	180	1	0.18	0.33 (20 min)	1:00pm-3:00pm	0.0594
3.	Solar submersible Water Pump for well pumping or drip irrigation	180	1	0.18	0.71 (42.8min in a day) (5 h/ week)	6:00pm-6:42 min48sec pm	0.1278
4.	Exhaust fan	120	6	0.72	3	1:00pm-3:00pm	2.16
5.	Electronic components for monitoring and control	200	1	0.2	12	6:00am-6:00pm	2.4
6.	Electric linear actuator	55	4	0.22	0.05 (3 min)	11:00am -11:1min 30sec am; 6:00pm-6:1min30sec pm	0.011
7.	Rotary electric actuator	150	8	1.2	0.06 (2 min)	10:58am-11:00 am; 12:58min-1:00pm	0.08
			Total power	**2.78**		**Total Energy consumption in a day**	**5.8**

Table 12. Planification of the greenhouse energy usage and load demand per summer day

Taking in to consideration the estimated working time in a summer day, summer daily energy consumption as well as the usage time of each electric load component, we have been able to determine in the below table, the energy demand for each 24 hours of each summer days (from September to May). Different energy demand profile is designed for winter months, (from June to August).

Day time	Greenhouse Daily Energy consumption per Hour (KWh)	Day time	Greenhouse Daily Energy consumption per Hour (KWh)
12:00 AM	0.08	12:00 Noon	0.28
1:00 AM	0.08	1:00 PM	1.0198
2:00 AM	0.08	2:00 PM	0.9398
3:00 AM	0.08	3:00 PM	0.9398
4:00 AM	0	4:00 PM	0.2
5:00 AM	0	5:00 PM	0.2
6:00 AM	0.2	6:00 PM	0.2133
7:00 AM	0.2	7:00 PM	0.08
8:00 AM	0.2	8:00 PM	0.08
9:00 AM	0.2	9:00 PM	0.08
10:00 AM	0.24	10:00 PM	0.08
11:00 AM	0.2855	11:00 PM	0.08
Total greenhouse daily energy consumption =5.8 KWh			

Table 13. Total greenhouse daily energy consumption in summer days

Day time	Greenhouse Daily Energy consumption per Hour (KWh)	Day time	Greenhouse Daily Energy consumption per Hour (KWh)
12:00 AM	0.08	12:00 Noon	0.2
1:00 AM	0.08	1:00 PM	0.2
2:00 AM	0.08	2:00 PM	0
3:00 AM	0.08	3:00 PM	0
4:00 AM	0	4:00 PM	0
5:00 AM	0	5:00 PM	0
6:00 AM	0	6:00 PM	0.2078
7:00 AM	0	7:00 PM	0.08
8:00 AM	0	8:00 PM	0.08
9:00 AM	0	9:00 PM	0.08
10:00 AM	0.2	10:00 PM	0.08
11:00 AM	0.2	11:00 PM	0.08
Total greenhouse daily energy consumption =1.7278 KWh			

Table 14. Daily energy consumption in winter (July and August)

In accordance with the objective set for our cooling technology (keeping the temperature T = 23-28 ° C and the relative humidity H = 70-85%.) and the summarized figure of data analysis of Kinshasa season and weather conditions (Figure 19), we have estimated the monthly greenhouse energy consumption. As the temperature and relative humidity is almost constant along a year (during summer months), then the daily greenhouse energy consumption has been considered to be constant in nine months (from September to May). As the during winter months (from June to August), the daily average temperature and relative humidity are below or in between our cooling technology objectives, For June, we have reduced in half the cooling energy demand (by reducing the working time of cooling system in Table 12) and for July and August we have considered only natural ventilation to be able to stabilize the temperature and humidity as the temperature and humidity in Kinshasa are very low during that period. In addition, from June to early October the wind speed is very highly capable and this fact empowers the natural ventilation to be sufficient to maintain temperature and relative humidity in the range fixed by the objective our cooling technology.

3.7.2. Monthly and Annual greenhouse energy consumption

Hour of a day	January	February	March	April	May	June	July	August	September	October	November	December
12:00 AM	0.08	0.08	0.08	0.08	0.08	0.08	0.08	0.08	0.08	0.08	0.08	0.08
1:00 AM	0.08	0.08	0.08	0.08	0.08	0.08	0.08	0.08	0.08	0.08	0.08	0.08
2:00 AM	0.08	0.08	0.08	0.08	0.08	0.08	0.08	0.08	0.08	0.08	0.08	0.08
3:00 AM	0.08	0.08	0.08	0.08	0.08	0.08	0.08	0.08	0.08	0.08	0.08	0.08
4:00 AM	0	0	0	0	0	0	0	0	0	0	0	0
5:00 AM	0	0	0	0	0	0	0	0	0	0	0	0
6:00 AM	0.2	0.2	0.2	0.2	0.2	0.2	0	0	0.2	0.2	0.2	0.2
7:00 AM	0.2	0.2	0.2	0.2	0.2	0.2	0	0	0.2	0.2	0.2	0.2
8:00 AM	0.2	0.2	0.2	0.2	0.2	0.2	0	0	0.2	0.2	0.2	0.2
9:00 AM	0.2	0.2	0.2	0.2	0.2	0.2	0	0	0.2	0.2	0.2	0.2
10:00 AM	0.24	0.24	0.24	0.24	0.24	0.24	0.2	0.2	0.24	0.24	0.24	0.24
11:00 AM	0.2855	0.2855	0.2855	0.2855	0.2855	0.2055	0.2	0.2	0.2855	0.2855	0.2855	0.2855
12:00 Noon	0.28	0.28	0.28	0.28	0.28	0.2	0.2	0.2	0.28	0.28	0.28	0.28
1:00 PM	1.0198	1.0198	1.0198	1.0198	1.0198	0.24	0.2	0.2	1.0198	1.0198	1.0198	1.0198
2:00 PM	0.9398	0.9398	0.9398	0.9398	0.9398	0.5699	0	0	0.9398	0.9398	0.9398	0.9398
3:00 PM	0.9398	0.9398	0.9398	0.9398	0.9398	0.9398	0	0	0.9398	0.9398	0.9398	0.9398
4:00 PM	0.2	0.2	0.2	0.2	0.2	0.2	0	0	0.2	0.2	0.2	0.2
5:00 PM	0.2	0.2	0.2	0.2	0.2	0.2	0	0	0.2	0.2	0.2	0.2
6:00 PM	0.2133	0.2133	0.2133	0.2133	0.2133	0.2133	0.2078	0.2078	0.2133	0.2133	0.2133	0.2133
7:00 PM	0.08	0.08	0.08	0.08	0.08	0.08	0.08	0.08	0.08	0.08	0.08	0.08
8:00 PM	0.08	0.08	0.08	0.08	0.08	0.08	0.08	0.08	0.08	0.08	0.08	0.08
9:00 PM	0.08	0.08	0.08	0.08	0.08	0.08	0.08	0.08	0.08	0.08	0.08	0.08
10:00 PM	0.08	0.08	0.08	0.08	0.08	0.08	0.08	0.08	0.08	0.08	0.08	0.08
11:00 PM	0.08	0.08	0.08	0.08	0.08	0.08	0.08	0.08	0.08	0.08	0.08	0.08
Energy demand in a day (KWh)	5.8382	5.8382	5.8382	5.8382	5.8382	4.5285	1.7278	1.7278	5.8382	5.8382	5.8382	5.8382
Days of each Month	31	28	31	30	31	30	31	31	30	31	30	31
Total Monthly Greenhouse energy demand (KWh/Month)	180.9842	163.4696	180.9842	175.146	180.9842	135.855	53.5618	53.5618	175.146	180.9842	175.146	180.9842
Total Annual greenhouse energy demand	1836.81 KWh/year or 1.83681 MWh/year											

Table 15.Monthly and Annual greenhouse energy consumption

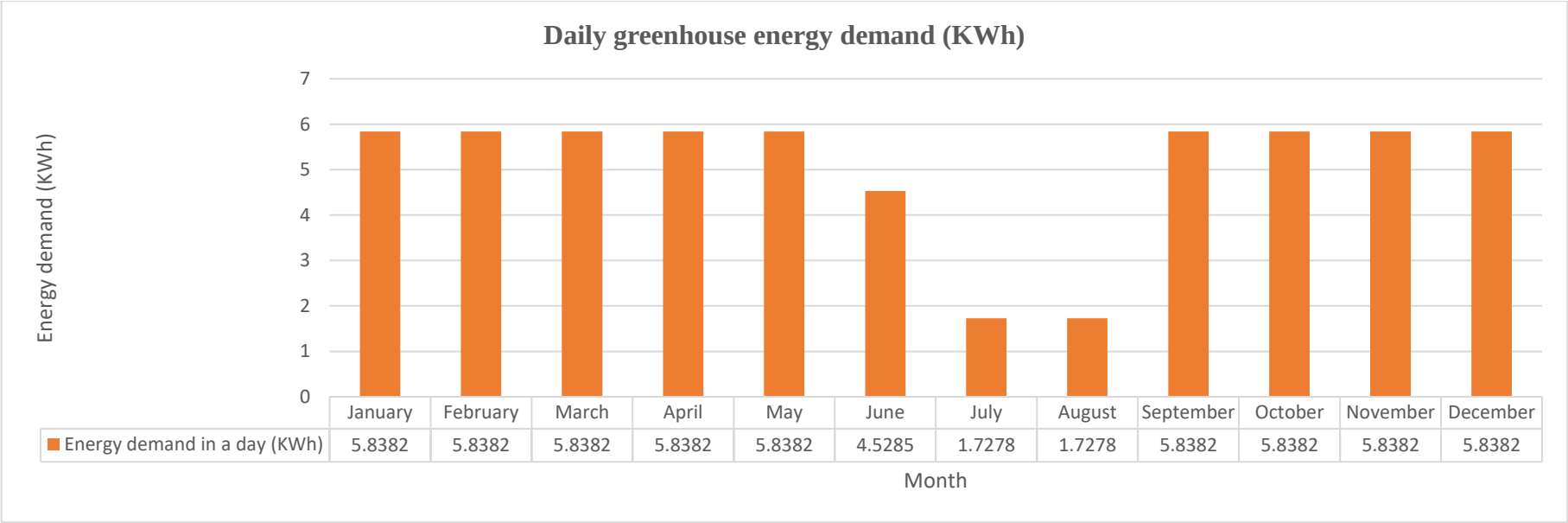

Figure 36. Daily greenhouse energy demand (KWh)

3.7.3. Average Monthly energy Demand showing different peaks

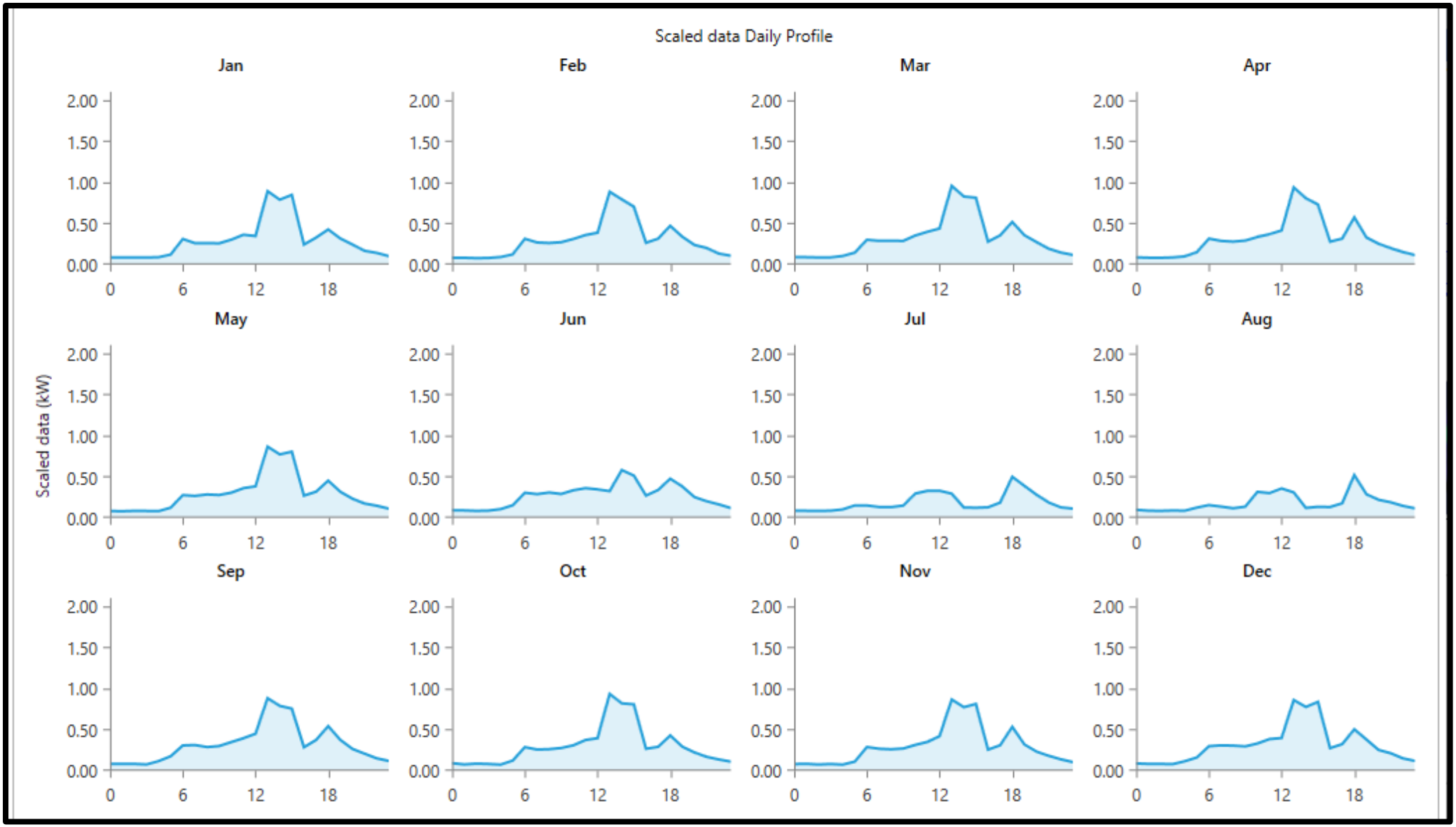

Figure 37. Monthly energy Demand showing different peak

3.7.4. Design of Horizontal Axial Wind Turbine -Solar PV Hybrid energy system

The hybrid energy system was designed using Helioscope integrated in HOMER Pro. Below are some specifications of the hybrid system with a storage system

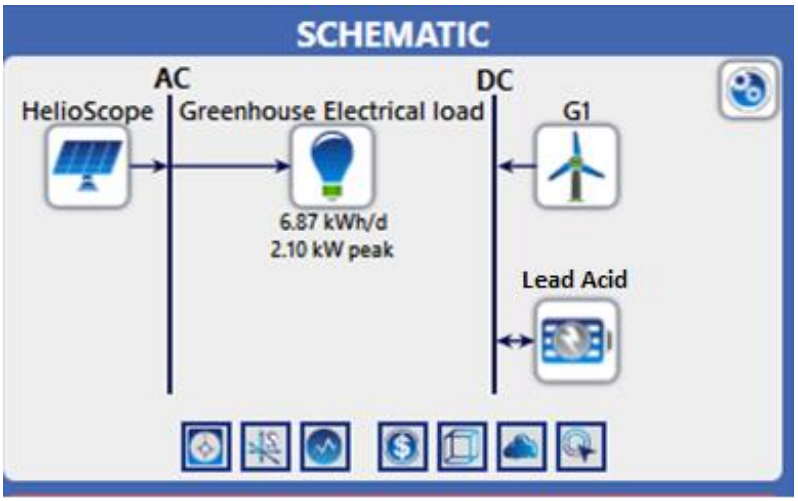

Figure 38. Schematic Greenhouse Electric load

3.7.5. Hybrid energy system components			
Items	**Description**	**Quantity**	**Other specification**
Solar Panel	Mono 280W	8	
Small Horizontal Wind Turbine	48V 600W	1	
Solar Battery	12V150AH	1	
Solar charge controller	48	1	
Wind turbine controller	48V	1	
Off grid inverter	48V 5000W	1	Replacing those from Heliscope software
PV cable	$4mm^2$	100m	
Total power generation	**2.70 KW**		

Table 16. Hybrid energy system components

3.7.6. Solar PV system

The Solar PV system design and sizing were performed using Helioscope software. Below is the annual report of the simulation of solar PV production and specification taken into consideration:

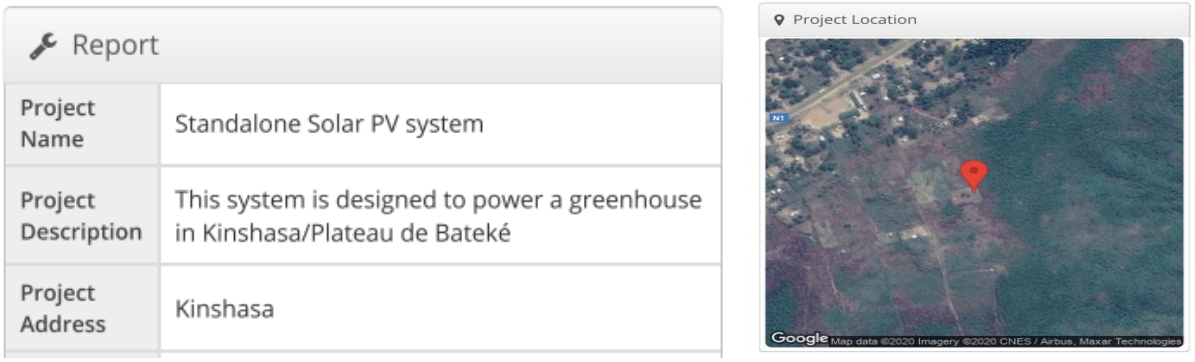

Figure 39. The site location.

System Metrics

Design	Greenhouse power system design
Module DC Nameplate	2.24 kW
Inverter AC Nameplate	1.92 kW Load Ratio: 1.17
Annual Production	2.602 MWh
Performance Ratio	73.1%
kWh/kWp	1,161.4
Weather Dataset	TMY, 10km Grid, meteonorm (meteonorm)
Simulator Version	ba7829daaf-726d75db9a-fd0d440941-8b7f968367

Figure 40. Solar PV annual energy

Field Segments

Description	Racking	Orientation	Tilt	Azimuth	Intrarow Spacing	Frame Size	Frames	Modules	Power
Field Segment 1	Flush Mount	Portrait (Vertical)	25°	180°	0.0 ft	1x1	8	8	2.24 kW

Components

Component	Name	Count
Inverters	M250 (240V) (Enphase)	8 (1.92 kW)
AC Branches	8 AWG (Copper)	1 (7,439.4 ft)
Module	REC Solar, REC280TP (280W)	8 (2.24 kW)

Figure 41. Field segments and components

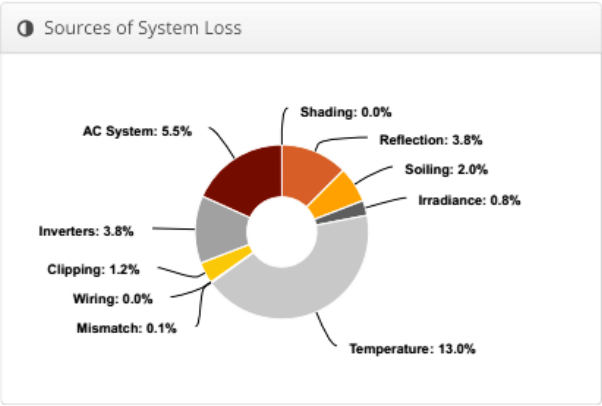

Figure 42. Solar PV energy technical loss

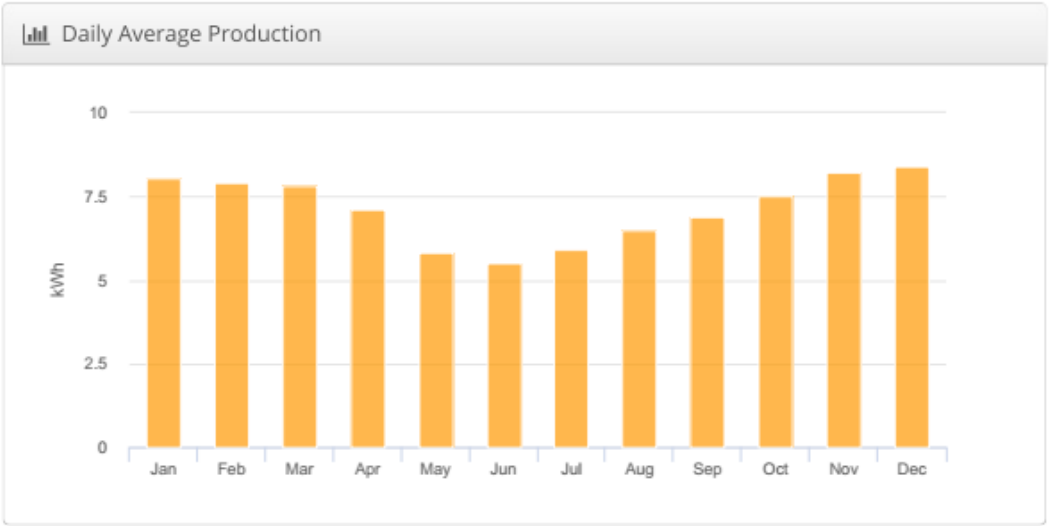

Figure 43. Daily Solar PV energy production

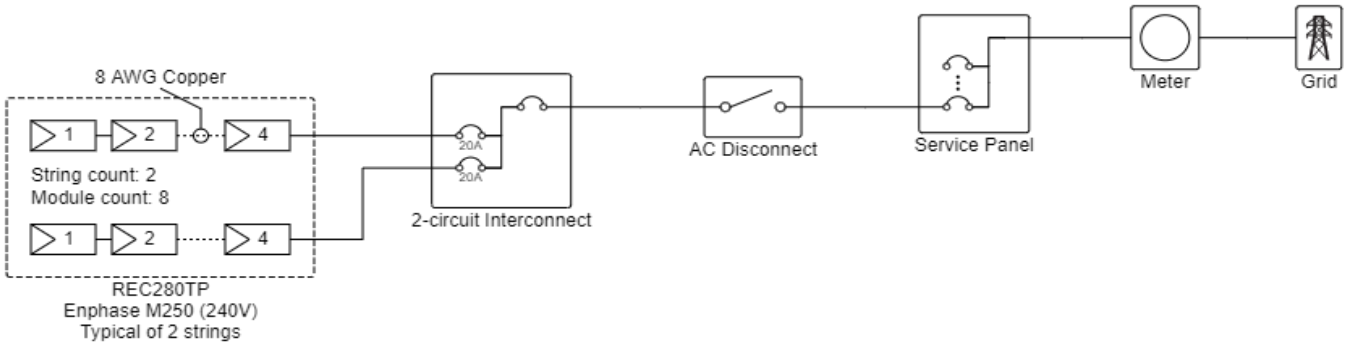

Module Specifications	
8x REC Solar REC280TP	
STC Rating	280 W
Vmp	31.9 V
Imp	8.78 A
Voc	39.2 V
Isc	9.44 A

Inverter Specifications	
8x Enphase M250 (240V)	
Max AC Power Rating	240 W
Max Input Voltage	48 V
Min AC Power Rating	0 W
Min Input Voltage	16 V

Wire Schedule		
Tier	Wire	Length

Figure 44. Electrical scheme/Inverter

Annual Production

	Description	Output	% Delta
Irradiance (kWh/m²)	Annual Global Horizontal Irradiance	1,715.6	
	POA Irradiance	1,589.8	-7.3%
	Shaded Irradiance	1,589.8	0.0%
	Irradiance after Reflection	1,529.7	-3.8%
	Irradiance after Soiling	1,499.1	-2.0%
	Total Collector Irradiance	**1,499.1**	**0.0%**
Energy (kWh)	Nameplate	3,358.7	
	Output at Irradiance Levels	3,330.4	-0.8%
	Output at Cell Temperature Derate	2,897.3	-13.0%
	Output After Mismatch	2,895.6	-0.1%
	Optimal DC Output	2,895.6	0.0%
	Constrained DC Output	2,861.4	-1.2%
	Inverter Output	2,753.1	-3.7%
	Energy to Grid	**2,601.5**	**-5.5%**
Temperature Metrics			
	Avg. Operating Ambient Temp		26.9 °C
	Avg. Operating Cell Temp		44.9 °C
Simulation Metrics			
	Operating Hours		4508
	Solved Hours		4508

Table 17. Solar PV annual Energy production

Condition Set

Description	Condition Set 1											
Weather Dataset	TMY, 10km Grid, meteonorm (meteonorm)											
Solar Angle Location	Meteo Lat/Lng											
Transposition Model	Perez Model											
Temperature Model	Sandia Model											
Temperature Model Parameters	Rack Type	a	b	Temperature Delta								
	Fixed Tilt	-3.56	-0.075	3°C								
	Flush Mount	-2.81	-0.0455	0°C								
Soiling (%)	J	F	M	A	M	J	J	A	S	O	N	D
	2	2	2	2	2	2	2	2	2	2	2	2
Irradiation Variance	5%											
Cell Temperature Spread	4° C											
Module Binning Range	-2.5% to 2.5%											
AC System Derate	0.50%											
Module Characterizations	Module	Uploaded By	Characterization									
	REC280TP (REC Solar)	Folsom Labs	Spec Sheet Characterization, PAN									
Component Characterizations	Device	Uploaded By	Characterization									
	M250 (240V) (Enphase)	Folsom Labs	CEC									

Table 18. Condition set for simulation

3.7.7. Wind turbine design and sizing

In this study, a rated 600 W small scale horizontal axis wind turbine with rotor radius of 1.8 m and Tip Speed Ratio of 6 was designed to work at low wind speed for greenhouse applications in Kinshasa. Based on the low wind speed characteristic of Kinshasa/ Plateau de Bateké weather condition, below are the required wind turbine specification needed to be associated to be associated to solar PV system in a small hybrid energy configuration:

Horizontal Axis Wind Turbine Specification	
Rated power	600W
Maximum Power	620W
Rated voltage	48V
Start-up wind speed	2m/s
Rated wind speed	13m/s
Survival wind speed	50m/s
Wheel diameter	1.5m
Tower height	6m
Number of blades	3
Generator type	Three phase permanent magnet AC synchronous generator
Control system	Electromagnet/wind wheel yaw
Speed regulation	Automatically adjust windward direction

Table 19. Horizontal Axis Wind Turbine Specification

3.7.8. Storage energy system

Energy storage technologies offer several significant benefits such as the improved stability of power quality and reliability of power supply. There are several methods for storing energy such as mechanical, electrical, chemical, electrochemical, and thermal. In this hybrid energy system, battery storage has been chosen to store energy. Based on the greenhouse energy demand and the energy usage hour, the role of battery is of supplying electricity for electronic components and lighting system.

The specification of that storage energy system is detailed in the table below:

Energy storage / Battery storage specification	
Type	Lead acid battery
Nominal Capacity	150Ah
Nominal battery Voltage	12VDC
Fast charge Time	8-16h
Cycle life	300-5000 times+DOD 80%
Overcharge tolerance	high
Self-discharge/month	5%
Maintenance requirement	3-6 Months

Table 20. Battery storage specification

3.8. GREENHOUSE COMPONENTS

For a synchronized performance of the proposed greenhouse system, those components are needed:

Items	Specifications	usage
Energy system (hybrid HAWT-Solar PV) with lead acid battery storage system	*Table 16, Table 17, Table 19 and Table 20*	To supply electricity to the entire greenhouse system
Covering system (sidewall and roof)	*Table 9*	Physical and thermal protection of crops
Shading system	Material: Polyethylene (PE) thick; Shading rate: 50%; Color: green (light reflection and absorption)	Shade net is used to provide shade against sunlight and control temperature.
Netting system	*Table 9, Table 9. Physical Properties of covering and netting system.*	to protect flowers, trees against frost, wide and hail damage. It is also used for fencing, lateral covering
Windows	1.4*32m	Close or open greenhouse air inlet
Misting system	Length: 32m; number of nozzles:16; diameter of nozzle hole:	For cooling air temperature in the greenhouse
Exhaust fans	*Table 11*	
Solar submersible pump		
Erecting system	Wooden sustain by concrete	Supporting the entire greenhouse system
Water tank	2000 liters	Storing water
Filters for misting system	5-micron, low pressure misting	Using advanced coconut carbon filtration to clear unclogged nozzles by eliminating sediments, rust, dirt and other water impurities.
Electric Actuators (linear)	29V55W, Speed 23mm/s, Stroke 1.6m Max. Load 800N	For window openings
Electric Actuators (rotary)	12V55W, 1600rpm	For the displacement of the shading system

3.9. CONFIGURATION OF THE PROPOSED FULL-SCALE GREENHOUSE

The proposed greenhouse has a "modified shed roof" and its area is of 13.5 m * 32 m. The structure has a side height of 8m to the top of main roof. The greenhouse has an air inlet opening area of $32m^2$ (1m * 32m) oriented perpendicular towards the main direction of wind flow (west for the Kinshasa region Figure 18). A window (for air inlet) with electric actuators is designed

to open or close the air inlet opening as needed. The greenhouse also has a secondary roof separated from the main roof by the air inlet opening. The misting system is located above the level of the secondary roof of the greenhouse and sprays water in a direction parallel to the slope of the main roof. Due to the elevated emplacement of the misting system, the water droplets from the misting nozzles would not reach the foliage of the plants (this hypothesis will be checked during testing phase). Then, the cooled air entering through the air inlet opening is led to the interior space of the greenhouse and exits to the opposite side area of 64m^2 (2m ×32 m) covered by a netting system of 60.8% of holes. In the event of a low wind speed and a high relative humidity rate which would have the additional consequence of increasing the temperature, a forced evacuation system using exhaust fans is started. There are six exhaust fans used for the volume of the proposed greenhouse. A shading system mounted on electric rotary actuators is temporarily rolled up or unrolled below the main roof, stabilizing the air temperature and the relative humidity, by the way, reducing the energy consumption of Exhaust fans. Moreover, a lighting system is used to compensate light deficits due to the shading system. An effective and efficient coordination of the proposed cooling configuration is developed for economical use of water and especially energy. This configuration based on the proposed energy usage planning (in Table 12) saves significantly the entire greenhouse energy consumption; only 5.8382 KWh/day in summer months and 1.7KWh/day in winter months (for 24 hours). To optimize the energy consumption of the greenhouse, a specific timing is set in Table 12, Table 13, Table 14 and Figure 36 for different cooling components (natural ventilation, misting system, shading system and exhaust fans).

Two submersible solar pumps are used. One for pumping water for the misting system, and another for supplying water in the tank and pumping water in an eventual drip irrigation system. Two water filters are used to filter water before entering the misting system, for prevention of nozzles clogging (Figure 45. Greenhouse configurationFigure 45).

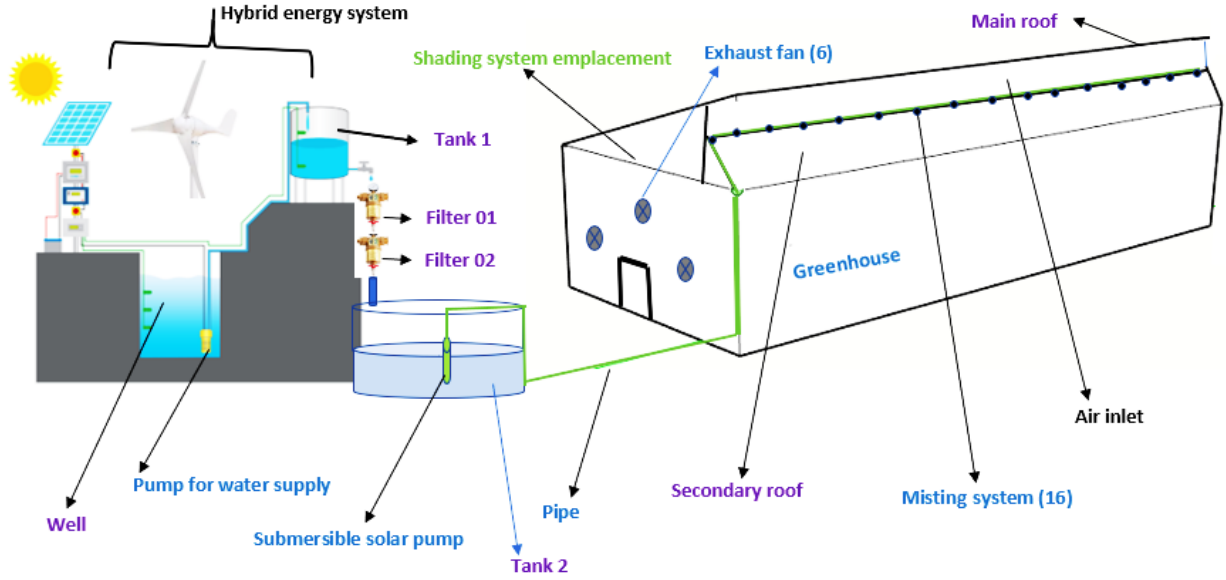

Figure 45. Greenhouse configuration

3.10. GREENHOUSE COST ESTIMATION

The cost estimation is summarized in the below table (the cost is in USA dollar, with an exchange rate of 1900 CDF =1$). The related tax charge is not taken into consideration and for international purchase, shipping cost is not considered. The platforms consulted for international prices are Alibaba and amazon, August 2020). The area of the proposed greenhouse being expressed in square meter (432m^2), the cost has been also estimated per square meter (m^2).

Item	**Quantity**	**Cost/Unit**	**Total Cost**	**Cost/m^2 of greenhouse**
Solar Panel (W)	2240	0.17	380.8	0.881481
Small Horizontal Wind Turbine	1	150	150	0.347222
Solar Battery	1	48	48	0.111111
Solar charge controller	1	45	45	0.104167
Wind turbine controller	1	51	51	0.118056
Inverters	3	60	180	0.416667
PV cable (m)	50	0.05	2.5	0.005787
Covering system for roof (m^2)	0.3	506	151.8	0.351389
Covering system sidewall (m^2)	0.15	455	68.25	0.157986
Shading system (m^2)	0.05	432	21.6	0.05
Netting system (m^2)	0.2	64	12.8	0.02963
Windows	2	22	44	0.101852
Misting system	1	30	30	0.069444
Exhaust fans	6	22	132	0.305556
Solar submersible pump	2	71	142	0.328704
Erecting system and concrete	1	50	50	0.115741
Water tank	1	60	60	0.138889
Filters for misting system water	2	4	8	0.018519
Electric linear actuators	4	14	56	0.12963
Electric rotary actuators	8	10	80	0.185185
Wire (m)	100	0.04	4	0.009259
Lighting	4	2.5	10	0.023148
Total greenhouse cost				**3.999421**

Table 21. Cost estimation USA dollar per square meter

The proposed greenhouse costs approximatively **3.99 USA dollars/m^2**

3.11. PROTOTYPE CONSTRUCTION AND IoT BASED TESTING

The prototyping phase of this research was conducted for the proof of concept and testing on the field the proposed greenhouse cooling system, for testing the performance of the full-scale designed and configured greenhouse. The cooling technology effectiveness was tested and its energy consumption was deduced from data recorded.

The full-scale greenhouse was miniaturized in keeping the same configuration and functioning mode. Its surface area was of 8.75 m^2 (representing the 1/49 surface of the full-scale greenhouse proposed in this research) and it was total empty during the testing phase. The front height was of 3 m and the back one of 2.5 m. The greenhouse was covered by a white and blue transparent polyethylene plastic. The shading system was of blue semitransparent polyethylene plastic. The misting system used was placed at 3m height (

Figure 51).

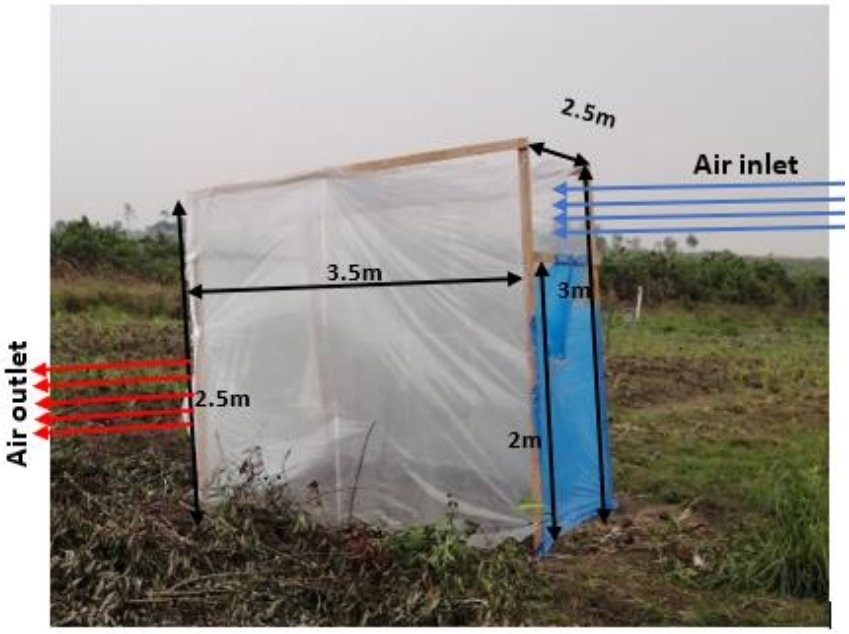

Figure 46. Prototype built for basic testing of concept

The IoT based testing and other testing approaches were performed to measure some key parameters such as:

- Indoor air temperature;
- Indoor relative humidity;
- Outdoor temperature;
- Outdoor relative humidity;
- Light transmission;
- Greenhouse infrared radiation;

- Indoor air circulation;
- Wind speed;
- Wind direction;
- Indoor airflow;
- Reactiveness of cooling system.

The description and specifications of IoT testing instruments and others are in below table:

Instrument/ Sensor	**Specification**	**usage**
Anemometer instrument	Type: NTK060-EN P1-3 **Air velocity measurement**: Unit m/s; Range 0-30; Resolution 0.1; Threshold 0.1; Accuracy ±5%. **Temperature measurement** Unit °C; Range -10 to 45; Resolution 0.2; Accuracy ±2%	The measurement of wind speed outside the greenhouse inlet. The instrument has also a thermometer measuring the outdoor temperature
Temperature and humidity sensor DHT22	Temperature Range: -40°C to 80°C; Temperature Accuracy: ± 0.5°C Humidity Range: 0% to 100% Humidity Accuracy: ± 2 to 5% Reading Rate 0.5Hz (once every 2 seconds)	For temperature and relative humidity measurement both indoor and outdoor
TEMP 18B20 sensor	Current Consumption: 1mA Resolution: 12 bits Conversion Time: < 750ms Humidity Range: 20-90% RH Humidity Accuracy: ±5% RH Temperature Range: 0-100 °C Temperature Accuracy: ±2% °C Operating Voltage: 3V to 5.5V	Indoor and outdoor temperature and relative humidity measurement
Light dependent Resistor (Photoresistor)	Max voltage @ 0 lux 200V Peak wavelength: 600nm Min. resistance 10lux 1.8kΩ Max. resistance 10lux 4.5kΩ Type. resistance 100lux 0.7kΩ Dark resistance after 1 sec 0.03MΩ Dark resistance after 5 sec 0.25MΩ	A photoresistor or light dependent resistor is an electronic component that is sensitive to light. When light falls upon it, then the resistance changes. It helped in measuring the influence of shading system on light transmittance
Airflow visualization test	A source of smoke placed in the greenhouse helping in the qualitative description of the airflow pattern	Descripting airflow pattern inside the greenhouse
Compass + GPS	Type: GARMIN Etrex GPS Satellite system: GPS + beidou; Positioning accuracy: 1m; Positioning time: 45s; Track navigation: Support; Compass: Support; Coordinate point storage: 1000 records; Data export format: TXT / GPX / CAD / BMP	For localization (long, latitude and altitude) and guiding in the choice of the greenhouse roof opening orientation
Watch and date record	Phone watch and computer	Measured different time needed for instance the

		reactiveness of the cooling system

Table 22. Description and specifications of the testing instruments

Two different sensors have been used to measure each thermo-physical parameter inside the greenhouse so to approach the data accuracy and eliminating eventual errors which could have occurred in using just one instrument.

Arduino sensors were mounted and installed with Arduino kits (see the appendix). The coding was performed on Arduino platform (in c+ programming language). Data were displayed simultaneously on Arduino screen LCD 1602 16 chars 2 lines Arduino and PC screen (via serial monitor). Data collected were stored on computer database through wire transmission mode.

Calibration of sensors

The calibration was made based on the thermometer included in the Anemometer Neoteck used in this research (detail of instrument can be seen in Table 22. Description and specifications of the testing instrumentsTable 22). It has been observed that the difference was negligible between the DHT11 sensor and the thermometer included in the Anemometer Neoteck.

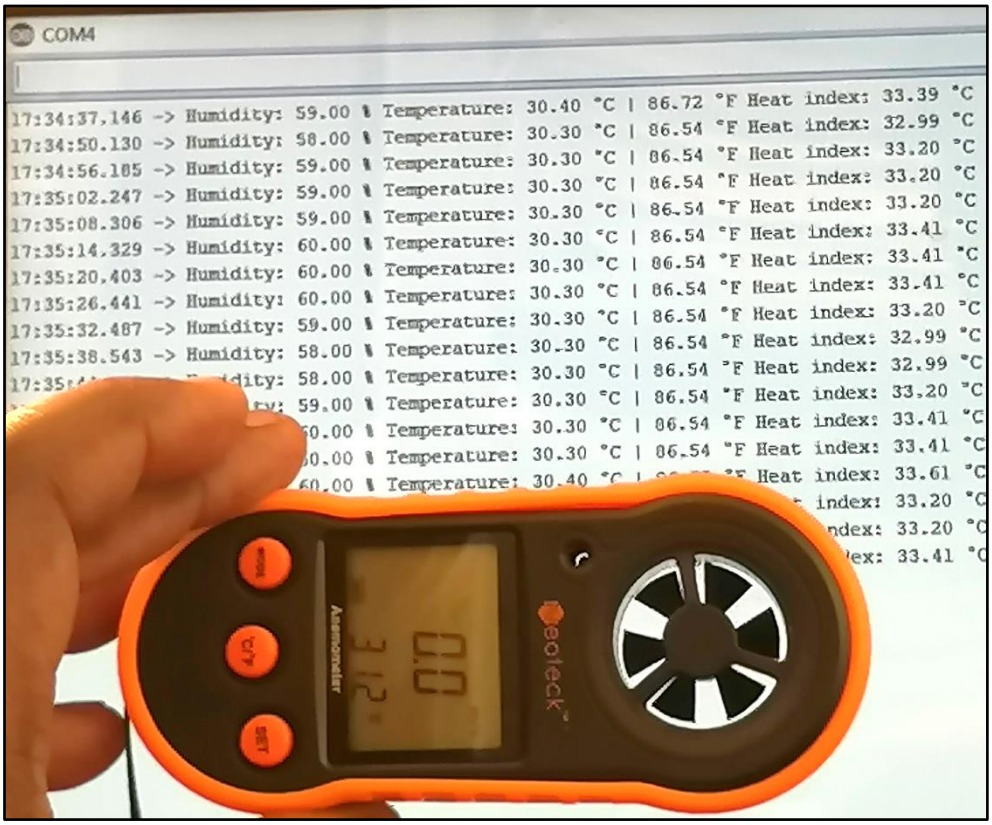

Figure 47. The calibration of DHT11 with Anemometer Neoteck

The difference between those instruments is of 2.9%.

DHT11 Temperature and relative humidity Arduino code

To run the DHT11 Temperature and relative humidity Arduino measurement instrument constructed in this Master thesis (seen in Figure 48), the below programming codes have been written and uploaded in the Arduino microcontroller.

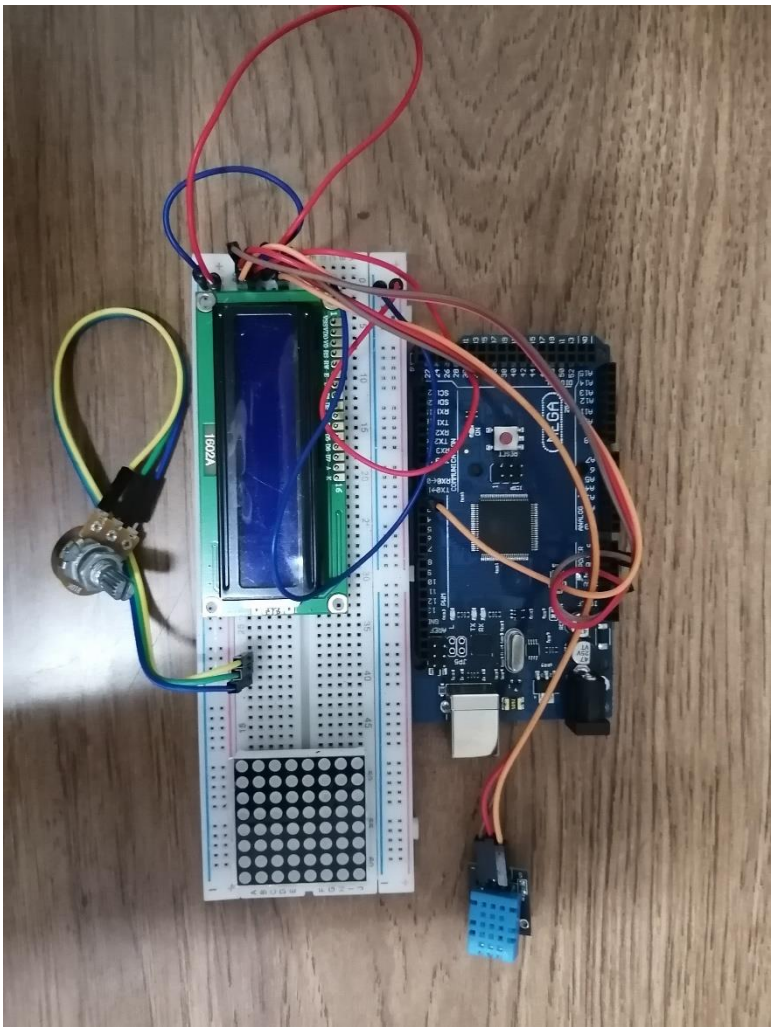

Figure 48. DHT11 Temperature and Relative humidity Arduino constructed instrument

```
/* Arduino code for DHT11 temperature and humidity sensors. By Constant Kunambu for Greenhouse testing phase */
// Include the libraries:
#include <Adafruit_Sensor.h>
#include <DHT.h>
// Set DHT pin:
#define DHTPIN 2
#define DHTTYPE DHT11   // DHT 11
DHT dht = DHT(DHTPIN, DHTTYPE);
void setup() {
  // Begin serial communication at a baud rate of 9600:
  Serial.begin(9600);
  // Setup sensor:
  dht.begin();
}
void loop() {
  // Wait a few seconds between measurements:
  delay(6000);
  // Reading temperature or humidity takes about 5 seconds!
  // Sensor readings may also be up to 5 seconds 'old' (it's a very slow sensor)
  // Read the humidity in %:
  float h = dht.readHumidity();
  // Read the temperature as Celsius:
```

```
  float t = dht.readTemperature();
  // Read the temperature as Fahrenheit:
  float f = dht.readTemperature(true);
  // Check if any reads failed and exit early (to try again):
  if (isnan(h) || isnan(t) || isnan(f)) {  Serial.println("Failed to read from DHT sensor!");
return;
  }
  // Compute heat index in Fahrenheit (default):
  float hif = dht.computeHeatIndex(f, h);
  // Compute heat index in Celsius:
  float hic = dht.computeHeatIndex(t, h, false);
  Serial.print("Humidity: ");
  Serial.print(h);
  Serial.print(" % ");
  Serial.print("Temperature: ");
  Serial.print(t);
  Serial.print(" \xC2\xB0");
  Serial.print("C | ");
  Serial.print(f);
  Serial.print(" \xC2\xB0");
  Serial.print("F ");
  Serial.print("Heat index: ");
  Serial.print(hic);
  Serial.print(" \xC2\xB0");
  Serial.print("C | ");
  Serial.print(hif);
  Serial.print(" \xC2\xB0");
  Serial.println("F");
}
```

Photoresistor code (Light Dependent Resistor)

To run the Light Dependent Resistor (Photoresistor) Arduino measurement instrument constructed in this master thesis (seen in), the below programming codes have been written and uploaded in the Arduino microcontroller.

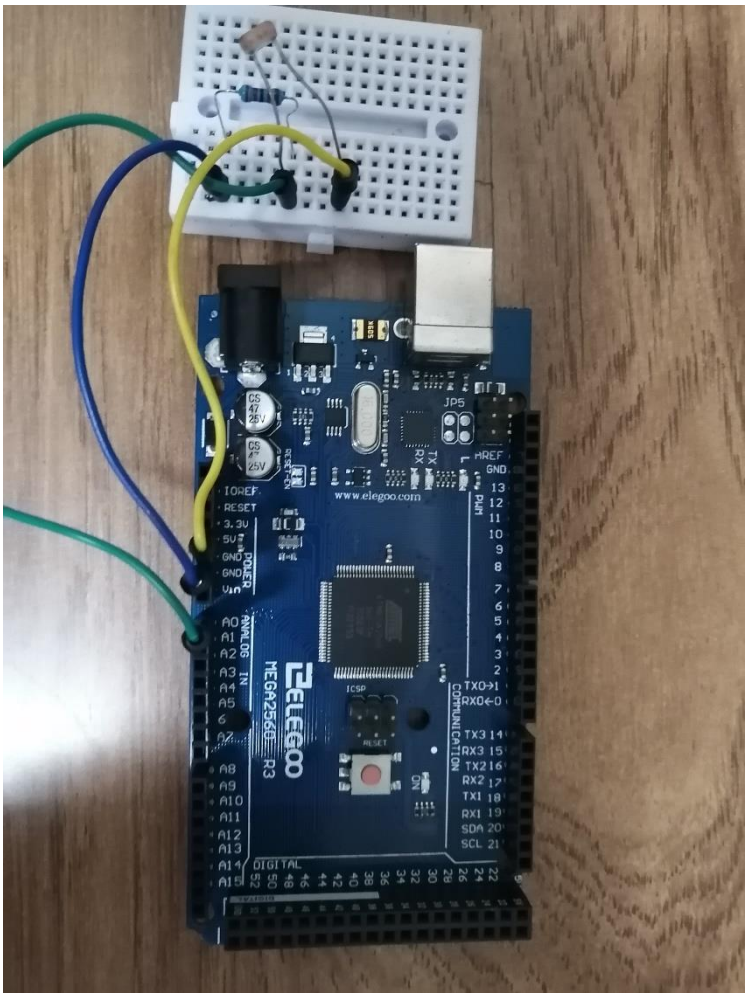

Figure 49. Photo resistor -LDR Arduino constructed instrument

```
const int LDR = A0;
int input_val = 0;

void setup()
{
  Serial.begin(9600);
}
void loop()
{
  input_val = analogRead(LDR);
  Serial.print("LDR Value is: ");
  Serial.println(input_val);
  delay(6000);
}
```

Conversion of LDR in Ohm (Ω) to Lux and Lux to W/m^2

RL=500/lux	R is the resistance connected to LDR (in our Arduino system R=1kΩ)
V0=5*(RL/(RL+R))	
V0=LDR_value*ADC_value	LDR_value is the Analog value read by micro-controller pin
lux=(250/V0)-50	ADC_value is system_voltage/Resolution of ADC
Where:	V0 is the analog measured voltage
RL is the resistance of LDR	lux is illumination calculated
	For the sunlight the conversion is of 0.0079W/m^2 per Lux.

CHAPTER 4. RESULTS AND DISCUSSION

From the analysis of data gathered in this Master Thesis, we highlighted some meteorological characteristics of the tropical savannah climate of Kinshasa. From the result, the annual average temperature was found to be 25.3 ° C, the annual average relative humidity of 82.5%, the annual precipitation is 1,400 mm and the direction of wind mainly from west with average speed of 3 m/s.

A specific greenhouse structure was designed and validated based on the result of data analysis of meteorological data of Kinshasa. The validated greenhouse structure was simulated in Ansys-Fluent. This greenhouse structure enabled a satisfactory air circulation, as shown in Ansys-Fluent simulation results, helped in decreasing rapidly the relative humidity and stabilizing the interior temperature. To manage effectively the relative humidity especially when the wind speed is low (0-1m/s), 6 exhaust fans were designed and simulated (on ANSYS Fluent) to be used for forced air evacuation.

The simulation in Ansys-Fluent has shown an even distribution of temperature and a satisfactory air circulation in the validated greenhouse structure. The temperature and pressure were found slightly high around the inlet and out let regions, especially for the wind speed of 3m/s (Figure 25). The air velocity in inlet region was also observed to be slightly high. This slight increasing of air velocity around inlet region was attributed to the specific roof structure and air inlet emplacement chosen and validated for the proposed greenhouse.

An air recirculation in the proposed full-scale greenhouse was clearly identified on velocity profiles (Figure 25 and Figure 26). And the same recirculation was observed during the air circulation visualization test in the miniaturized greenhouse prototype (Figure 50).

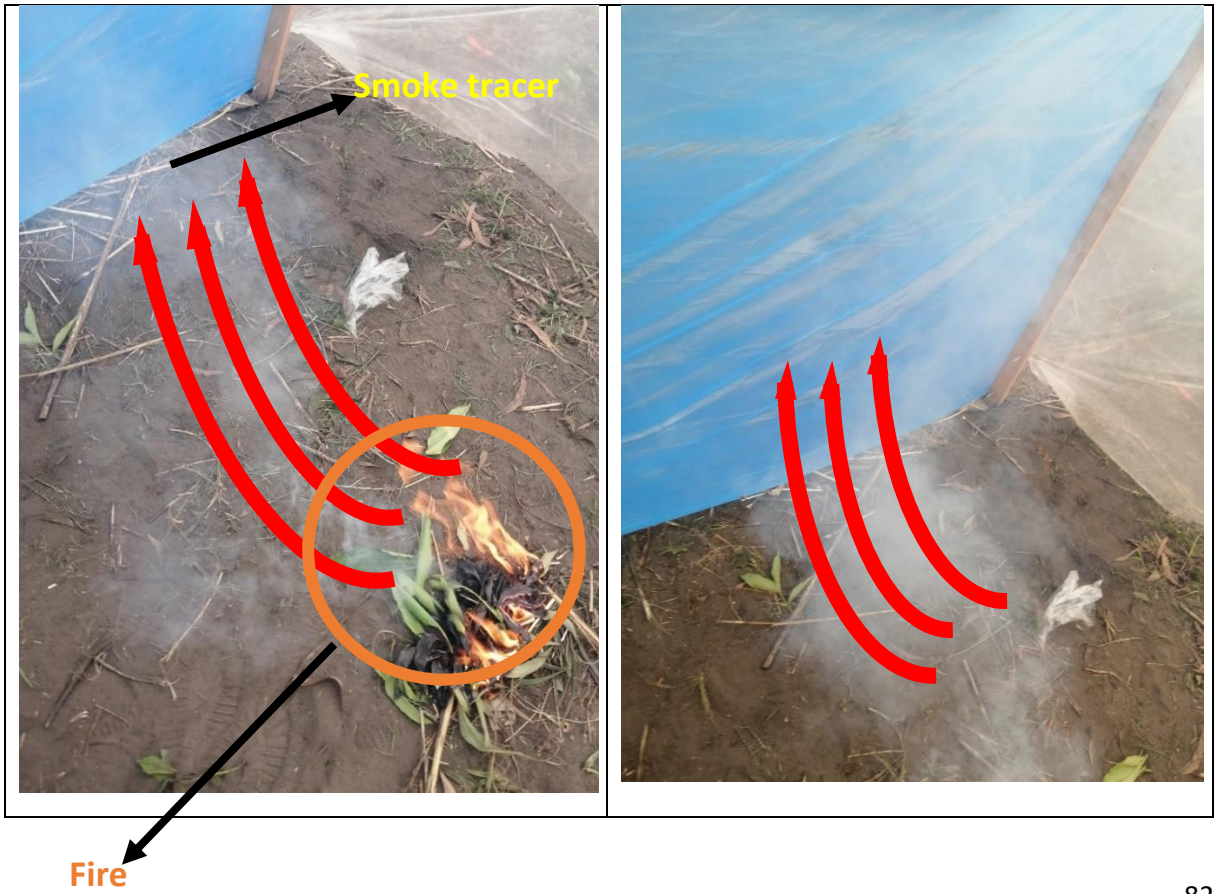

Figure 50. Airflow visualization test

The proposed greenhouse in its miniaturized form was built in Kinshasa Menkao (4.2099771 S; 15.7011222 E). The testing phase was carried out between 12:00 noon to 1:00 PM (time when the solar irradiation is maximal in Kinshasa, Figure 11). The DHT11 sensor, LDR and PC data recording station were placed in the outlet region (Figure 51). The smoke source for air circulation visualization test was placed in the middle of the miniaturized greenhouse (region with low pressure and where the air recirculation has been observed clearly in CDF simulation profiles).

Figure 51. Misting system used in the testing phase and sensors location

The result of the shading testing has shown a little impact on light transmittance. The shading system did not quite affect light transmittance in the greenhouse (Figure 52) but had a high contribution in the stabilization of the relative humidity at 64%. A slight temperature drop was observed from 30°C to 29.2°C in 1 minute and 18 seconds due to the use of shading system (This can be seen on Figure 52.The influence of shading system measured by LDRFigure 52 from 12:21:10 PM to 12:22:28 PM, where the shading system slightly reduced the light transmittance).

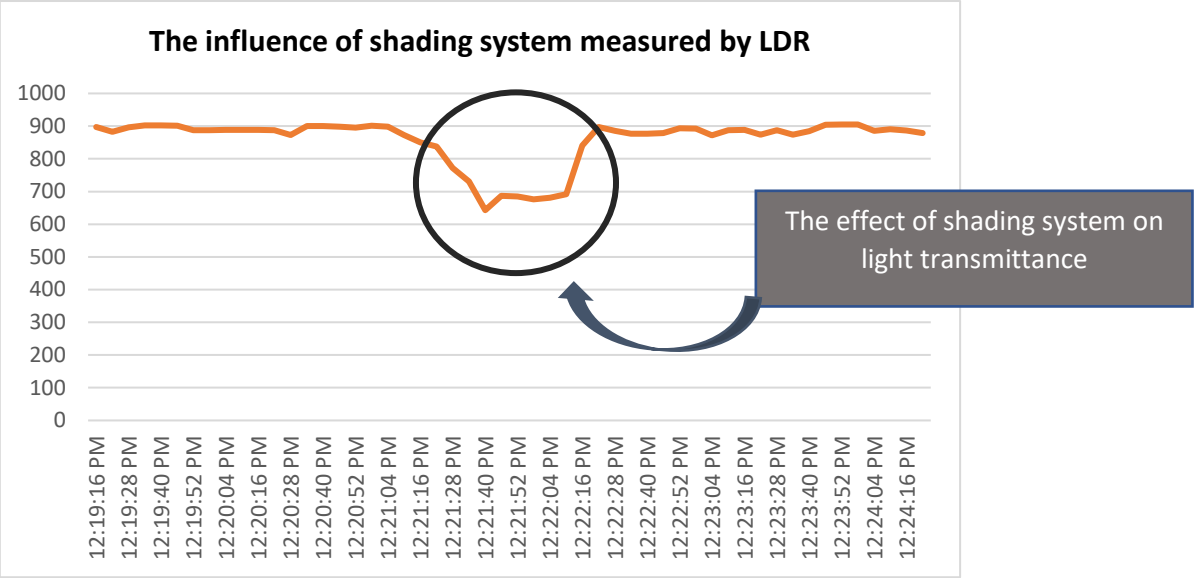

Figure 52.The influence of shading system measured by LDR

The result of the cooling test (in the miniaturized greenhouse) has shown a rapid and sharp drop in inside greenhouse temperature and a corresponding increase in inside relative humidity. The temperature changes occur quickly, within 48 seconds (from 12:58:48 to12:59:30, Figure 53), upon use of the configured cooling system (Figure 54 , Figure 55 and Table 25 of data acquisition table in Appendix) compared the average outside temperature of 30.4°C observed during the testing phase (Table 23 in Appendix).

Compared to greenhouse fan pad systems, where conditions vary greatly when cooling occurs, the greenhouse system tests showed that inside greenhouse conditions remained almost stable for the entirety of the operation period. The magnitude of these changes depended on the initial inside greenhouse conditions and the volume of water misted. The configuration of the misting system used in testing phase has shown a water consumption of 0.42 $L.h^{-1}.m^{-2}$ (see the Flow rate measurement in appendix Figure 59).

The proposed greenhouse in its miniaturized design and under Kinshasa outdoor conditions, provided 1°C to 7 ° C of cooling compared to the outside temperature (Figure 53 and Table 23). The cooling system has shown a high reactiveness. The temperature drop due to the misted water has been observed just 48 seconds after spraying water from the misting system for the spraying duration of 1minute 11seconds (12:58:48 PM to 12:59:59 PM). The temperature reached its lowest level 23°C after 10 minutes 11 seconds (Figure 53) and started increasing slowly. The temperature was stabilized under the initial temperature for 22 minutes.

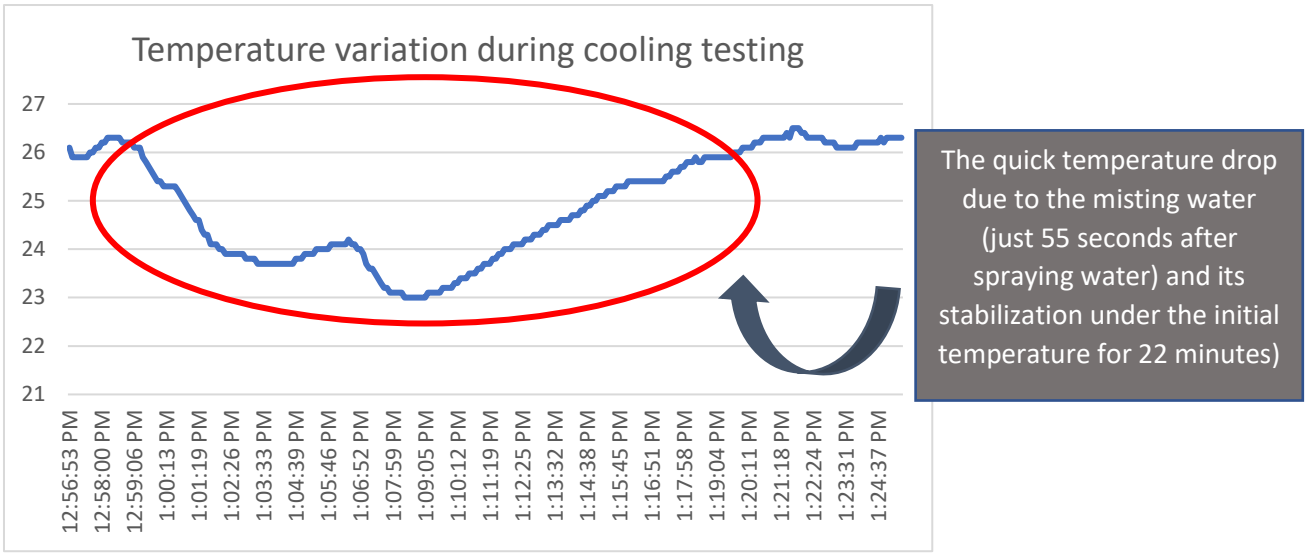

Figure 53. Temperature variation during cooling testing

The management of relative humidity has been identified to be the big challenge for greenhouse used in Kinshasa with a tropical savannah climate where relative humidity remains very high along the year. The cooling system proposed in this research has shown an increasing in relative humidity of 1% to 24% during the testing phase (from 63% to 87%, Figure 54 and Table 25 in appendix). The repercussion, in terms of the effect on interior relative humidity were rapid, after the activation of the cooling system. In just 3 minutes 31(from 12:58:48 PM to 1:02:13 PM) seconds after activating the misting system, the relative humidity increased by 21% followed by a short stagnation period and slight drop due to the air circulation and 4 minutes 57 seconds later, the relative humidity reached its highest level of 87%. We have observed a drastic increasing in relative humidity of 24% in a short time (8minutes 28 seconds) and a linear drop towards the initial value. The quick stabilization of relative humidity while the temperature remained at lower than its initial value was realized thanks to the designed roof shape and the air inlet emplacement which have favored a good greenhouse indoor air circulation playing the role of dehumidifier.

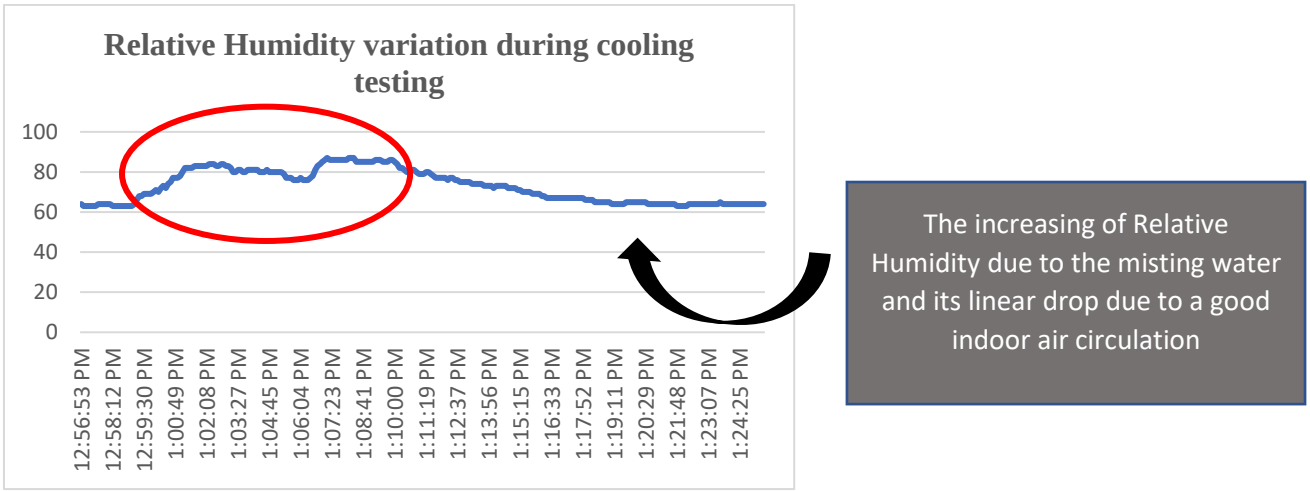

Figure 54. Relative Humidity variation during the testing phase

Some remarkable heterogeneity has been observed during a same phase nobly during the increasing phase of relative humidity and decreasing phase of temperature. Ideally, after the activation of misting system, the relative humidity is supposed to increase while the temperature decreases. A remarkable heterogeneity is seen on Figure 55, where instead of observing respectively the increasing and decreasing of relative humidity and air temperature, we observe a reverse scenario where the relative humidity slightly decreases while the air temperature slightly increases. This would likely be the mere consequence of an abrupt change in air velocity and the position of DHT11 sensor placed in the outlet region, where the temperature is inclined to be high as demonstrated in the result of CFD temperature simulation (Figure 30, Figure 31 and Figure 32).

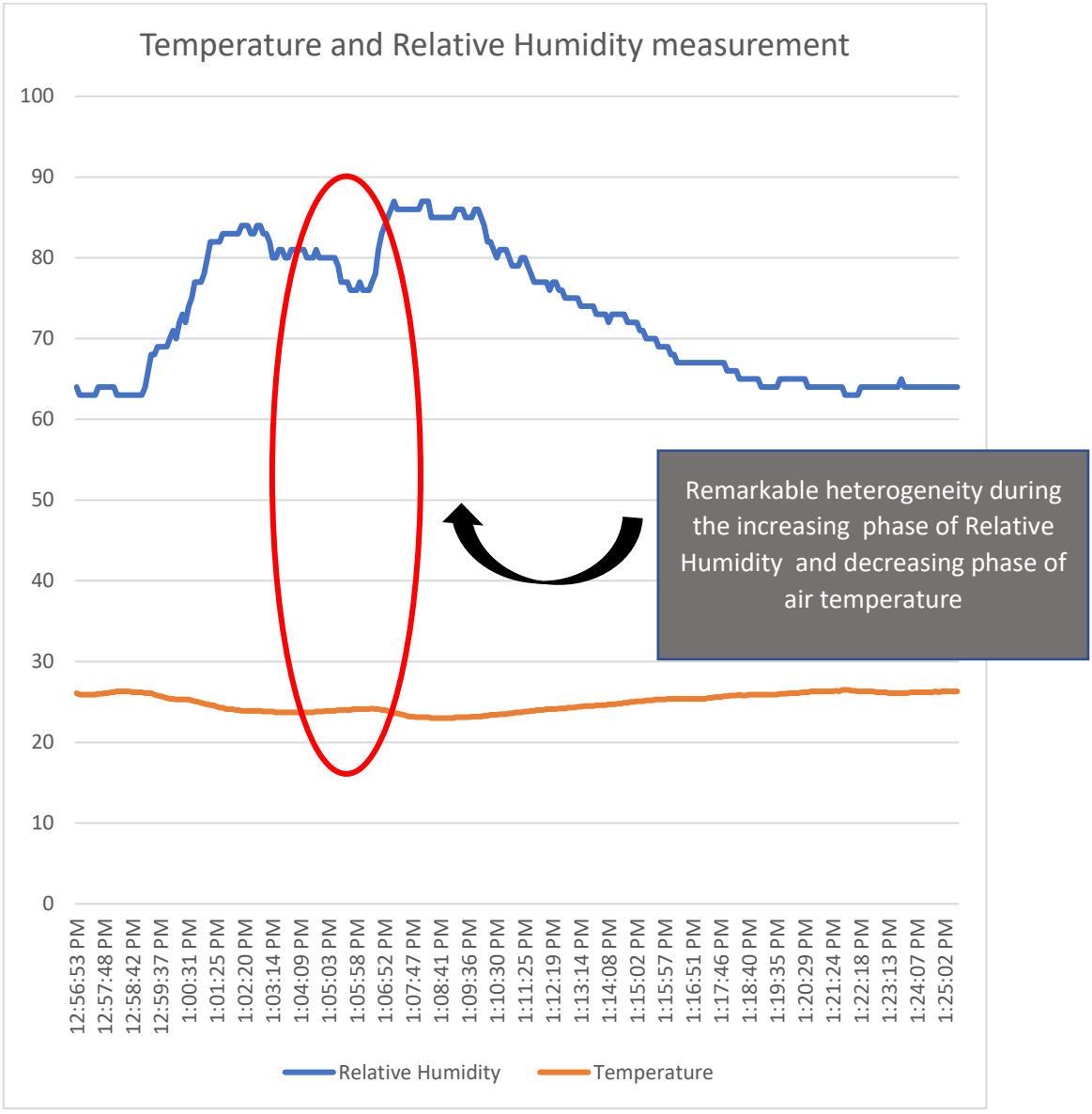

Figure 55. Temperature and Relative Humidity measurement

A design and sizing of a Hybrid Wind-Solar PV energy system with the storage system as a backup were meticulously carried out for the full-scale greenhouse. A specific cooling configuration was proposed based on energy efficiency and the running cost. An effective and efficient coordination of the proposed cooling configuration was developed for an economical

use of water and especially energy in the entire greenhouse. This configuration based on the designed energy usage planning (in Table 12) saves significantly the entire greenhouse energy consumption; only 5.8382 KWh/day in summer months and 1.7KWh/day in winter months (for 24 hours). To optimize the energy consumption of the greenhouse, a specific timing was set in Table 12, Table 13, Table 14 and Figure 36 for different cooling components (natural ventilation, misting system, shading system and exhaust fans). The cost of the proposed greenhouse was estimated to be 3.94 USA dollar per square meter, cost which made the proposed greenhouse affordable.

Based on the objective and the aim of this study, the above compiled results are satisfactory. However, our study had several limitations notably, the lack of carrying out the experimentation of electric actuators for window and shading system, the construction a small size of the prototype using only one mist nozzle, the absence of exhaust fans during the testing phase and the absence of the designed hybrid energy system during the testing experimentation. Those limitations restricted our study from a full demonstration of the concept. Those limitation were mainly due to the financial and time constraints. The main reason of not overcoming those limitations was the Covid-19 pandemic coerced us to slightly change our research topic (by removing the smart and automation chapter from our study) and pushed us to change the location of the prototype construction (initially in Tlemcen). In addition, the covid-19 pandemic effect rendered the equipment shipping quasi impossible in the needed time.

CONCLUSION AND RECOMMANDATIONS

In many countries of Africa notably the Democratic Republic of Congo farmers suffer from high yield losses, which mainly is the result of unfavorable and/or unpredictable weather conditions (including climate change effect) for crops. Thus, in the quest to gain superiority over crop yield, there is the need to provide favorable micro climate conditions necessary for plants (vegetables and fruits) to produce maximum yield. It has been also highlighted that the greenhouse components and cooling technologies come with high cost of investments and involve high-energy consumption.

This work was geared towards identifying the current challenges that exist within the greenhouse sector in the savannah tropical climate and developing a new type of greenhouse more adequate, energetically efficient and affordable for small as well as large farmers thus, to boost their yield which remain low due to several reasons including the exclusive dependence on natural climatic factors such as rain, seasons instability and climate change effect.

The proposed greenhouse (13.5m×32m) uses a new energy efficient cooling method designed and tested for savanna tropical climates in emphasizing more on the simplicity of technology, use of local materials, affordability and energy efficiency. A specific cooling configuration was proposed based on energy efficiency and the running cost. The proposed greenhouse cooling system is mainly based on natural ventilation sustained by a misting system, a shading system and 6 exhaust fans. An effective and efficient coordination of the proposed cooling configuration was developed for an economical use of water and especially energy in the entire greenhouse. This configuration based on the designed energy usage planning saves significantly the entire greenhouse energy consumption; only 5.8382 KWh/day in summer and 1.7KWh/day in winter. The energy consumption was optimized by a specific timing set for different cooling components (natural ventilation, misting system, shading system and exhaust fans). The prototype provided 1°C to 7 ° C of cooling compared to the outside temperature. The cooling system proposed in this research has shown an increase in relative humidity of 1% to 24% during the testing phase. A design and sizing of a Hybrid Wind-Solar PV energy system with the storage system were meticulously carried out for the full-scale greenhouse. Finally, the cost of the proposed full-scale greenhouse was estimated to be 3.94 USA dollar per square meter, cost which made the proposed greenhouse affordable.

The result of this research has provided a new tropical greenhouse structure with an adequate energy efficient cooling configuration meeting the meteorological constraints of savannah tropical climate. This offers a new perspective for modern agriculture and can boost significantly food production (especially vegetables and fruits) in Democratic Republic of Congo/Kinshasa as well as in other African countries with similar weather conditions.

We recommend further full-scale testing for the proposed greenhouse for providing a full demonstration of the concept and we strongly suggest future studies may be oriented towards a design of a smart monitoring and control as well as the automated system that should optimize the use of energy and water in the proposed greenhouse.

REFERENCES

1. Abdel-Ghany, A. M., Al-Helal, I. M., Alzahrani, S. M. Alsadon, A. A., Ali, I. M., & Elleithy, R. M. (2012). Covering materials incorporating radiation-preventing Techniques to meet greenhouse cooling challenges in arid regions: A review. The Scientific World Journal.

2. Abdel-Ghany, A. M., Al-Helal, I. M., Picuno, P., & Shady, M. R. (2016). Modified plastic net-houses as alternative agricultural structures for saving energy and water in hot and sunny regions. Renewable Energy.

3. Abdel-Ghany, A. M., Goto, E., & Kozai, T. (2006). Evaporation characteristics in a naturally ventilated, fog-cooled greenhouse. Renewable Energy.

4. Abu-Hamdeh, N. H., & Almitani, K. H. (2016). Solar liquid desiccant regeneration and nanofluids in evaporative cooling for greenhouse food production in Saudi Arabia. Solar Energy.

5. Alejandra Jimenez, Santiago Jimenez, Pablo Lozada, and Cristhy Jimenez, "Wireless sensors network in the efficient management of greenhouse crops," in Proceedings of the Nineth International Conference on Information Technology: New Generations (ITNG), Las Vegas, 1618 April 2012, pp. 680685.

6. Arcidiacono, C., D'Emilio, A., Mazzarella, R., & Leonardi, C. (2006). Covering materials to improve greenhouse microclimate during summer in hot climates. Acta Horticulturae.

7. Attar, I., Naili, N., Khalifa, N., Hazami, M., Lazaar, M., & Farhat, A. (2014). Experimental study of an air conditioning system to control a greenhouse microclimate. Energy Conversion and Management.

8. Baeza, E., Perez-Parra, J., Montero, J., Bailey, B., L opez, J., & Gazquez, J. (2009). Analysis of the role of sidewall vents on buoyancy-driven natural ventilation in parral-type greenhouses with and without insect screens using computational fluid dynamics. Biosystems Engineering.

9. Banik, P., & Ganguly, A. (2017). Performance and economic analysis of a floricultural greenhouse with distributed fan-pad evaporative cooling coupled with solar desiccation. Solar Energy.

10. Bank, w., 2016. The household electrification rate in sub-Saharan Africa is the lowest in the world, Washington DC: World Bank.

11. Bao, Yan Sheng, Wei Yao, and Wei Zhang. 2012. "Design of Wireless Sensor Network Based on PSoC." Advanced Materials Research 433–440: 5568–72. https://doi.org/10.4028/www.scientific.net/AMR.

12. Boulard, T. (2011). Advantages and constraints of CFD greenhouse modelling. Acta Horticulturae.

13. Campen, J. B., & Bot, G. P. A. (2003). Determination of greenhouse specific aspects of ventilation using three-dimensional computational fluid dynamics. Biosystems Engineering.

14. Campiotti, C. A., Morosinotto, G., Puglisi, G., Schettini, E., & Vox, G. (2016). Performance evaluation of a solar cooling plant applied for greenhouse thermal control. Agriculture and Agricultural Science Procedia.

15. Ceylan, I., Ergun, A., Acar, B., & Aydin, M. (2016). Psychometric and thermodynamic analysis of new ground source evaporative cooling system. Energy and Buildings.

16. Chen, J., Cai, Y., Xu, F., Hu, H., & Ai, Q. (2014). Analysis and optimization of the fan-pad evaporative cooling system for greenhouse based on CFD. Advances in Mechanical Engineering.

17. Chou, S. K., Chua, K. J., Ho, J. C., & Ooi, C. L. (2004). On the study of an energy-efficient greenhouse for heating, cooling and dehumidification applications. Applied Energy.

18. Chu, C., Lan, T., Tasi, R., Wu, T., & Yang, C. (2017). Wind-driven natural ventilation of greenhouses with vegetation. Biosystems Engineering.

19. Critten, D. L., & Bailey, B. J. (2002). A review of greenhouse engineering developments during the 1990s. Agricultural and forest Meteorology,

20. Critten, D. L., & Bailey, B. J. (2002). A review of greenhouse engineering developments during the 1990s. Agricultural and forest Meteorology.

21. Cuce, P. M., & Riffat, S. (2016). A state-of-the-art review of evaporative cooling systems for building applications. Renewable and Sustainable Energy Reviews.

22. Dehbi, A., & Mourad, A. I. (2016). Durability of mono-layer versus tri-layers LDPE films used as greenhouse cover: Comparative study. Arabian Journal of Chemistry.

23. Despommier, D. (2011). The vertical farm: controlled environment agriculture carried out in tall buildings would create greater food safety and security for large urban populations. Journal für Verbraucherschutz und Lebensmittelsicherheit,

24. Djevic, M., and A. Dimitrijevic. 2009. “Energy Consumption for Different Greenhouse Constructions.” Energy 34 (9): 1325–31. https://doi.org/10.1016/j.energy.

25. El-Maghlany, W. M., Teamah, M. A., & Tanaka, H. (2015). Optimum design and orientation of the greenhouses for maximum capture of solar energy in North Tropical Region. Energy Conversion and Management.

26. Environment effect on plants, Colorado State University, 2013. Available http://www.cmg.colostate.edu/gardennotes.shtml

27. Espinoza, K., Lopez, A., Valera, D., Molina-Aiz, F., Torres, J., & Pena, A. (2017). Effects of ventilator configuration on the flow pattern of a naturally-ventilated three-span Mediterranean greenhouse. Biosystems Engineering.

28. Farrell, E., Hassan, M. I., Tufa, R. A., Tuomiranta, A., Avci, A. H., Politano, A., & Arafat, H. A. (2017). Reverse electrodialysis powered greenhouse concept for water-and energy-self-sufficient agriculture. Applied Energy,

29. Feuilloley, P., & Issanchou, G. (1996). Greenhouse covering materials measurement and modelling of Thermal properties using the hot box method, and condensation effects. Journal of Agricultural Engineering Research.

30. Flores-Velazquez, J., Montero, J. I., Baeza, E. J., & Lopez, J. C. (2014). Mechanical and natural ventilation systems in a greenhouse designed using computational fluid dynamics. International Journal of Agricultural and Biological Engineering.

31. Franco, Antonio, Diego L. Valera, and Araceli Peña. 2014. “Energy Efficiency in Greenhouse Evaporative Cooling Techniques: Cooling Boxes versus Cellulose Pads.” Energies 7 (3): 1427–47. https://doi.org/10.3390/en7031427.

32. Ganguly, A., Misra, D., & Ghosh, S. (2010). Modeling and analysis of solar photovoltaic-electrolyzer-fuel cell hybrid power system integrated with a floriculture greenhouse. Energy and Buildings.

33. Ghosal, M. K., Tiwari, G. N., & Srivastava, N. S. L. (2003). Modeling and experimental validation of a greenhouse with evaporative cooling by moving water film over external shade cloth. Energy and Buildings.

34. Ghosh, A., & Ganguly, A. (2017). Performance analysis of a partially closed solar regenerated desiccant assisted cooling system for greenhouse lettuce cultivation. Solar Energy.

35. Giacomelli G, Castilla N, Vanhenten E, Mears D, Sase S (2008) Innovation in greenhouse engineering. Acta Hortic

36. Guan, L., Bennett, M., & Bell, J. (2015). Evaluating the potential use of direct evaporative cooling in Australia. Energy and Buildings.

37. Gupta, M. J., & Chandra, P. (2002). Effect of greenhouse design parameters on conservation of energy for greenhouse environmental control. Energy.

38. Gupta, R., Tiwari, G. N., Kumar, A., & Gupta, Y. (2012). Calculation of total solar fraction for different orientation of greenhouse using 3D-shadow analysis in Auto-CAD. Energy and Buildings.

39. Guzman-Cruz, R., Castaneda-Miranda, R., Garcia-Escalante, J. J., Lopez-Cruz, I. L., Lara-Herrera, A., & De la Rosa, J. I. (2009). Calibration of a greenhouse climate model using evolutionary algorithms. Biosystems Engineering.

40. Hasni, A., Taibi, R., Draoui, B., & Boulard, T. (2011). Optimization of greenhouse climate model parameters using particle swarm optimization and genetic algorithms. Energy Procedia.

41. Hassanien, E. R. H., Li, M., & Lin, W. D. (2016). Advanced applications of solar energy in agricultural greenhouses. Renewable and Sustainable Energy Reviews.

42. He, K. S., Chen, D. A., Sun, L. J., Liu, Z. L., & Huang, Z. Y. (2015). The effect of vent openings on the microclimate inside multi-span greenhouses during summer and winter seasons. Engineering Applications of Computational Fluid Mechanics.

43. He, K. S., Chen, D. A., Sun, L. J., Liu, Z. L., & Huang, Z. Y. (2015). The effect of vent openings on the microclimate inside multi-span greenhouses during summer and winter seasons. Engineering Applications of Computational Fluid Mechanics.

44. Helmy, M. A., Eltawil, M., Ado-shieshaa, R. R., & El-Zan, N. M. (2013). Enhancing the evaporative cooling performance of fan-pad system using alternative pad materials and water film over the greenhouse roof. Agricultural Engineering International: CIGR Journal.

45. Hochmuth, Maynard and. 2007. "The Physiology of Vegetable Crops, 2nd Edition." In The Physiology of Vegetable Crops,.

46. Ismail, R. S. &. W. I. W., (2013). A Review of Greenhouse Climate Control a. ournal of Agricultural Science and Applications.

47. Ismail, Ramin Shamshiri & Wan Ishak Wan. 2013. "A Review of Greenhouse Climate Control a." ournal of Agricultural Science and Applications.

48. Ithaca, NY. 2020. https://cuaes.cals.cornell.edu/greenhouses/. Accessed june 3, 2020. https://cuaes.cals.cornell.edu/greenhouses/.

49. Janssen, L. H., Wams, H. E., & van Hasselt, P. R. (1992). Temperature dependence of chlorophyll fluorescence induction and photosynthesis in tomato as affected by temperature and light conditions during growth. Journal of Plant Physiology.

50. Katsoulas, N., Baille, A., & Kittas, C. (2001). Effect of misting on transpiration and conductances of a greenhouse rose canopy. Agricultural and Forest Meteorology.

51. Katsoulas, N., Kitta, E., Kittas, C., Tsirogiannis, I. L., Stamati, E., & Sayvas, D. (2006). Greenhouse cooling by a fog system: Effects on microclimate and on production and quality of a soilless pepper crop. Acta Horticulturae.

52. Katsoulas, N., Sapounas, A., De Zwart, F., Dieleman, J. A., & Stanghellini, C. (2015). Reducing ventilation requirements in semi-closed greenhouses increases water use efficiency. Agricultural Water Management.

53. Kittas, C., Bartzanas, T., & Jaffrin, A. (2000). Greenhouse evaporative cooling: measurement and data analysis. International Conference and British-Israeli Workshop on Greenhouse Techniques towards the 3rd Millennium.

54. Kittas, C., Katsoulas, N., Bartzanas, T., & Bakker, S. (2013). Greenhouse climate control and energy use. In FAO plant production and protection paper. 217. Good Agricultural Practices for greenhouse vegetable crops: Principles for Mediterranean climate areas (pp. 63e95) (Rome).

55. Kittas, C., Katsoulas, N., Bartzanas, T., & Bakker, S. (2013). Greenhouse climate control and energy use. In FAO plant production and protection paper. 217. Good Agricultural Practices for greenhouse vegetable crops: Principles for Mediterranean climate areas (pp. 63-95) (Rome).

56. Kittas, C., Katsoulas, N., Bartzanas, T., & Bakker, S. (2013). Greenhouse climate control and energy use. In FAO plant production and protection paper. 217. Good Agricultural Practices for greenhouse vegetable crops: Principles for Mediterranean climate areas (pp. 63-95) (Rome).

57. L. M. Mortensen “Effect of relative humidity on growth and flowering of some greenhouse plants,” Sci. Horticulture.

58. Lawrence, J. L., P. M. Titus & D. O. Clarke Harris. (2011). Protected agriculture and its potential role in achieving food and nutritional security in the Caribbean Region. University of the West Indies, St Augustine Campus. Caribbean Agricultural Research and Development Institute (CARDI).

59. Lee, H. W., Lee, J. W., Diop, S., & Na, O. H. (2014). Measurement of overall heat transfer coefficient of covering material with thermal screens for plastic greenhouse. Acta Horticulturae.

60. Lee, S., Lee, I., & Kim, R. (2018). Evaluation of wind-driven natural ventilation of single-span greenhouses built on reclaimed coastal land. Biosystems Engineering.

61. Li, A., Huang, L., & Zhang, T. (2017). Field test and analysis of microclimate in naturally ventilated single-sloped greenhouses. Energy and Buildings.

62. Lopez, Jose Chen. 2018. Pro-mix L'influence de la lumière sur la croissance. Accessed June 02, 2020. https://www.pthorticulture.com/fr/zone-du-savoir/influence-de-la-lumiere-sur-la-croissance.

63. Lychnos, G., & Davies, P. A. (2012). Modelling and experimental verification of a solar-powered liquid desiccant cooling system for greenhouse food production in hot climates. Energy.

64. Marucci, A., & Cappuccini, A. (2016). Dynamic photovoltaic greenhouse: Energy balance in completely clear sky condition during the hot period. Energy.

65. Mashonjowa, E., Ronsse, F., Milford, J. R., & Pieters, J. G. (2013). Modelling the thermal performance of a naturally ventilated greenhouse in Zimbabwe using a dynamic greenhouse climate model. Solar Energy.

66. McCartney, Lucas, and Mark G. Lefsrud. 2018. “Field Trials of the Natural Ventilation Augmented Cooling (NVAC) Greenhouse.” *Biosystems Engineering* 174: 159–72. https://doi.org/10.1016/j.biosystemseng.2018.07.004.

67. Mobtaker, H., Ajabshirchi, Y., Ranjbar, S., & Matloobi, M. (2019). Simulation of thermal performance of solar greenhouse in north-west of Iran: An experimental validation. Renewable Energy.

68. Mohammadi, B., Ranjbar, S. F., & Ajabshirchi, Y. (2018). Application of dynamic model to predict some inside environment variables in a semi-solar greenhouse. Information Processing in Agriculture.

69. Murakami, K., Fukuoka, N., & Noto, S. (2017). Improvement of greenhouse microenvironment and sweetness of melon (Cucumis melo L.) fruits by greenhouse shading with a new kind of near-infrared ray-cutting net in mid-summer. Scientia Horticulturae.

70. Nurarif & Kusuma, 2016).(2013. "No Title No Title." Journal of Chemical Information and Modeling 53 (9): 1689–99. https://doi.org/10.1017/CBO9781107415324.004.

71. Paul J. Kramer, "Soil moisture in relation to plant growth," Bot. Rev., Vol. 10, no. 9, pp. 52559, Nov. 1944.

72. Piscia, D., Munoz, P., Panad C., & Montero, J. I. (2015). A method of coupling CFD and energy balance simulations to study humidity control in unheated greenhouses. Computers and Electronics in Agriculture.

73. PNUD, 2013. RAPPORT NATIONAL ENERGIE DURABLE POUR TOUS A L'HORIZON 2030, KInshasa DRC: PNUD.

74. Poly-Tex. 2020. https://www.poly-tex.com/products/xa-30-commercial-greenhouse.html. Accessed june 1, 2020. https://www.poly-tex.com/products/xa-30-commercial-greenhouse.html.

75. Raya, V., Parra, M., & Cid, M. C. (2006). Influence of changes in cover and height on the climate of Canary-screenhouses for tomato growth: Preliminary results. Acta Horticulturae.

76. Runkle, E. S., Jaster, P., Heins, R. D., & Thill, C. (2002). Environmental conditions under an experimental near infra-red reflecting greenhouse film. Acta Horticulturae.

77. Sanchez-Hermosilla, J., Paez, F., Rincon, V. J., & Callejon, A. J. (2013). Evaluation of a fog cooling system for applying plantprotection products in a greenhouse tomato crop. Crop Protection.

78. Santolini, E., Pulvirenti, B., Benni, S., Barbaresi, L., Torreggiani, D., & Tassinari, P. (2018). Numerical study of wind-driven natural ventilation in a greenhouse with screens. Computers and Electronics in Agriculture.

79. Sethi, V. P. (2009). On the selection of shape and orientation of a greenhouse: Thermal modeling and experimental validation. Solar Energy.

80. Sethi, V. P., & Sharma, S. K. (2007). Survey of cooling technologies for worldwide agricultural greenhouse applications. Solar Energy.

81. Shen, Y., & Yu, S. L. (2002). Cooling methods for greenhouse in tropical region. Acta Horticulturae.

82. Singh, G., Singh, P. P., Lubana, P. P. S., & Singh, K. G. (2006). Formulation and validation of a mathematical model of the microclimate of a greenhouse. Renewable Energy.

83. Singh, G., Singh, P. P., Lubana, P. P. S., & Singh, K. G. (2006). Formulation and validation of a mathematical model of the microclimate of a greenhouse. Renewable Energy.

84. Soriano, T., Hernandez, J., Morales, M. I., Escobar, I., & Castilla, N. (2004a). Radiation transmission differences in east-west oriented plastic greenhouses. Acta Horticulturae.

85. Soriano, T., Montero, J. I., Sanchez-Guerrero, M. C., Medrano, E., Anton, A., Hern andez, J., et al. (2004). A study of direct solar radiation transmission in asymmetrical multi-span greenhouses using scale models and simulation models. Biosystems Engineering.

86. Stanciu, C., Stanciu, D., & Dobrovicescu, A. (2016). Effect of greenhouse orientation with respect to E-W axis on its required heating and cooling loads. Energy Procedia.

87. Stefani, L., Zanon, M., Modesti, M., Ugel, E., Vox, G., & Schettini, E. (2008). Reduction of the environmental impact of plastic films for green house covering by using fluoropolymeric materials. Acta Horticulturae.

88. Tamimi, E., & Kacira, M. (2013). Analysis of climate uniformity in a naturally ventilated greenhouse equipped with high
pressure fogging system using computational fluid dynamics. Acta Horticulturae.

89. Teitel, M., Montero, J. I., & Baeza, E. J. (2012). Greenhouse design: Concepts and trends. Acta Horticulturae.

90. von Zabeltitz, C. (2011). Integrated Greenhouse Systems for Mild Climates. Integrated Greenhouse Systems for Mild

Climates Climate Conditions, Design, Construction, Maintenance, Climate Control. Springer-Verlag. Wedemark, Germany.

91. von Zabeltitz, C. (2011). Integrated Greenhouse Systems for Mild Climates. Integrated Greenhouse Systems for Mild Climates Climate Conditions, Design, Construction, Maintenance, Climate Control. Springer-Verlag. Wedemark, Germany.

92. Wang, X., Luo, J., & Li, X. (2013). CFD based study of heterogeneous microclimate in a typical Chinese greenhouse in Central China. Journal of Integrative Agriculture.

93. Watson, Richard T., Marie-Claude Boudreau, and Marc W. van Iersel. 2018. "Simulation of Greenhouse Energy Use: An Application of Energy Informatics." Energy Informatics 1 (1): 1–14. https://doi.org/10.1007/s42162-018-0005-7.

94. Wei, B., Guo, S., Wang, J., Li, J., Wang, J., Zhang, J., et al. (2016). Thermal performance of single span greenhouses with removable back walls. Biosystems Engineering.

95. Willits, D. H. (2001). SE-structures and environment: The effect of cloth characteristics on the cooling performance of external shade cloths for greenhouses. Journal of Agricultural Engineering Research.

96. Willits, D. H., & Peet, M. M. (2000). Intermittent application of water to an externally mounted greenhouse shade cloth to modify cooling performance. Transactions of the ASAE, 43(5).

97. Xiao-wei, W., Jin-yao, L., & Xiao-ping, L. (2013). CFD based study of heterogeneous microclimate in a typical Chinese greenhouse in Central China. Journal of Integrative Agriculture.

98. Xu, J., Li, Y., Wanga, R. Z., Liu, W., & Zhou, P. (2015). Experimental performance of evaporative cooling pad systems in greenhouses in humid subtropical climates. Applied Energy.

99. Yang, S. H., & Rhee, J. H. (2013). Utilization and performance evaluation of a surplus air heat pump system for greenhouse cooling and heating. Applied Energy.

100. Yildirim, N., & Bilir, L. (2017). Evaluation of a hybrid system for a nearly zero energy greenhouse. Energy Conversion and Management.

101. Yiming, Zhou, Yang Xianglong, Guo Xishan, Zhou Mingang, and Wang Liren. 2007. "A Design of Greenhouse Monitoring & Control System Based on ZigBee Wireless Sensor Network." 2007 International Conference on Wireless Communications, Networking and Mobile Computing, WiCOM 2007. https://doi.org/10.1109/WICOM.2007.638.

APPENDIX

Figure 56. Anemometer

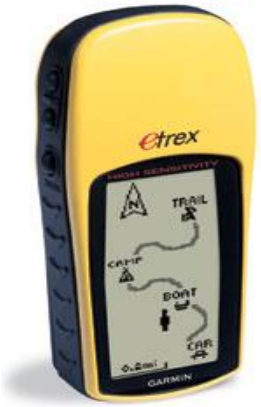

Figure 57. GPS including Compass

Figure 58. Misting system used in testing phase

Figure 59. The calculation of the misting flow rate

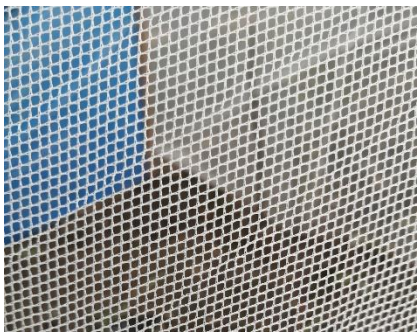

Figure 60. Netting system use for testing

Figure 61. Shading system use for testing

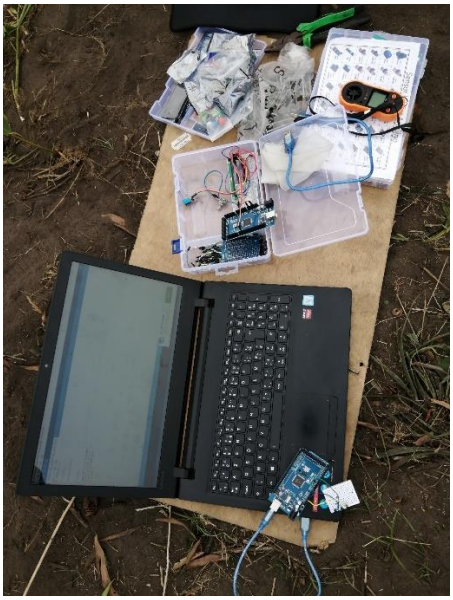

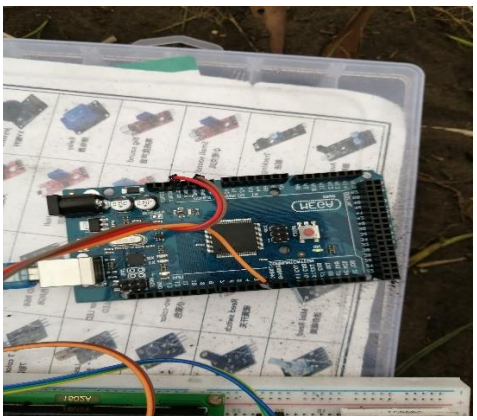


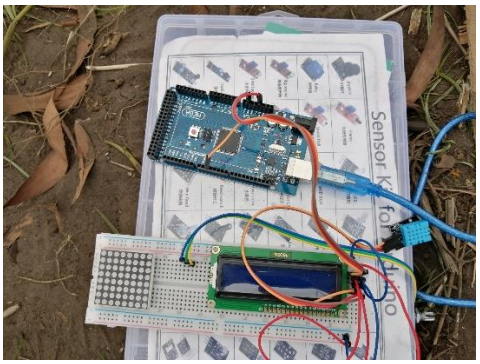

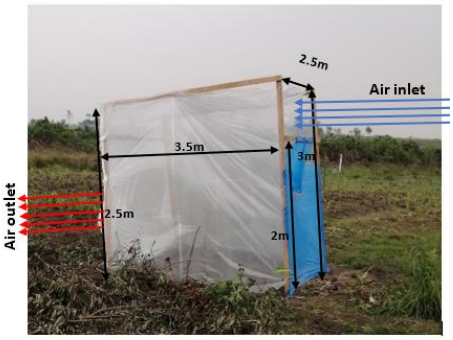



Average UV (Ultra Violet) index in Kinshasa, Democratic Republic of Congo

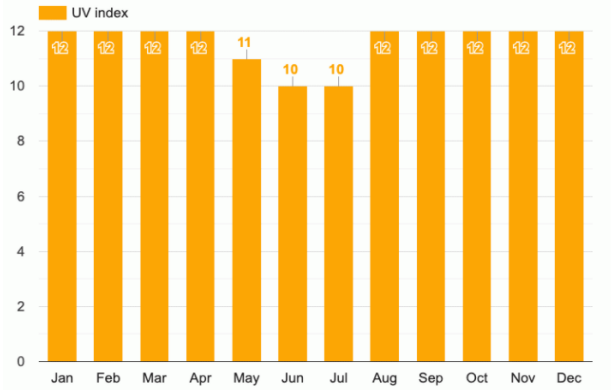

Figure 62. Average UV index Kinshasa, Democratic Republic of Congo

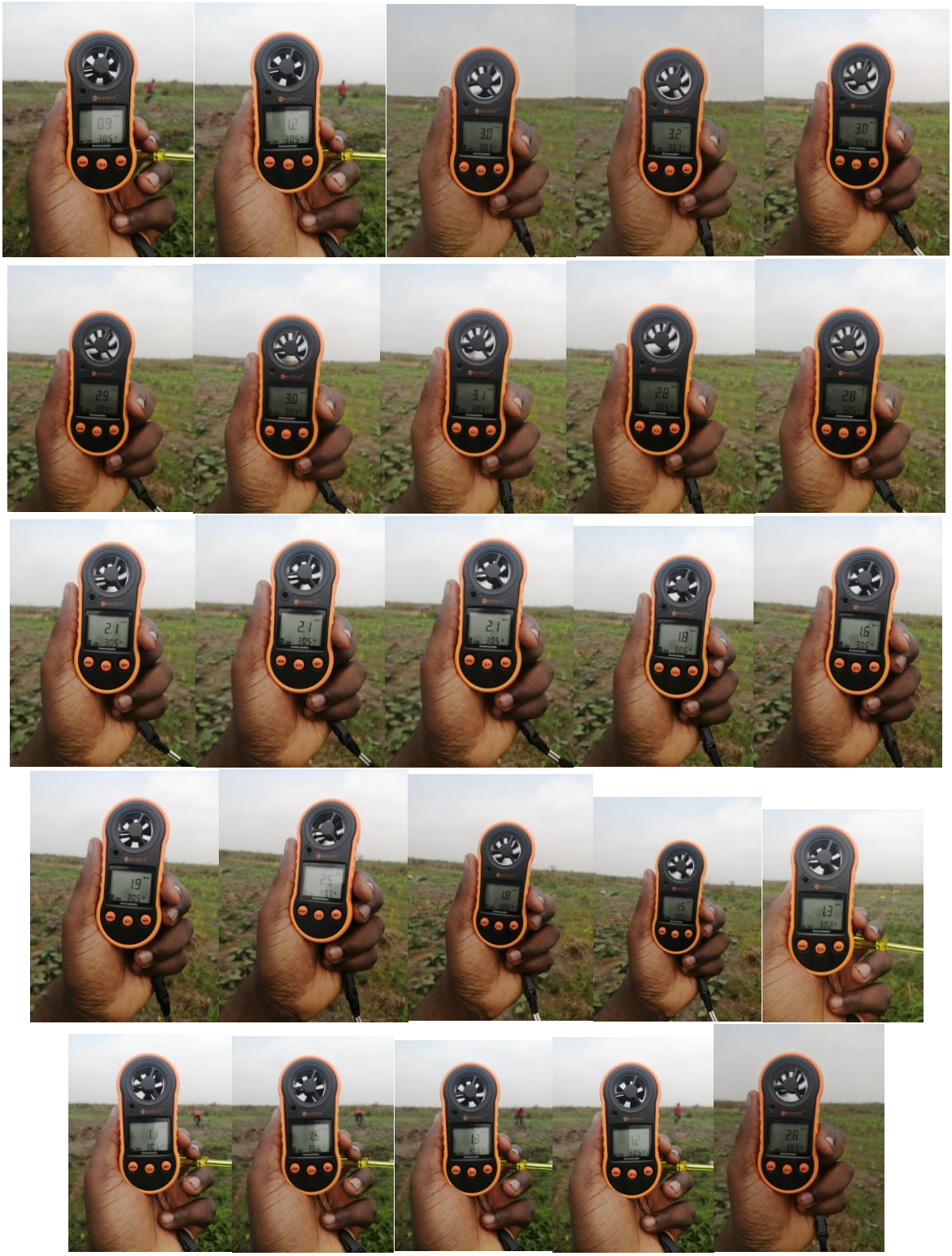

RECORDED DATA FROM TESTING PHASE (LDR, LIGHT PENETRATION)

12:19:16.132 -> LDR Value is: 897
12:19:22.141 -> LDR Value is: 883
12:19:28.148 -> LDR Value is: 896
12:19:34.150 -> LDR Value is: 902
12:19:40.155 -> LDR Value is: 902
12:19:46.156 -> LDR Value is: 901
12:19:52.175 -> LDR Value is: 888
12:19:58.171 -> LDR Value is: 888
12:20:04.177 -> LDR Value is: 889
12:20:10.173 -> LDR Value is: 889
12:20:16.201 -> LDR Value is: 889
12:20:22.209 -> LDR Value is: 888
12:20:28.209 -> LDR Value is: 873
12:20:34.221 -> LDR Value is: 900
12:20:40.225 -> LDR Value is: 900
12:20:46.231 -> LDR Value is: 898
12:20:52.231 -> LDR Value is: 895
12:20:58.259 -> LDR Value is: 901
12:21:04.257 -> LDR Value is: 898
12:21:10.251 -> LDR Value is: 873
12:21:16.254 -> LDR Value is: 850
12:21:22.289 -> LDR Value is: 838
12:21:28.272 -> LDR Value is: 772
12:21:34.277 -> LDR Value is: 731
12:21:40.309 -> LDR Value is: 643
12:21:46.321 -> LDR Value is: 687
12:21:52.329 -> LDR Value is: 855
12:21:58.336 -> LDR Value is: 676
12:22:04.338 -> LDR Value is: 681
12:22:10.348 -> LDR Value is: 692
12:22:16.351 -> LDR Value is: 841
12:22:22.361 -> LDR Value is: 897
12:22:28.367 -> LDR Value is: 886
12:22:34.355 -> LDR Value is: 877
12:22:40.371 -> LDR Value is: 877
12:22:46.392 -> LDR Value is: 879
12:22:52.371 -> LDR Value is: 893
12:22:58.396 -> LDR Value is: 892
12:23:04.411 -> LDR Value is: 872
12:23:10.407 -> LDR Value is: 888
12:23:16.443 -> LDR Value is: 889
12:23:22.437 -> LDR Value is: 874
12:23:28.425 -> LDR Value is: 888
12:23:34.434 -> LDR Value is: 874
12:23:40.453 -> LDR Value is: 885
12:23:46.462 -> LDR Value is: 904

OUTSIDE TEMPERATURE AND WIND SPEED

Outside wind speed (m/s)	Outside Temperature (°C)
0.9	30.5
1.2	30.5
3	30.3
3.2	30.3
3	30.4
2.9	30.4
3	30.4
3.1	30.4
2.8	30.5
2.8	30.5
2.1	30.5
2.1	30.5
2.1	30.5
1.8	30.6
1.6	30.6
1.9	30.5
2.5	30.7
1.8	30.5
1.5	30.5
1.3	30.2
1.1	30.5
1.5	30.5
1.3	30.6
1.2	30.5
2.8	30.3

Table 23. Outside wind speed and outside Temperature

12:23:52.463 -> LDR Value is: 905
12:23:58.477 -> LDR Value is: 905
12:24:04.488 -> LDR Value is: 886
12:24:10.487 -> LDR Value is: 891
12:24:16.479 -> LDR Value is: 887
12:24:22.489 -> LDR Value is: 879

Table 24. Photoresistor recorded data for light testing

RECORDED DATA FROM TESTING PHASE (DHT11, TEMPERATURE AND RELATIVE HUMIDITY)

12:56:53.123 -> Humidity: 64.00 % Temperature: 26.10 °C | 78.98 °F Heat index: 27.19 °C | 80.95 °F
12:56:59.199 -> Humidity: 63.00 % Temperature: 25.90 °C | 78.62 °F Heat index: 26.92 °C | 80.46 °F
12:57:05.244 -> Humidity: 63.00 % Temperature: 25.90 °C | 78.62 °F Heat index: 26.92 °C | 80.46 °F
12:57:11.294 -> Humidity: 63.00 % Temperature: 25.90 °C | 78.62 °F Heat index: 26.92 °C | 80.46 °F
12:57:17.361 -> Humidity: 63.00 % Temperature: 25.90 °C | 78.62 °F Heat index: 26.92 °C | 80.46 °F
12:57:23.401 -> Humidity: 63.00 % Temperature: 25.90 °C | 78.62 °F Heat index: 26.92 °C | 80.46 °F
12:57:29.438 -> Humidity: 63.00 % Temperature: 25.90 °C | 78.62 °F Heat index: 26.92 °C | 80.46 °F
12:57:35.507 -> Humidity: 64.00 % Temperature: 26.00 °C | 78.80 °F Heat index: 27.07 °C | 80.73 °F
12:57:41.558 -> Humidity: 64.00 % Temperature: 26.00 °C | 78.80 °F Heat index: 27.07 °C | 80.73 °F
12:57:47.603 -> Humidity: 64.00 % Temperature: 26.10 °C | 78.98 °F Heat index: 27.19 °C | 80.95 °F
12:57:53.651 -> Humidity: 64.00 % Temperature: 26.10 °C | 78.98 °F Heat index: 27.19 °C | 80.95 °F
12:57:59.700 -> Humidity: 64.00 % Temperature: 26.20 °C | 79.16 °F Heat index: 27.32 °C | 81.17 °F
12:58:05.744 -> Humidity: 64.00 % Temperature: 26.20 °C | 79.16 °F Heat index: 27.32 °C | 81.17 °F
12:58:11.819 -> Humidity: 63.00 % Temperature: 26.30 °C | 79.34 °F Heat index: 27.39 °C | 81.31 °F
12:58:17.864 -> Humidity: 63.00 % Temperature: 26.30 °C | 79.34 °F Heat index: 27.39 °C | 81.31 °F
12:58:23.910 -> Humidity: 63.00 % Temperature: 26.30 °C | 79.34 °F Heat index: 27.39 °C | 81.31 °F
12:58:29.961 -> Humidity: 63.00 % Temperature: 26.30 °C | 79.34 °F Heat index: 27.39 °C | 81.31 °F
12:58:36.007 -> Humidity: 63.00 % Temperature: 26.30 °C | 79.34 °F Heat index: 27.39 °C | 81.31 °F
12:58:42.055 -> Humidity: 63.00 % Temperature: 26.20 °C | 79.16 °F Heat index: 27.27 °C | 81.09 °F
12:58:48.119 -> Humidity: 63.00 % Temperature: 26.20 °C | 79.16 °F Heat index: 27.27 °C | 81.09 °F
12:58:54.162 -> Humidity: 63.00 % Temperature: 26.20 °C | 79.16 °F Heat index: 27.27 °C | 81.09 °F
12:59:00.236 -> Humidity: 63.00 % Temperature: 26.20 °C | 79.16 °F Heat index: 27.27 °C | 81.09 °F
12:59:06.282 -> Humidity: 64.00 % Temperature: 26.10 °C | 78.98 °F Heat index: 27.19 °C | 80.95 °F
12:59:12.318 -> Humidity: 66.00 % Temperature: 26.10 °C | 78.98 °F Heat index: 27.28 °C | 81.10 °F
12:59:18.364 -> Humidity: 68.00 % Temperature: 26.10 °C | 78.98 °F Heat index: 27.36 °C | 81.24 °F
12:59:24.446 -> Humidity: 68.00 % Temperature: 25.90 °C | 78.62 °F Heat index: 27.09 °C | 80.76 °F
12:59:30.486 -> Humidity: 69.00 % Temperature: 25.80 °C | 78.44 °F Heat index: 26.98 °C | 80.57 °F
12:59:36.520 -> Humidity: 69.00 % Temperature: 25.70 °C | 78.26 °F Heat index: 26.85 °C | 80.33 °F
12:59:42.589 -> Humidity: 69.00 % Temperature: 25.60 °C | 78.08 °F Heat index: 26.02 °C | 78.83 °F
12:59:48.625 -> Humidity: 69.00 % Temperature: 25.50 °C | 77.90 °F Heat index: 25.91 °C | 78.63 °F
12:59:54.700 -> Humidity: 70.00 % Temperature: 25.40 °C | 77.72 °F Heat index: 25.82 °C | 78.48 °F
13:00:00.747 -> Humidity: 71.00 % Temperature: 25.40 °C | 77.72 °F Heat index: 25.85 °C | 78.53 °F
13:00:06.792 -> Humidity: 70.00 % Temperature: 25.30 °C | 77.54 °F Heat index: 25.71 °C | 78.28 °F
13:00:12.839 -> Humidity: 72.00 % Temperature: 25.30 °C | 77.54 °F Heat index: 25.77 °C | 78.38 °F

Beginning of cooling system

13:00:18.893 -> Humidity: 73.00 % Temperature: 25.30 °C | 77.54 °F Heat index: 25.79 °C | 78.42 °F
13:00:24.939 -> Humidity: 72.00 % Temperature: 25.30 °C | 77.54 °F Heat index: 25.77 °C | 78.38 °F
13:00:30.997 -> Humidity: 74.00 % Temperature: 25.30 °C | 77.54 °F Heat index: 25.82 °C | 78.47 °F
13:00:37.047 -> Humidity: 75.00 % Temperature: 25.20 °C | 77.36 °F Heat index: 25.73 °C | 78.32 °F
13:00:43.082 -> Humidity: 77.00 % Temperature: 25.10 °C | 77.18 °F Heat index: 25.68 °C | 78.22 °F
13:00:49.160 -> Humidity: 77.00 % Temperature: 25.00 °C | 77.00 °F Heat index: 25.57 °C | 78.02 °F
13:00:55.196 -> Humidity: 77.00 % Temperature: 24.90 °C | 76.82 °F Heat index: 25.46 °C | 77.82 °F
13:01:01.267 -> Humidity: 78.00 % Temperature: 24.80 °C | 76.64 °F Heat index: 25.37 °C | 77.67 °F
13:01:07.311 -> Humidity: 80.00 % Temperature: 24.70 °C | 76.46 °F Heat index: 25.31 °C | 77.57 °F
13:01:13.368 -> Humidity: 82.00 % Temperature: 24.60 °C | 76.28 °F Heat index: 25.26 °C | 77.46 °F
13:01:19.406 -> Humidity: 82.00 % Temperature: 24.60 °C | 76.28 °F Heat index: 25.26 °C | 77.46 °F
13:01:25.475 -> Humidity: 82.00 % Temperature: 24.40 °C | 75.92 °F Heat index: 25.04 °C | 77.07 °F
13:01:31.523 -> Humidity: 82.00 % Temperature: 24.30 °C | 75.74 °F Heat index: 24.93 °C | 76.87 °F
13:01:37.567 -> Humidity: 83.00 % Temperature: 24.30 °C | 75.74 °F Heat index: 24.95 °C | 76.91 °F
13:01:43.619 -> Humidity: 83.00 % Temperature: 24.10 °C | 75.38 °F Heat index: 24.73 °C | 76.52 °F
13:01:49.672 -> Humidity: 83.00 % Temperature: 24.10 °C | 75.38 °F Heat index: 24.73 °C | 76.52 °F
13:01:55.723 -> Humidity: 83.00 % Temperature: 24.10 °C | 75.38 °F Heat index: 24.73 °C | 76.52 °F
13:02:01.795 -> Humidity: 83.00 % Temperature: 24.00 °C | 75.20 °F Heat index: 24.62 °C | 76.32 °F
13:02:07.846 -> Humidity: 83.00 % Temperature: 24.00 °C | 75.20 °F Heat index: 24.62 °C | 76.32 °F
13:02:13.893 -> Humidity: 84.00 % Temperature: 23.90 °C | 75.02 °F Heat index: 24.54 °C | 76.17 °F
13:02:19.928 -> Humidity: 84.00 % Temperature: 23.90 °C | 75.02 °F Heat index: 24.54 °C | 76.17 °F
13:02:26.003 -> Humidity: 84.00 % Temperature: 23.90 °C | 75.02 °F Heat index: 24.54 °C | 76.17 °F
13:02:32.048 -> Humidity: 83.00 % Temperature: 23.90 °C | 75.02 °F Heat index: 24.51 °C | 76.12 °F
13:02:38.099 -> Humidity: 83.00 % Temperature: 23.90 °C | 75.02 °F Heat index: 24.51 °C | 76.12 °F
13:02:44.139 -> Humidity: 84.00 % Temperature: 23.90 °C | 75.02 °F Heat index: 24.54 °C | 76.17 °F
13:02:50.213 -> Humidity: 84.00 % Temperature: 23.90 °C | 75.02 °F Heat index: 24.54 °C | 76.17 °F
13:02:56.248 -> Humidity: 83.00 % Temperature: 23.80 °C | 74.84 °F Heat index: 24.40 °C | 75.92 °F
13:03:02.300 -> Humidity: 83.00 % Temperature: 23.80 °C | 74.84 °F Heat index: 24.40 °C | 75.92 °F
13:03:08.349 -> Humidity: 82.00 % Temperature: 23.80 °C | 74.84 °F Heat index: 24.38 °C | 75.88 °F
13:03:14.411 -> Humidity: 80.00 % Temperature: 23.80 °C | 74.84 °F Heat index: 24.32 °C | 75.78 °F
13:03:20.465 -> Humidity: 80.00 % Temperature: 23.70 °C | 74.66 °F Heat index: 24.21 °C | 75.59 °F
13:03:26.531 -> Humidity: 81.00 % Temperature: 23.70 °C | 74.66 °F Heat index: 24.24 °C | 75.63 °F
13:03:32.568 -> Humidity: 81.00 % Temperature: 23.70 °C | 74.66 °F Heat index: 24.24 °C | 75.63 °F
13:03:38.638 -> Humidity: 80.00 % Temperature: 23.70 °C | 74.66 °F Heat index: 24.21 °C | 75.59 °F
13:03:44.675 -> Humidity: 80.00 % Temperature: 23.70 °C | 74.66 °F Heat index: 24.21 °C | 75.59 °F
13:03:50.716 -> Humidity: 81.00 % Temperature: 23.70 °C | 74.66 °F Heat index: 24.24 °C | 75.63 °F
13:03:56.793 -> Humidity: 81.00 % Temperature: 23.70 °C | 74.66 °F Heat index: 24.24 °C | 75.63 °F
13:04:02.833 -> Humidity: 81.00 % Temperature: 23.70 °C | 74.66 °F Heat index: 24.24 °C | 75.63 °F
13:04:08.868 -> Humidity: 81.00 % Temperature: 23.70 °C | 74.66 °F Heat index: 24.24 °C | 75.63 °F
13:04:14.917 -> Humidity: 81.00 % Temperature: 23.70 °C | 74.66 °F Heat index: 24.24 °C | 75.63 °F
13:04:20.995 -> Humidity: 80.00 % Temperature: 23.70 °C | 74.66 °F Heat index: 24.21 °C | 75.59 °F
13:04:27.027 -> Humidity: 80.00 % Temperature: 23.70 °C | 74.66 °F Heat index: 24.21 °C | 75.59 °F
13:04:33.074 -> Humidity: 80.00 % Temperature: 23.70 °C | 74.66 °F Heat index: 24.21 °C | 75.59 °F
13:04:39.134 -> Humidity: 81.00 % Temperature: 23.80 °C | 74.84 °F Heat index: 24.35 °C | 75.83 °F
13:04:45.178 -> Humidity: 80.00 % Temperature: 23.80 °C | 74.84 °F Heat index: 24.32 °C | 75.78 °F
13:04:51.242 -> Humidity: 80.00 % Temperature: 23.80 °C | 74.84 °F Heat index: 24.32 °C | 75.78 °F
13:04:57.286 -> Humidity: 80.00 % Temperature: 23.90 °C | 75.02 °F Heat index: 24.43 °C | 75.98 °F
13:05:03.342 -> Humidity: 80.00 % Temperature: 23.90 °C | 75.02 °F Heat index: 24.43 °C | 75.98 °F

13:05:09.407 -> Humidity: 80.00 % Temperature: 23.90 °C | 75.02 °F Heat index: 24.43 °C | 75.98 °F
13:05:15.438 -> Humidity: 80.00 % Temperature: 23.90 °C | 75.02 °F Heat index: 24.43 °C | 75.98 °F
13:05:21.487 -> Humidity: 79.00 % Temperature: 24.00 °C | 75.20 °F Heat index: 24.52 °C | 76.13 °F
13:05:27.559 -> Humidity: 77.00 % Temperature: 24.00 °C | 75.20 °F Heat index: 24.47 °C | 76.04 °F
13:05:33.609 -> Humidity: 77.00 % Temperature: 24.00 °C | 75.20 °F Heat index: 24.47 °C | 76.04 °F
13:05:39.660 -> Humidity: 77.00 % Temperature: 24.00 °C | 75.20 °F Heat index: 24.47 °C | 76.04 °F
13:05:45.704 -> Humidity: 76.00 % Temperature: 24.00 °C | 75.20 °F Heat index: 24.44 °C | 75.99 °F
13:05:51.749 -> Humidity: 76.00 % Temperature: 24.10 °C | 75.38 °F Heat index: 24.55 °C | 76.19 °F
13:05:57.792 -> Humidity: 76.00 % Temperature: 24.10 °C | 75.38 °F Heat index: 24.55 °C | 76.19 °F
13:06:03.844 -> Humidity: 77.00 % Temperature: 24.10 °C | 75.38 °F Heat index: 24.58 °C | 76.24 °F
13:06:09.918 -> Humidity: 76.00 % Temperature: 24.10 °C | 75.38 °F Heat index: 24.55 °C | 76.19 °F
13:06:15.960 -> Humidity: 76.00 % Temperature: 24.10 °C | 75.38 °F Heat index: 24.55 °C | 76.19 °F
13:06:21.999 -> Humidity: 76.00 % Temperature: 24.10 °C | 75.38 °F Heat index: 24.55 °C | 76.19 °F
13:06:28.062 -> Humidity: 77.00 % Temperature: 24.20 °C | 75.56 °F Heat index: 24.69 °C | 76.43 °F
13:06:34.096 -> Humidity: 78.00 % Temperature: 24.10 °C | 75.38 °F Heat index: 24.60 °C | 76.28 °F
13:06:40.149 -> Humidity: 81.00 % Temperature: 24.10 °C | 75.38 °F Heat index: 24.68 °C | 76.43 °F
13:06:46.212 -> Humidity: 83.00 % Temperature: 24.00 °C | 75.20 °F Heat index: 24.62 °C | 76.32 °F
13:06:52.252 -> Humidity: 84.00 % Temperature: 24.00 °C | 75.20 °F Heat index: 24.65 °C | 76.37 °F
13:06:58.327 -> Humidity: 85.00 % Temperature: 23.90 °C | 75.02 °F Heat index: 24.56 °C | 76.22 °F
13:07:04.367 -> Humidity: 86.00 % Temperature: 23.70 °C | 74.66 °F Heat index: 24.37 °C | 75.87 °F
13:07:10.441 -> Humidity: 87.00 % Temperature: 23.60 °C | 74.48 °F Heat index: 24.29 °C | 75.72 °F
13:07:16.464 -> Humidity: 86.00 % Temperature: 23.60 °C | 74.48 °F Heat index: 24.26 °C | 75.67 °F
13:07:22.530 -> Humidity: 86.00 % Temperature: 23.50 °C | 74.30 °F Heat index: 24.15 °C | 75.47 °F
13:07:28.565 -> Humidity: 86.00 % Temperature: 23.40 °C | 74.12 °F Heat index: 24.04 °C | 75.27 °F
13:07:34.642 -> Humidity: 86.00 % Temperature: 23.30 °C | 73.94 °F Heat index: 23.93 °C | 75.08 °F
13:07:40.689 -> Humidity: 86.00 % Temperature: 23.20 °C | 73.76 °F Heat index: 23.82 °C | 74.88 °F
13:07:46.734 -> Humidity: 86.00 % Temperature: 23.20 °C | 73.76 °F Heat index: 23.82 °C | 74.88 °F
13:07:52.783 -> Humidity: 86.00 % Temperature: 23.10 °C | 73.58 °F Heat index: 23.71 °C | 74.68 °F
13:07:58.856 -> Humidity: 86.00 % Temperature: 23.10 °C | 73.58 °F Heat index: 23.71 °C | 74.68 °F
13:08:04.898 -> Humidity: 87.00 % Temperature: 23.10 °C | 73.58 °F Heat index: 23.74 °C | 74.73 °F
13:08:10.952 -> Humidity: 87.00 % Temperature: 23.10 °C | 73.58 °F Heat index: 23.74 °C | 74.73 °F
13:08:17.000 -> Humidity: 87.00 % Temperature: 23.10 °C | 73.58 °F Heat index: 23.74 °C | 74.73 °F
13:08:23.037 -> Humidity: 85.00 % Temperature: 23.00 °C | 73.40 °F Heat index: 23.57 °C | 74.43 °F
13:08:29.098 -> Humidity: 85.00 % Temperature: 23.00 °C | 73.40 °F Heat index: 23.57 °C | 74.43 °F
13:08:35.152 -> Humidity: 85.00 % Temperature: 23.00 °C | 73.40 °F Heat index: 23.57 °C | 74.43 °F
13:08:41.199 -> Humidity: 85.00 % Temperature: 23.00 °C | 73.40 °F Heat index: 23.57 °C | 74.43 °F
13:08:47.270 -> Humidity: 85.00 % Temperature: 23.00 °C | 73.40 °F Heat index: 23.57 °C | 74.43 °F
13:08:53.303 -> Humidity: 85.00 % Temperature: 23.00 °C | 73.40 °F Heat index: 23.57 °C | 74.43 °F
13:08:59.374 -> Humidity: 85.00 % Temperature: 23.00 °C | 73.40 °F Heat index: 23.57 °C | 74.43 °F
13:09:05.404 -> Humidity: 85.00 % Temperature: 23.00 °C | 73.40 °F Heat index: 23.57 °C | 74.43 °F
13:09:11.452 -> Humidity: 86.00 % Temperature: 23.10 °C | 73.58 °F Heat index: 23.71 °C | 74.68 °F
13:09:17.508 -> Humidity: 86.00 % Temperature: 23.10 °C | 73.58 °F Heat index: 23.71 °C | 74.68 °F
13:09:23.567 -> Humidity: 86.00 % Temperature: 23.10 °C | 73.58 °F Heat index: 23.71 °C | 74.68 °F
13:09:29.621 -> Humidity: 85.00 % Temperature: 23.10 °C | 73.58 °F Heat index: 23.68 °C | 74.63 °F
13:09:35.680 -> Humidity: 85.00 % Temperature: 23.10 °C | 73.58 °F Heat index: 23.68 °C | 74.63 °F
13:09:41.704 -> Humidity: 85.00 % Temperature: 23.20 °C | 73.76 °F Heat index: 23.79 °C | 74.83 °F
13:09:47.784 -> Humidity: 86.00 % Temperature: 23.20 °C | 73.76 °F Heat index: 23.82 °C | 74.88 °F
13:09:53.828 -> Humidity: 86.00 % Temperature: 23.20 °C | 73.76 °F Heat index: 23.82 °C | 74.88 °F

13:09:59.866 -> Humidity: 85.00 % Temperature: 23.20 °C | 73.76 °F Heat index: 23.79 °C | 74.83 °F
13:10:05.923 -> Humidity: 84.00 % Temperature: 23.30 °C | 73.94 °F Heat index: 23.88 °C | 74.98 °F
13:10:11.965 -> Humidity: 82.00 % Temperature: 23.30 °C | 73.94 °F Heat index: 23.83 °C | 74.89 °F
13:10:18.030 -> Humidity: 82.00 % Temperature: 23.40 °C | 74.12 °F Heat index: 23.94 °C | 75.09 °F
13:10:24.071 -> Humidity: 81.00 % Temperature: 23.40 °C | 74.12 °F Heat index: 23.91 °C | 75.04 °F
13:10:30.123 -> Humidity: 80.00 % Temperature: 23.40 °C | 74.12 °F Heat index: 23.88 °C | 74.99 °F
13:10:36.194 -> Humidity: 81.00 % Temperature: 23.50 °C | 74.30 °F Heat index: 24.02 °C | 75.24 °F
13:10:42.223 -> Humidity: 81.00 % Temperature: 23.50 °C | 74.30 °F Heat index: 24.02 °C | 75.24 °F
13:10:48.299 -> Humidity: 81.00 % Temperature: 23.50 °C | 74.30 °F Heat index: 24.02 °C | 75.24 °F
13:10:54.337 -> Humidity: 80.00 % Temperature: 23.60 °C | 74.48 °F Heat index: 24.10 °C | 75.39 °F
13:11:00.399 -> Humidity: 79.00 % Temperature: 23.60 °C | 74.48 °F Heat index: 24.08 °C | 75.34 °F
13:11:06.450 -> Humidity: 79.00 % Temperature: 23.70 °C | 74.66 °F Heat index: 24.19 °C | 75.54 °F
13:11:12.480 -> Humidity: 79.00 % Temperature: 23.70 °C | 74.66 °F Heat index: 24.19 °C | 75.54 °F
13:11:18.556 -> Humidity: 80.00 % Temperature: 23.70 °C | 74.66 °F Heat index: 24.21 °C | 75.59 °F
13:11:24.581 -> Humidity: 80.00 % Temperature: 23.80 °C | 74.84 °F Heat index: 24.32 °C | 75.78 °F
13:11:30.642 -> Humidity: 79.00 % Temperature: 23.80 °C | 74.84 °F Heat index: 24.30 °C | 75.74 °F
13:11:36.696 -> Humidity: 78.00 % Temperature: 23.90 °C | 75.02 °F Heat index: 24.38 °C | 75.89 °F
13:11:42.763 -> Humidity: 77.00 % Temperature: 23.90 °C | 75.02 °F Heat index: 24.36 °C | 75.84 °F
13:11:48.814 -> Humidity: 77.00 % Temperature: 24.00 °C | 75.20 °F Heat index: 24.47 °C | 76.04 °F
13:11:54.850 -> Humidity: 77.00 % Temperature: 24.00 °C | 75.20 °F Heat index: 24.47 °C | 76.04 °F
13:12:00.909 -> Humidity: 77.00 % Temperature: 24.00 °C | 75.20 °F Heat index: 24.47 °C | 76.04 °F
13:12:06.965 -> Humidity: 77.00 % Temperature: 24.10 °C | 75.38 °F Heat index: 24.58 °C | 76.24 °F
13:12:13.001 -> Humidity: 76.00 % Temperature: 24.10 °C | 75.38 °F Heat index: 24.55 °C | 76.19 °F
13:12:19.064 -> Humidity: 77.00 % Temperature: 24.10 °C | 75.38 °F Heat index: 24.58 °C | 76.24 °F
13:12:25.101 -> Humidity: 77.00 % Temperature: 24.10 °C | 75.38 °F Heat index: 24.58 °C | 76.24 °F
13:12:31.165 -> Humidity: 76.00 % Temperature: 24.20 °C | 75.56 °F Heat index: 24.66 °C | 76.39 °F
13:12:37.198 -> Humidity: 76.00 % Temperature: 24.20 °C | 75.56 °F Heat index: 24.66 °C | 76.39 °F
13:12:43.270 -> Humidity: 75.00 % Temperature: 24.20 °C | 75.56 °F Heat index: 24.63 °C | 76.34 °F
13:12:49.296 -> Humidity: 75.00 % Temperature: 24.30 °C | 75.74 °F Heat index: 24.74 °C | 76.54 °F
13:12:55.340 -> Humidity: 75.00 % Temperature: 24.30 °C | 75.74 °F Heat index: 24.74 °C | 76.54 °F
13:13:01.404 -> Humidity: 75.00 % Temperature: 24.30 °C | 75.74 °F Heat index: 24.74 °C | 76.54 °F
13:13:07.470 -> Humidity: 75.00 % Temperature: 24.40 °C | 75.92 °F Heat index: 24.85 °C | 76.74 °F
13:13:13.505 -> Humidity: 74.00 % Temperature: 24.40 °C | 75.92 °F Heat index: 24.83 °C | 76.69 °F
13:13:19.567 -> Humidity: 74.00 % Temperature: 24.50 °C | 76.10 °F Heat index: 24.94 °C | 76.89 °F
13:13:25.628 -> Humidity: 74.00 % Temperature: 24.50 °C | 76.10 °F Heat index: 24.94 °C | 76.89 °F
13:13:31.648 -> Humidity: 74.00 % Temperature: 24.50 °C | 76.10 °F Heat index: 24.94 °C | 76.89 °F
13:13:37.703 -> Humidity: 74.00 % Temperature: 24.50 °C | 76.10 °F Heat index: 24.94 °C | 76.89 °F
13:13:43.765 -> Humidity: 73.00 % Temperature: 24.60 °C | 76.28 °F Heat index: 25.02 °C | 77.04 °F
13:13:49.822 -> Humidity: 73.00 % Temperature: 24.60 °C | 76.28 °F Heat index: 25.02 °C | 77.04 °F
13:13:55.855 -> Humidity: 73.00 % Temperature: 24.60 °C | 76.28 °F Heat index: 25.02 °C | 77.04 °F
13:14:01.917 -> Humidity: 73.00 % Temperature: 24.60 °C | 76.28 °F Heat index: 25.02 °C | 77.04 °F
13:14:07.982 -> Humidity: 72.00 % Temperature: 24.70 °C | 76.46 °F Heat index: 25.11 °C | 77.19 °F
13:14:14.024 -> Humidity: 73.00 % Temperature: 24.70 °C | 76.46 °F Heat index: 25.13 °C | 77.24 °F
13:14:20.064 -> Humidity: 73.00 % Temperature: 24.70 °C | 76.46 °F Heat index: 25.13 °C | 77.24 °F
13:14:26.119 -> Humidity: 73.00 % Temperature: 24.80 °C | 76.64 °F Heat index: 25.24 °C | 77.43 °F
13:14:32.189 -> Humidity: 73.00 % Temperature: 24.80 °C | 76.64 °F Heat index: 25.24 °C | 77.43 °F
13:14:38.217 -> Humidity: 73.00 % Temperature: 24.90 °C | 76.82 °F Heat index: 25.35 °C | 77.63 °F
13:14:44.280 -> Humidity: 72.00 % Temperature: 24.90 °C | 76.82 °F Heat index: 25.33 °C | 77.59 °F

13:14:50.319 -> Humidity: 72.00 % Temperature: 25.00 °C | 77.00 °F Heat index: 25.44 °C | 77.78 °F
13:14:56.389 -> Humidity: 72.00 % Temperature: 25.00 °C | 77.00 °F Heat index: 25.44 °C | 77.78 °F
13:15:02.423 -> Humidity: 72.00 % Temperature: 25.10 °C | 77.18 °F Heat index: 25.55 °C | 77.98 °F
13:15:08.491 -> Humidity: 71.00 % Temperature: 25.10 °C | 77.18 °F Heat index: 25.52 °C | 77.93 °F
13:15:14.530 -> Humidity: 71.00 % Temperature: 25.10 °C | 77.18 °F Heat index: 25.52 °C | 77.93 °F
13:15:20.572 -> Humidity: 70.00 % Temperature: 25.20 °C | 77.36 °F Heat index: 25.60 °C | 78.09 °F
13:15:26.643 -> Humidity: 70.00 % Temperature: 25.20 °C | 77.36 °F Heat index: 25.60 °C | 78.09 °F
13:15:32.677 -> Humidity: 70.00 % Temperature: 25.20 °C | 77.36 °F Heat index: 25.60 °C | 78.09 °F
13:15:38.736 -> Humidity: 70.00 % Temperature: 25.30 °C | 77.54 °F Heat index: 25.71 °C | 78.28 °F
13:15:44.772 -> Humidity: 69.00 % Temperature: 25.30 °C | 77.54 °F Heat index: 25.69 °C | 78.24 °F
13:15:50.847 -> Humidity: 69.00 % Temperature: 25.30 °C | 77.54 °F Heat index: 25.69 °C | 78.24 °F
13:15:56.877 -> Humidity: 69.00 % Temperature: 25.30 °C | 77.54 °F Heat index: 25.69 °C | 78.24 °F
13:16:02.939 -> Humidity: 69.00 % Temperature: 25.40 °C | 77.72 °F Heat index: 25.80 °C | 78.43 °F
13:16:08.981 -> Humidity: 68.00 % Temperature: 25.40 °C | 77.72 °F Heat index: 25.77 °C | 78.39 °F
13:16:15.034 -> Humidity: 68.00 % Temperature: 25.40 °C | 77.72 °F Heat index: 25.77 °C | 78.39 °F
13:16:21.112 -> Humidity: 67.00 % Temperature: 25.40 °C | 77.72 °F Heat index: 25.74 °C | 78.34 °F
13:16:27.145 -> Humidity: 67.00 % Temperature: 25.40 °C | 77.72 °F Heat index: 25.74 °C | 78.34 °F
13:16:33.181 -> Humidity: 67.00 % Temperature: 25.40 °C | 77.72 °F Heat index: 25.74 °C | 78.34 °F
13:16:39.256 -> Humidity: 67.00 % Temperature: 25.40 °C | 77.72 °F Heat index: 25.74 °C | 78.34 °F
13:16:45.289 -> Humidity: 67.00 % Temperature: 25.40 °C | 77.72 °F Heat index: 25.74 °C | 78.34 °F
13:16:51.338 -> Humidity: 67.00 % Temperature: 25.40 °C | 77.72 °F Heat index: 25.74 °C | 78.34 °F
13:16:57.405 -> Humidity: 67.00 % Temperature: 25.40 °C | 77.72 °F Heat index: 25.74 °C | 78.34 °F
13:17:03.446 -> Humidity: 67.00 % Temperature: 25.40 °C | 77.72 °F Heat index: 25.74 °C | 78.34 °F
13:17:09.516 -> Humidity: 67.00 % Temperature: 25.40 °C | 77.72 °F Heat index: 25.74 °C | 78.34 °F
13:17:15.559 -> Humidity: 67.00 % Temperature: 25.40 °C | 77.72 °F Heat index: 25.74 °C | 78.34 °F
13:17:21.618 -> Humidity: 67.00 % Temperature: 25.50 °C | 77.90 °F Heat index: 25.85 °C | 78.54 °F
13:17:27.646 -> Humidity: 67.00 % Temperature: 25.50 °C | 77.90 °F Heat index: 25.85 °C | 78.54 °F
13:17:33.701 -> Humidity: 67.00 % Temperature: 25.60 °C | 78.08 °F Heat index: 25.96 °C | 78.74 °F
13:17:39.757 -> Humidity: 67.00 % Temperature: 25.60 °C | 78.08 °F Heat index: 25.96 °C | 78.74 °F
13:17:45.804 -> Humidity: 67.00 % Temperature: 25.60 °C | 78.08 °F Heat index: 25.96 °C | 78.74 °F
13:17:51.843 -> Humidity: 67.00 % Temperature: 25.70 °C | 78.26 °F Heat index: 26.07 °C | 78.93 °F
13:17:57.902 -> Humidity: 66.00 % Temperature: 25.70 °C | 78.26 °F Heat index: 26.05 °C | 78.89 °F
13:18:03.956 -> Humidity: 66.00 % Temperature: 25.80 °C | 78.44 °F Heat index: 26.90 °C | 80.42 °F
13:18:10.016 -> Humidity: 66.00 % Temperature: 25.80 °C | 78.44 °F Heat index: 26.90 °C | 80.42 °F
13:18:16.059 -> Humidity: 66.00 % Temperature: 25.80 °C | 78.44 °F Heat index: 26.90 °C | 80.42 °F
13:18:22.127 -> Humidity: 65.00 % Temperature: 25.90 °C | 78.62 °F Heat index: 26.99 °C | 80.58 °F
13:18:28.165 -> Humidity: 65.00 % Temperature: 25.80 °C | 78.44 °F Heat index: 26.87 °C | 80.37 °F
13:18:34.227 -> Humidity: 65.00 % Temperature: 25.80 °C | 78.44 °F Heat index: 26.87 °C | 80.37 °F
13:18:40.285 -> Humidity: 65.00 % Temperature: 25.90 °C | 78.62 °F Heat index: 26.99 °C | 80.58 °F
13:18:46.310 -> Humidity: 65.00 % Temperature: 25.90 °C | 78.62 °F Heat index: 26.99 °C | 80.58 °F
13:18:52.376 -> Humidity: 65.00 % Temperature: 25.90 °C | 78.62 °F Heat index: 26.99 °C | 80.58 °F
13:18:58.431 -> Humidity: 65.00 % Temperature: 25.90 °C | 78.62 °F Heat index: 26.99 °C | 80.58 °F
13:19:04.469 -> Humidity: 64.00 % Temperature: 25.90 °C | 78.62 °F Heat index: 26.96 °C | 80.52 °F
13:19:10.531 -> Humidity: 64.00 % Temperature: 25.90 °C | 78.62 °F Heat index: 26.96 °C | 80.52 °F
13:19:16.574 -> Humidity: 64.00 % Temperature: 25.90 °C | 78.62 °F Heat index: 26.96 °C | 80.52 °F
13:19:22.617 -> Humidity: 64.00 % Temperature: 25.90 °C | 78.62 °F Heat index: 26.96 °C | 80.52 °F
13:19:28.704 -> Humidity: 64.00 % Temperature: 25.90 °C | 78.62 °F Heat index: 26.96 °C | 80.52 °F
13:19:34.742 -> Humidity: 64.00 % Temperature: 25.90 °C | 78.62 °F Heat index: 26.96 °C | 80.52 °F

13:19:40.790 -> Humidity: 65.00 % Temperature: 26.00 °C | 78.80 °F Heat index: 27.11 °C | 80.80 °F
13:19:46.829 -> Humidity: 65.00 % Temperature: 26.00 °C | 78.80 °F Heat index: 27.11 °C | 80.80 °F
13:19:52.900 -> Humidity: 65.00 % Temperature: 26.00 °C | 78.80 °F Heat index: 27.11 °C | 80.80 °F
13:19:58.933 -> Humidity: 65.00 % Temperature: 26.10 °C | 78.98 °F Heat index: 27.23 °C | 81.02 °F
13:20:05.001 -> Humidity: 65.00 % Temperature: 26.10 °C | 78.98 °F Heat index: 27.23 °C | 81.02 °F
13:20:11.064 -> Humidity: 65.00 % Temperature: 26.10 °C | 78.98 °F Heat index: 27.23 °C | 81.02 °F
13:20:17.113 -> Humidity: 65.00 % Temperature: 26.10 °C | 78.98 °F Heat index: 27.23 °C | 81.02 °F
13:20:23.139 -> Humidity: 65.00 % Temperature: 26.20 °C | 79.16 °F Heat index: 27.36 °C | 81.25 °F
13:20:29.195 -> Humidity: 65.00 % Temperature: 26.20 °C | 79.16 °F Heat index: 27.36 °C | 81.25 °F
13:20:35.262 -> Humidity: 64.00 % Temperature: 26.20 °C | 79.16 °F Heat index: 27.32 °C | 81.17 °F
13:20:41.296 -> Humidity: 64.00 % Temperature: 26.30 °C | 79.34 °F Heat index: 27.44 °C | 81.39 °F
13:20:47.350 -> Humidity: 64.00 % Temperature: 26.30 °C | 79.34 °F Heat index: 27.44 °C | 81.39 °F
13:20:53.410 -> Humidity: 64.00 % Temperature: 26.30 °C | 79.34 °F Heat index: 27.44 °C | 81.39 °F
13:20:59.450 -> Humidity: 64.00 % Temperature: 26.30 °C | 79.34 °F Heat index: 27.44 °C | 81.39 °F
13:21:05.521 -> Humidity: 64.00 % Temperature: 26.30 °C | 79.34 °F Heat index: 27.44 °C | 81.39 °F
13:21:11.562 -> Humidity: 64.00 % Temperature: 26.30 °C | 79.34 °F Heat index: 27.44 °C | 81.39 °F
13:21:17.616 -> Humidity: 64.00 % Temperature: 26.30 °C | 79.34 °F Heat index: 27.44 °C | 81.39 °F
13:21:23.660 -> Humidity: 64.00 % Temperature: 26.30 °C | 79.34 °F Heat index: 27.44 °C | 81.39 °F
13:21:29.708 -> Humidity: 64.00 % Temperature: 26.40 °C | 79.52 °F Heat index: 27.57 °C | 81.62 °F
13:21:35.757 -> Humidity: 64.00 % Temperature: 26.30 °C | 79.34 °F Heat index: 27.44 °C | 81.39 °F
13:21:41.821 -> Humidity: 64.00 % Temperature: 26.50 °C | 79.70 °F Heat index: 27.70 °C | 81.85 °F
13:21:47.886 -> Humidity: 63.00 % Temperature: 26.50 °C | 79.70 °F Heat index: 27.64 °C | 81.75 °F
13:21:53.918 -> Humidity: 63.00 % Temperature: 26.50 °C | 79.70 °F Heat index: 27.64 °C | 81.75 °F
13:21:59.975 -> Humidity: 63.00 % Temperature: 26.40 °C | 79.52 °F Heat index: 27.52 °C | 81.53 °F
13:22:06.023 -> Humidity: 63.00 % Temperature: 26.40 °C | 79.52 °F Heat index: 27.52 °C | 81.53 °F
13:22:12.086 -> Humidity: 63.00 % Temperature: 26.30 °C | 79.34 °F Heat index: 27.39 °C | 81.31 °F
13:22:18.144 -> Humidity: 64.00 % Temperature: 26.30 °C | 79.34 °F Heat index: 27.44 °C | 81.39 °F
13:22:24.182 -> Humidity: 64.00 % Temperature: 26.30 °C | 79.34 °F Heat index: 27.44 °C | 81.39 °F
13:22:30.236 -> Humidity: 64.00 % Temperature: 26.30 °C | 79.34 °F Heat index: 27.44 °C | 81.39 °F
13:22:36.291 -> Humidity: 64.00 % Temperature: 26.30 °C | 79.34 °F Heat index: 27.44 °C | 81.39 °F
13:22:42.325 -> Humidity: 64.00 % Temperature: 26.30 °C | 79.34 °F Heat index: 27.44 °C | 81.39 °F
13:22:48.393 -> Humidity: 64.00 % Temperature: 26.20 °C | 79.16 °F Heat index: 27.32 °C | 81.17 °F
13:22:54.437 -> Humidity: 64.00 % Temperature: 26.20 °C | 79.16 °F Heat index: 27.32 °C | 81.17 °F
13:23:00.507 -> Humidity: 64.00 % Temperature: 26.20 °C | 79.16 °F Heat index: 27.32 °C | 81.17 °F
13:23:06.562 -> Humidity: 64.00 % Temperature: 26.20 °C | 79.16 °F Heat index: 27.32 °C | 81.17 °F
13:23:12.597 -> Humidity: 64.00 % Temperature: 26.10 °C | 78.98 °F Heat index: 27.19 °C | 80.95 °F
13:23:18.663 -> Humidity: 64.00 % Temperature: 26.10 °C | 78.98 °F Heat index: 27.19 °C | 80.95 °F
13:23:24.693 -> Humidity: 64.00 % Temperature: 26.10 °C | 78.98 °F Heat index: 27.19 °C | 80.95 °F
13:23:30.752 -> Humidity: 64.00 % Temperature: 26.10 °C | 78.98 °F Heat index: 27.19 °C | 80.95 °F
13:23:36.801 -> Humidity: 65.00 % Temperature: 26.10 °C | 78.98 °F Heat index: 27.23 °C | 81.02 °F
13:23:42.866 -> Humidity: 64.00 % Temperature: 26.10 °C | 78.98 °F Heat index: 27.19 °C | 80.95 °F
13:23:48.903 -> Humidity: 64.00 % Temperature: 26.10 °C | 78.98 °F Heat index: 27.19 °C | 80.95 °F
13:23:54.962 -> Humidity: 64.00 % Temperature: 26.20 °C | 79.16 °F Heat index: 27.32 °C | 81.17 °F
13:24:01.026 -> Humidity: 64.00 % Temperature: 26.20 °C | 79.16 °F Heat index: 27.32 °C | 81.17 °F
13:24:07.060 -> Humidity: 64.00 % Temperature: 26.20 °C | 79.16 °F Heat index: 27.32 °C | 81.17 °F
13:24:13.106 -> Humidity: 64.00 % Temperature: 26.20 °C | 79.16 °F Heat index: 27.32 °C | 81.17 °F
13:24:19.177 -> Humidity: 64.00 % Temperature: 26.20 °C | 79.16 °F Heat index: 27.32 °C | 81.17 °F
13:24:25.222 -> Humidity: 64.00 % Temperature: 26.20 °C | 79.16 °F Heat index: 27.32 °C | 81.17 °F

13:24:31.259 -> Humidity: 64.00 % Temperature: 26.20 °C | 79.16 °F Heat index: 27.32 °C | 81.17 °F
13:24:37.315 -> Humidity: 64.00 % Temperature: 26.20 °C | 79.16 °F Heat index: 27.32 °C | 81.17 °F
13:24:43.383 -> Humidity: 64.00 % Temperature: 26.30 °C | 79.34 °F Heat index: 27.44 °C | 81.39 °F
13:24:49.437 -> Humidity: 64.00 % Temperature: 26.20 °C | 79.16 °F Heat index: 27.32 °C | 81.17 °F
13:24:55.484 -> Humidity: 64.00 % Temperature: 26.30 °C | 79.34 °F Heat index: 27.44 °C | 81.39 °F
13:25:01.541 -> Humidity: 64.00 % Temperature: 26.30 °C | 79.34 °F Heat index: 27.44 °C | 81.39 °F
13:25:07.573 -> Humidity: 64.00 % Temperature: 26.30 °C | 79.34 °F Heat index: 27.44 °C | 81.39 °F
13:25:13.618 -> Humidity: 64.00 % Temperature: 26.30 °C | 79.34 °F Heat index: 27.44 °C | 81.39 °F
13:25:19.694 -> Humidity: 64.00 % Temperature: 26.30 °C | 79.34 °F Heat index: 27.44 °C | 81.39 °F
13:25:25.740 -> Humidity: 64.00 % Temperature: 26.30 °C | 79.34 °F Heat index: 27.44 °C | 81.39 °F

Table 25. Temperature, Relative Humidity and Heat index from testing phase

ANSYS-FLUENT SIMULATION REPORT

1. File Report

Table 1. File Information for CFX 1

Case	CFX 1
File Path	C:\Users\HP PRO\PROJET-BON_files\dp0\CFX-1\CFX\CFX_005.res
File Date	26 septembre 2020
File Time	05:03:24
File Type	CFX5
File Version	19.2

2. Mesh Report

Table 2. Mesh Information for CFX 1

Domain	Nodes	Elements
Default Domain	18659	83997

3. Physics Report

Table 3. Domain Physics for CFX 1

Domain - Default Domain	
Type	Fluid
Location	B220
Materials	
Air Ideal Gas	
Fluid Definition	Material Library

Boundary - Boundary 2	
Type	OPENING
Location	F238.220
Settings	
Flow Direction	Normal to Boundary Condition
Flow Regime	Subsonic
Heat Transfer	Opening Temperature
Opening Temperature	2.6000e+01 [C]
Mass And Momentum	Opening Pressure and Direction
Relative Pressure	0.0000e+00 [atm]
Turbulence	Medium Intensity and Eddy Viscosity Ratio

Boundary - Boundary 6	
Type	OUTLET
Location	F222.220, F224.220, F226.220, F228.220, F230.220, F232.220
Settings	
Flow Regime	Subsonic
Mass And Momentum	Normal Speed
Normal Speed	2.3000e+00 [m s^-1]
Boundary - Boundary 3	
Type	WALL
Location	F236.220
Settings	
Heat Transfer	Adiabatic
Mass And Momentum	No Slip Wall
Wall Roughness	Smooth Wall

Boundary - Boundary 4	
Type	WALL
Location	F234.220, F240.220
Settings	
Heat Transfer	Heat Transfer Coefficient
Heat Transfer Coefficient	5.5000e-01 [W m^-2 K^-1]
Outside Temperature	2.9900e+02 [K]
Mass And Momentum	No Slip Wall
Wall Roughness	Smooth Wall
Boundary - Boundary 5	
Type	WALL
Location	F221.220, F223.220, F225.220, F227.220, F229.220, F231.220, F235.220, F237.220, F239.220, F241.220, F242.220
Settings	
Heat Transfer	Heat Flux
Heat Flux in	8.0000e+02 [W m^-2]
Mass And Momentum	No Slip Wall
Wall Roughness	Smooth Wall

4. Solution Report

Table 5. Boundary Flows for CFX 1

Location	Type	Mass Flow	Momentum		
			X	Y	Z
Boundary 1	Boundary	5.6819e+01	8.5954e-07	-1.1560e+02	2.0481e-04
Boundary 2	Boundary	-5.3137e+01	-4.6382e-02	4.7495e+01	2.4843e+01
Boundary 3	Boundary	0.0000e+00	-8.8895e-04	-4.2666e-01	2.3705e+02
Boundary 4	Boundary	0.0000e+00	3.2149e-04	3.0011e+01	-2.6211e+02
Boundary 5	Boundary	0.0000e+00	6.2190e-02	3.7551e+01	8.3365e-02
Boundary 6	Boundary	-3.6813e+00	-1.5584e-02	9.9393e-01	1.3516e-01

1. File Report

Table 1. File Information for CFX

Case	CFX
File Path	C:\Users\HP PRO\PROJET-BON_files\dp0\CFX\CFX\CFX_011.res
File Date	28 septembre 2020
File Time	11:24:23
File Type	CFX5
File Version	19.2

2. Mesh Report

Table 2. Mesh Information for CFX

Domain	Nodes	Elements
Default Domain	18659	83997

3. Physics Report

Table 3. Domain Physics for CFX

Domain - Default Domain	
Type	Fluid
Location	B220
Materials	
Air Ideal Gas	
Fluid Definition	Material Library
Morphology	Continuous Fluid

Table 4. Boundary Physics for CFX

Domain	**Boundaries**	
Default Domain	**Boundary - Boundary 1**	
	Type	INLET
	Location	F233.220
	Settings	
	Flow Direction	Normal to Boundary Condition
	Flow Regime	Subsonic
	Heat Transfer	Total Temperature
	Total Temperature	2.7000e+01 [C]
	Mass And Momentum	Mass Flow Rate
	Mass Flow Rate	1.1366e+02 [kg s^-1]
	Mass Flow Rate Area	As Specified
	Turbulence	Medium Intensity and Eddy Viscosity Ratio

Boundary - Boundary 2	
Type	OPENING
Location	F238.220
Settings	
Flow Direction	Normal to Boundary Condition
Flow Regime	Subsonic
Heat Transfer	Static Temperature
Static Temperature	2.8000e+01 [C]
Mass And Momentum	Opening Pressure and Direction
Relative Pressure	0.0000e+00 [atm]
Turbulence	Medium Intensity and Eddy Viscosity Ratio

Boundary - Boundary 3	
Type	WALL
Location	F221.220, F222.220, F223.220, F224.220, F225.220, F226.220, F227.220, F228.220, F229.220, F230.220, F231.220, F232.220, F235.220, F237.220, F239.220, F241.220, F242.220
Settings	
Heat Transfer	Heat Transfer Coefficient
Heat Transfer Coefficient	3.3000e-01 [W m^-2 K^-1]
Outside Temperature	2.5000e+01 [C]
Mass And Momentum	No Slip Wall
Wall Roughness	Smooth Wall

Boundary - Boundary 4	
Type	WALL
Location	F234.220, F240.220
Settings	
Heat Transfer	Heat Flux
Heat Flux in	1.0000e+03 [W m^-2]
Mass And Momentum	No Slip Wall
Wall Roughness	Smooth Wall
Boundary - Boundary 5	
Type	WALL
Location	F236.220
Settings	
Heat Transfer	Adiabatic
Mass And Momentum	No Slip Wall
Wall Roughness	Smooth Wall

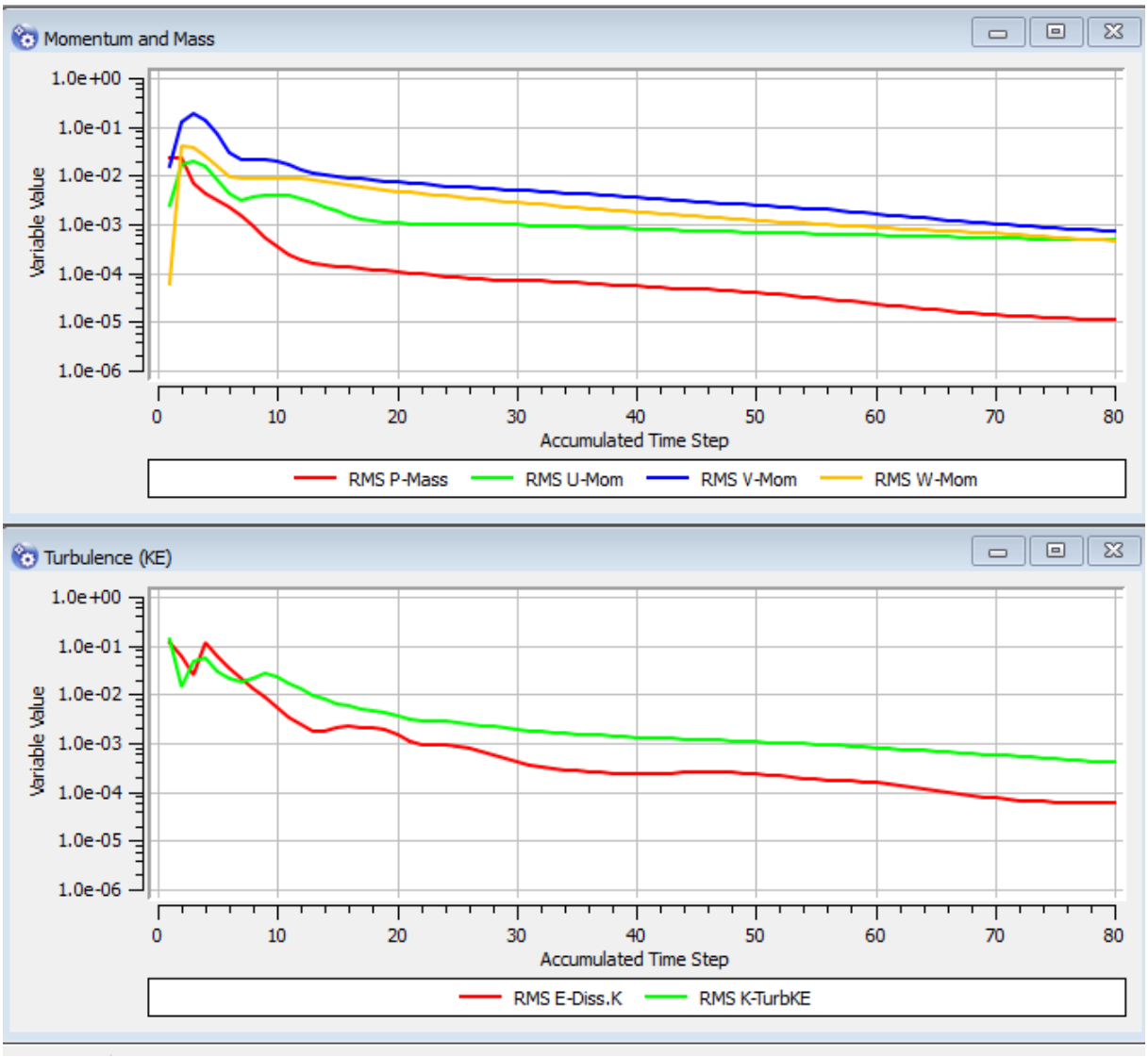
Momentum and Mass
1.0e+00
1.0e-01
1.0e-02
1.0e-03
1.0e-04
1.0e-05
1.0e-06
Variable Value
0
10
20
30
40
50
60
70
80
Accumulated Time Step
RMS P-Mass
RMS U-Mom
RMS V-Mom
RMS W-Mom
Turbulence (KE)
1.0e+00
1.0e-01
1.0e-02
1.0e-03
1.0e-04
1.0e-05
1.0e-06
Variable Value
0
10
20
30
40
50
60
70
80
Accumulated Time Step
RMS E-Diss.K
RMS K-TurbKE

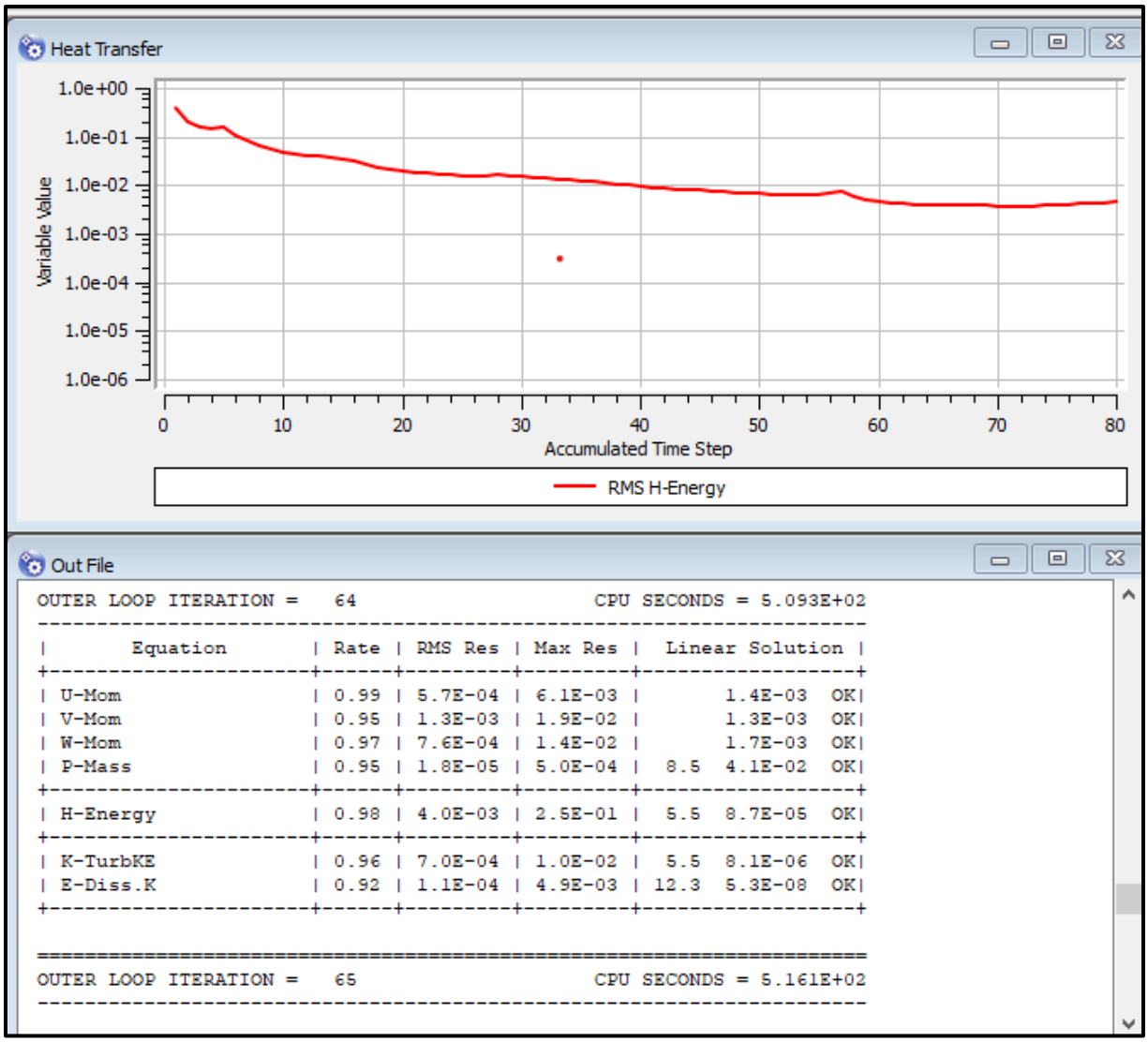
Heat Transfer
1.0e+00
1.0e-01
1.0e-02
1.0e-03
1.0e-04
1.0e-05
1.0e-06
Variable Value
0
10
20
30
40
50
60
70
80
Accumulated Time Step
RMS H-Energy
Out File
OUTER LOOP ITERATION = 64 CPU SECONDS = 5.093E+02
Equation	Rate	RMS Res	Max Res	Linear Solution
U-Mom	0.99	5.7E-04	6.1E-03	1.4E-03 OK
V-Mom	0.95	1.3E-03	1.9E-02	1.3E-03 OK
W-Mom	0.97	7.6E-04	1.4E-02	1.7E-03 OK
P-Mass	0.95	1.8E-05	5.0E-04	8.5 4.1E-02 OK
H-Energy	0.98	4.0E-03	2.5E-01	5.5 8.7E-05 OK
K-TurbKE	0.96	7.0E-04	1.0E-02	5.5 8.1E-06 OK
E-Diss.K	0.92	1.1E-04	4.9E-03	12.3 5.3E-08 OK
OUTER LOOP ITERATION = 65 CPU SECONDS = 5.161E+02